Convention on Long-range Transboundary Air Pollution

emep

*Co-operative programme for monitoring and evaluation of the long-range transmission of air pollutants in Europe*

STATUS REPORT
2/2017 July 2017

# Assessment of heavy metal transboundary pollution on regional and national scales, transition to the new EMEP grid

Status Report 2/2017

msc-e & ccc

**EMEP Status Report 2/2017**

**July 2017**

# Assessment of heavy metal transboundary pollution on regional and national scales, transition to the new EMEP grid


METEOROLOGICAL SYNTHESIZING CENTRE - EAST

I.Ilyin, O.Rozovskaya, O.Travnikov

CHEMICAL CO-ORDINATING CENTRE

W. Aas



**MCS-E**

Meteorological Synthesizing Centre - East

2nd Roshchinsky proezd, 8/5
115419 Moscow
Russia
Phone.: +7 926 906 91 78
Fax: +7 495 956 19 44
E-mail: msce@msceast.org
Internet: www.msceast.org

**CCC**
Norwegian Institute for Air Research (NILU)

P.O. Box 100NO-2027 Kjeller
Norway
Phone: +47 63 89 80 00
Fax: +47 63 89 80 50
E-mail: kjetil.torseth@nilu.no
Internet: www.nilu.no

## CONTENTS

# EXECUTIVE SUMMARY

Heavy metal pollution remains a matter of public concern despite significant mitigation efforts undertaken under the UNECE Convention on Long-range Transboundary Air Pollution (hereafter, CLRTAP or the Convention). Decline in pollution levels over the past two decades has resulted in reduced impact for both human health and biota. However, human health and ecosystems continue to be at risk in many UNECE countries [*Maas and Grennfelt*, 2016]. Heavy metals that are within the scope of the Convention include lead (Pb), cadmium (Cd) and mercury (Hg). Collection and analysis of variety of information related to heavy metal pollution and transboundary transport are performed by research centres of the Co-operative Programme for Monitoring and Evaluation of Long-range Transmission of Air Pollutants in Europe (EMEP).

This Status Report outlines recent activities of the EMEP Centres in the field of heavy metal pollution assessment performed in accordance with the workplan of the Convention for 2016-2017 [ECE/EB.AIR/133/Add.1]. The major topics presented in the report include assessment of heavy metal pollution in the EMEP region based both on monitoring and modelling, further development and improvement of the modelling approaches associated with transition to the new EMEP grid, co-operation with national experts in the framework of case studies on heavy metal pollution in selected EMEP countries, and collaboration with other Bodies to the Convention, international organisations and programmes.

Model assessment of heavy metal pollution levels in the EMEP domain for 2015 was carried out using gridded emission data on lead, cadmium and mercury provided by CEIP. The total values of anthropogenic heavy metal emissions in the EMEP countries for 2015 are lower than the corresponding values for 2014 in previous submission and amount to 3704 tonnes for lead, 200 tonnes for cadmium and 142 tonnes for mercury. Detailed information on heavy metal emissions in each country, as well as the gap-filling methods that have been used for the 2015 Gridding Nomenclature for Reporting (GNFR) inventory can be found in the CEIP Technical Report 01/2017 [*Tista et al*., 2017]. Auxiliary information on emissions height distribution and chemical speciation of mercury emissions was prepared by MSC-E based on expert estimates. Besides, a global inventory of mercury anthropogenic emissions [*AMAP/UNEP*, 2013] was used for mercury simulations on a global scale and evaluation of boundary conditions for regional modelling.

Measurements of lead and cadmium in the EMEP region in 2014 were carried out at 66 sites, and mercury – at 28 sites. In total, 22 Parties to the Convention report heavy metal data to EMEP, 8 of these fulfil their monitoring obligations as defined in the EMEP monitoring strategy [*UNECE*, 2009] with at least one level 2 site with both air and precipitation measurements of heavy meals and mercury in air and precipitation. The lowest concentrations for all elements were generally found in northern Scandinavia, and the highest ones were noted for central and south-eastern Europe. It should be noted that some of the high concentrations are due to too high detection limit of the method applied, i.e. Cd in aerosols in Portugal, and Hg in precipitation in Portugal and Ireland. The EBAS database [http://ebas.nilu.no], which hosts data from EMEP, GAW, AMAP, CAMP, HELCOM, ACTRIS and more, has been improved this year to include additional metadata and information on quality assurance. A more detailed information about the sites and the measurement methods are found in the EMEP/CCC data report for 2015 [*Aas and Nizzetto*, 2017].

Lead, cadmium and mercury pollution levels in the EMEP region were assessed for 2015. The highest pollution levels of these heavy metals took place in the central part of Europe (Poland, northern Italy, western and south-western Germany). The lowest levels were noted for the northern part of Scandinavia and the Russian Arctic. Heavy metal deposition in the EMEP region was formed by EMEP anthropogenic, EMEP secondary and non-EMEP sources. Secondary sources made the largest contribution to lead and cadmium deposition that exceeded half of total deposition in 45 countries for lead and in 29 counties for cadmium. EMEP anthropogenic sources contributed from 25% to 50%, and non-EMEP sources – less than 15% to deposition in most of countries. In case of mercury non-EMEP sources contributed more than 50% of total deposition in majority of the EMEP countries. Contribution of transboundary deposition of lead, cadmium, and mercury exceeded the deposition caused by national anthropogenic sources in 39, 42, and 33 countries, respectively. In most of the EMEP countries 60-90% of emitted heavy metals were transported beyond the national borders.

The major direction of further development of the Global EMEP Multi-media Modelling System (GLEMOS) during the past year was related to transition of the EMEP operational modelling to the new EMEP grid. The work started a few years ago was continued with adaptation and testing of pollutant-specific modules for new contaminants (particle-bound heavy metals and a selected persistent organic pollutant) as well as preparation of additional input data. Besides, the GLEMOS modelling system underwent considerable structural revision aimed to prepare it for public distribution as open-source software. Pilot simulations of lead and cadmium pollution performed with GLEMOS on the new EMEP grid demonstrate good succession between the old and new model versions for assessment of transboundary transport between the EMEP countries and ecosystem-specific deposition. However, evaluation of wind re-suspension of heavy metals requires further refinement including estimates of long-term accumulation of the pollutants in topsoil. Besides, anthropogenic emission data with fine spatial resolution is needed for improvement of the model performance for simulations on the new grid. In addition, model study of mercury chemistry and other processes in the atmosphere was finished and main conclusions were formulated to direct further model development. All results of the study were published in a series of peer-reviewed papers [*Travnikov et al.*, 2017; *Bieser et al.,* 2017; *Angot et al*., 2016].

Co-operation with Parties to the Convention in the framework of the country-specific case studies of heavy metal pollution with fine spatial resolution was continued. The first phase of the country-specific study for Poland has been complete this year. In this phase, a variety of input information (emissions, measurements, meteorological data etc.) were collected, model simulations of the country pollution by cadmium were performed and analysed. Further analysis of the transition to the new EMEP grid on a country scale showed improvement of the model performance at background regional stations in Poland and neighbouring areas. It was also shown that heavy metal emissions from some source categories (e.g. residential combustion) could have significant uncertainties and needed further refinement. Besides, the need to revise emissions data for Eastern Europe was demonstrated to improve quality of the model assessment. The study for Poland will be continued including further analysis of pollution levels over the whole territory and selected cities of the country.

MSC-E also collaborated with national experts from Italy and Russia supporting their activities on heavy metal assessment. In particular, the Centre provided ENEA (Italy) with calculated air concentrations of lead, cadmium, mercury and the second priority metals (arsenic, nickel, chromium,

copper, zinc and selenium) required for determining boundary conditions of the national model domain. The Centre also collaborated with experts from Russia performing initial analysis of measurements from the national monitoring network for heavy metals. The observations were compared with modelling results to evaluate uncertainties of measurements, national emission data and secondary emissions.

Another important aspect of MSC-E activities is collaboration with subsidiary bodies to the Convention and other international organisations. All results of the research and development were presented and discussed at the EMEP Task Force on Measurements and Modelling (TFMM). In particular, the progress in transition of the GLEMOS modelling system to the new EMEP grid was reported and pilot results of model simulations of heavy metal pollution on a country scale for Poland were presented. Important topics of pollution assessment were suggested for discussion at future meetings of the Task Force: (1) modelling of wind suspension of mineral dust and harmonization of land-cover data within the Convention and (2) peculiarities of evaluation of "grid cell-averaged" modelled pollution levels against "point" values of measurements at monitoring sites.

MSC-E also continues co-operation with the Working Group on Effects (WGE). Ecosystem-specific deposition of lead, cadmium and mercury is calculated annually for the EMEP region and individual EMEP countries to support work of the effect community. All variety of information is available at the MSC-E website [www.msceast.org]. This year MSC-E has also started a new joint activity with the Coordination Centre for Effects focused on evaluation of critical loads exceedances for mercury on a hemispheric scale. For this purpose, MSC-E performed modelling of mercury deposition to forests and (semi-)natural vegetation in the boreal and temperate region of the Northern Hemisphere under the current conditions (2010) and in future (2035).

EMEP closely collaborates with the United Nations Environment Programme (UN Environment). A new Global Mercury Assessment 2018 is now under development in accordance with the request of the UN Environment Governing Council (Decision 27/12). MSC-E takes part in the assessment coordinating work of an international group of experts focused on modelling of mercury pollution on global and regional scales. Besides, in cooperation with other EMEP Centres, MSC-E performs regular model assessment of atmospheric pollution of the Baltic Sea by various pollutants including heavy metals. This work is carried out in accordance with the Memorandum of Understanding between CLRTAP and the Baltic Marine Environment Protection Commission (HELCOM).

Future directions of MSC-E activities will be aimed at further improvement of heavy metal pollution assessment in the EMEP region. Further development and evaluation of the Global EMEP Multi-media Modelling System (GLEMOS) will include additional testing of the model performance and refinement of wind re-suspension of heavy metals on the new EMEP grid, and analysis of the key factors affecting mercury accumulation in and exchange between the environmental media. Country-specific case studies will be continued for a number of countries (Poland, the United Kingdom, Russia) using detailed national emission and monitoring data and in close cooperation with national experts. Finally, MSC-E will continue co-operation with subsidiary bodies of the Convention (WGE, TFMM, TF HTAP), international organizations (UN Environment, AMAP, HELCOM etc.) and national experts. These directions of future research and development are reflected in MSC-E proposals for the EMEP workplan for 2018-2019 and the updated Mandate of the Centre.

# INTRODUCTION

Heavy metal pollution remains a matter of public concern despite significant mitigation efforts undertaken under the UNECE Convention on Long-range Transboundary Air Pollution (hereafter, CLRTAP or the Convention). Decline in pollution levels over the past two decades has resulted in reduced impact for both human health and biota. However, human health and ecosystems continue to be at risk in many UNECE countries [*Maas and Grennfelt*, 2016]. Therefore, as it is stated in the report of the *ad hoc* policy review group [ECE/EB.AIR/WG.5/2017/3], the Convention is recommended to pursue mitigation activities as well as scientific and technical work on heavy metals within the UNECE region.

Heavy metals that are within the scope of the Convention include lead (Pb), cadmium (Cd) and mercury (Hg). Collection and analysis of variety of information related to heavy metal pollution and transboundary transport are performed by research centres of the Co-operative Programme for Monitoring and Evaluation of Long-range Transmission of Air Pollutants in Europe (EMEP). These are the Centre of Emission Inventories and Projections (CEIP), the Chemical Coordinating Centre (CCC), the Meteorological Synthesizing Centre – East (MSC-E) and the Centre for Integrated Assessment Modelling (CIAM). More detailed information on the EMEP structure and operational activities of the research centres is available at the EMEP website [www.emep.int].

This Status Report outlines recent activities of the EMEP Centres in the field of heavy metal pollution assessment performed in accordance with the workplan of the Convention for 2016-2017 [ECE/EB.AIR/133/Add.1]. The major topics presented in the report include assessment of heavy metal pollution in the EMEP region based both on monitoring and modelling, further development and improvement of the modelling approaches associated with transition to the new EMEP grid, co-operation with national experts in the framework of case studies on heavy metal pollution in selected EMEP countries, and collaboration with other Bodies to the Convention, international organisations and programmes.

Assessment of heavy metal pollution of the EMEP region covers various aspects relating to emissions reporting, monitoring and modelling activities (*Chapter 1*). Gridded emission data on lead, cadmium and mercury is prepared by CEIP based on reported data and expert estimates. Annual results of measurements of lead, cadmium and mercury concentration in air and precipitation at the EMEP monitoring network are reported by CCC along with brief analysis of data quality. This is important information both for characterizing pollution levels and evaluation of modelling results. Model assessment performed by MSC-E consists of evaluation of current pollution levels of heavy metals in the EMEP region. In particular, it includes model calculations of concentration and deposition fields and transboundary fluxes of lead, cadmium and mercury in 2015 as well as analysis of pollution changes between the two successive years (2014 and 2015). In addition, information on heavy metal pollution of the Arctic sector of the EMEP region is also presented to facilitate cooperation between the Convention and the Arctic Monitoring and Assessment Program (AMAP).

The major direction of further development of the Global EMEP Multi-media Modelling System (GLEMOS) during the past year was related to transition of the EMEP operational modelling to the new EMEP grid (*Chapter 2*). The work started a few years ago was continued with adaptation and

testing of pollutant-specific modules for new contaminants (particle-bound heavy metals and a selected persistent organic pollutant) as well as preparation of additional input data. Besides, the GLEMOS modelling system underwent considerable structural revision aimed to prepare it for public distribution as open-source software. Pilot simulations on the new grid were performed for lead and cadmium and included analysis of spatial patterns, source-receptor relationships, and ecosystem-specific deposition fluxes as well as evaluation of model performance against measurements. In addition, model study of mercury chemistry and other processes in the atmosphere was finished and main conclusions were formulated to direct further model development.

MSC-E continued co-operation with Parties to the Convention in the framework of case studies of heavy metal pollution on a scale of individual countries. The first phase of the country-specific study for Poland has been complete this year (*Chapter 3*). In this phase, a variety of input information (emissions, measurements, meteorological data etc.) were collected, model simulations of the country pollution by cadmium were performed and analysed, and main directions for the next phase of the study were formulated. Particular attention was paid to testing the model performance in modelling with fine spatial resolution on a country scale and analysis of factors affecting pollution levels in the country. The study for Poland will be continued including further analysis of pollution levels over the whole territory and selected cities of the country. In addition, MSC-E co-operated with national experts from Italy and Russia supporting their activities on heavy metal assessment and development national monitoring network, respectively (*Section 4.1*).

Another important aspect of MSC-E activities is collaboration with subsidiary bodies to the Convention and other international organisations (*Chapter 4*). All results of the research and development were presented and discussed at the EMEP Task Force on Measurements and Modelling (TFMM). Besides, information on ecosystem-specific deposition of mercury was provided to the Working Group on Effects (WGE) for evaluation of critical load exceedances on a hemispheric scale. Moreover, the Centre worked in close co-operation with other international organizations and programmes (the United Nations Environmental Programme, the Arctic Monitoring and Assessment Programme, Helsinki Commission etc.) to broaden dissemination of the scientific and policy oriented information generated within EMEP.

Detailed information on heavy metal pollution levels in the EMEP region and in individual countries as well as transboundary transport are presented at the MSC-E website [www.msceast.org]. Additionally, information on heavy metal pollution in the countries of Eastern Europe, Caucasus and Central Asia (EECCA) is given in Russian [www.ru.msceast.org]. Significant efforts were undertaken by the Centre during the past year to improve accessibility and visibility of assessment results at the website. For this purpose, the internal database and visualization mechanisms were considerably revised.

# 1. HEAVY METAL POLLUTION OF THE EMEP REGION

## 1.1. Emission data for model assessment

Model assessment of heavy metal pollution levels in the EMEP domain for 2015 was carried out using gridded emission data on lead, cadmium and mercury provided by CEIP. Detailed information on heavy metal emissions in each country, as well as the gap-filling methods that have been used for the 2015 GNFR inventory can be found in the CEIP Technical Report 01/2017 [*Tista et al*., 2017]. Information on emission distribution with height is important for modelling of atmospheric transport of heavy metals. In order to estimate distribution of emissions with height MSC-E utilized sector-split emission information provided by the EMEP countries. Height distributions for different emission sectors were averaged taking into account a sector contribution to the total emission. It was assumed that heavy metal emission was distributed between three lowest model layers (0-70 m; 70-150 m and 150-300 m). Mercury is emitted to the atmosphere in elemental, gaseous oxidized and particulate forms. Atmospheric behaviour of mercury strongly depends on its form. The speciation of mercury emissions is not included in the information reported by the Parties to the Convention. Therefore, expert estimates of mercury emission speciation have been used by MSC-E. For calculations of mercury levels speciation of mercury emissions derived from global emission dataset [*AMAP/UNEP*, 2013] was applied.

The total values of anthropogenic heavy metal emissions in the EMEP countries for 2015 are lower than the corresponding values for 2014 in previous submission and amount to 3704 tonnes for lead, 200 tonnes for cadmium and 142 tonnes for mercury. The value of lead emissions is about 41 tonnes lower in comparison to the lead emissions used for model calculation for 2014. The total emissions of cadmium and mercury have decreased in comparison with the previous year by 4 tonnes and 25 tonnes, respectively.

The changes of lead, cadmium and mercury emissions in each country are expressed as $100*(E_{2015} - E_{2014})/E_{2014}$ (%), where $E_{2014}$ and $E_{2015}$ are previous and current emissions in 2017 Submission and 2017 Submission, respectively. The changes are illustrated in Fig. 1.1. Negative values indicate a decrease of emissions, while positive values illustrate an increase of emissions from 2014 to 2015.

Emissions in Belarus, Bosnia and Herzegovina, the Czech Republic, Estonia, France, Greece, Ireland, Malta, Monaco, Sweden and Switzerland decreased compared to the emission values of all three metals for 2014. The increase of the heavy metal emission values was noted for Albania, Azerbaijan, Hungary, Liechtenstein, Lithuania, Luxembourg, Montenegro, Portugal and Serbia.

In Bulgaria, Malta and Monaco emissions of lead have decreased over 2.5, 6.5 and 3 times, respectively (Fig. 1.1a). Emissions of cadmium in Kazakhstan and Monaco have decreased over 2 and 4.5 times, respectively (Fig. 1.1b). In Lithuania, mercury emissions have increased almost 3.5 times (Fig. 1.1c). Heavy metal emissions in Iceland have significantly changed compared to the previous year. For example, lead emissions increased more than 9 times (Fig. 1.1a). This is due to the fact that Iceland submitted national data for the first time. Spatial distributions of lead, cadmium and mercury emissions used in the modelling are shown in Fig. 1.2.

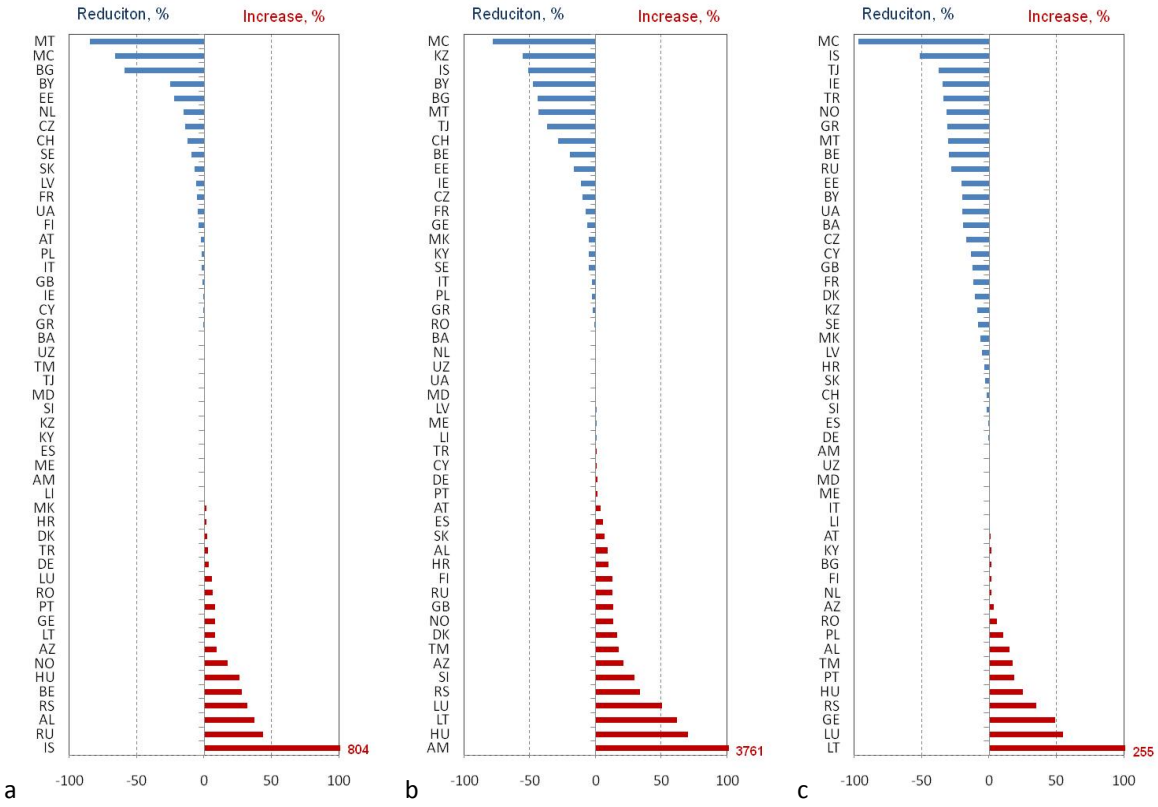


***Fig. 1.1.*** *Relative changes of annual total emissions of lead (a), cadmium (b) and mercury (c) between 2014 and 2015, %*

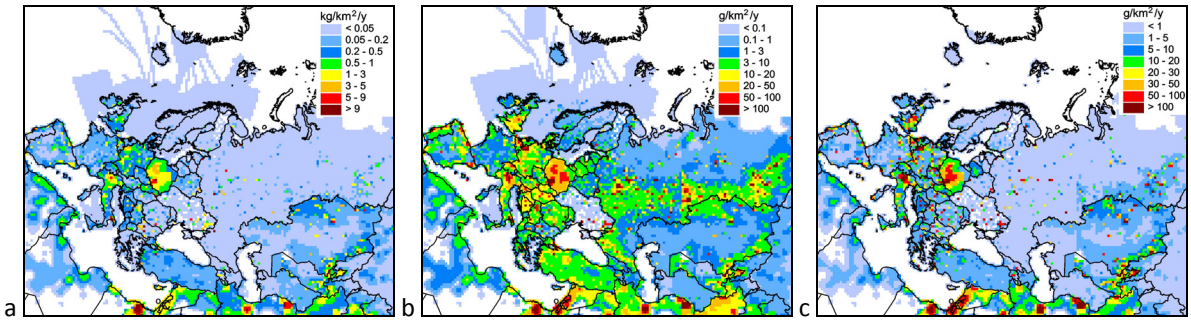


***Fig. 1.2.*** *Spatial distribution of lead (a), cadmium (b)and mercury (c) anthropogenic emissions over the EMEP domain in 2015*

Due to long atmospheric residence time mercury is dispersed over global scale. Therefore, assessment of mercury pollution in the EMEP countries requires data on mercury anthropogenic emissions on a global scale. The global inventory of mercury anthropogenic emissions for 2010 was used for mercury simulations on he global scale and evaluation of boundary conditions for regional modelling. A new updated emissions inventory has been developed as a part of the UNEP Global Mercury Assessment 2013 [*AMAP/UNEP*, 2013].

## 1.2. EMEP monitoring network of heavy metals

### *Measurement network*

In 2015, there were 34 sites measuring heavy metals (cadmium or lead) in both aerosols and precipitation, and altogether there were 66 measurement sites. 28 sites were measuring mercury in either air and precipitation, 12 of these with concurrent measurements in air and precipitation. In total, 22 Parties to the Convention report heavy metal data to EMEP, 8 of these fulfil their monitoring obligations as defined in the EMEP monitoring strategy [*UNECE*, 2009] with at least one level 2 site with both air and precipitation measurements of heavy meals and mercury in air and precipitation. A number of countries have been reporting heavy metals within the EMEP area in connection with different national and international programmers such as HELCOM, AMAP and OSPAR. Detailed information about the sites and the measurement methods are found in EMEP/CCC's data report on heavy metals and POPs [*Aas and Nizzetto*, 2017].

### *Observed concentration level of Pb, Cd and Hg in 2015*

Annual averages of Pb, Cd and Hg concentrations in precipitation and in air in 2015 are presented in Fig. 1.3-1.8. The lowest concentrations for all elements are generally found in Scandinavia, and the highest in Central and Eastern Europe. Some of the high concentrations are due to too high detection limit of the method, i.e. Cd in aerosols in Portugal, and Hg in precipitation in Portugal and Ireland.

For lead, the highest concentration in aerosols is observed in Hungary followed by sites in Poland, Belgium and Netherlands. In precipitation, the highest volume weighted annual means are observed in Slovakia and Denmark.

For cadmium, the highest concentration in aerosols is at the northern Finnish site followed by sites in Hungary and Latvia, if not considering the Portuguese site with high detection limit. The Finnish site is probably influenced by high emissions from the smelters at the Kola Peninsula in Russia. In precipitation, the highest level is seen at the Italian site, which is situated not very far outside Rome.

For total gaseous and elemental mercury it is somewhat strange regional pattern with highest concentration in Greenland (DK10) and lowest in Slovenia. There are several months missing for DK10, and for Slovenia there has been some instrumental problem, so these observations should be used with care. In precipitation, the highest levels are seen in Estonia and Latvia, if excluding the sites with high detection limits.

A more detailed discussion of temporal and spatial resolution of heavy metals in Europe is found in *Tørseth et al*. [2012] and in the EMEP/CCC data report for 2015 [*Aas and Nizzetto*, 2017].

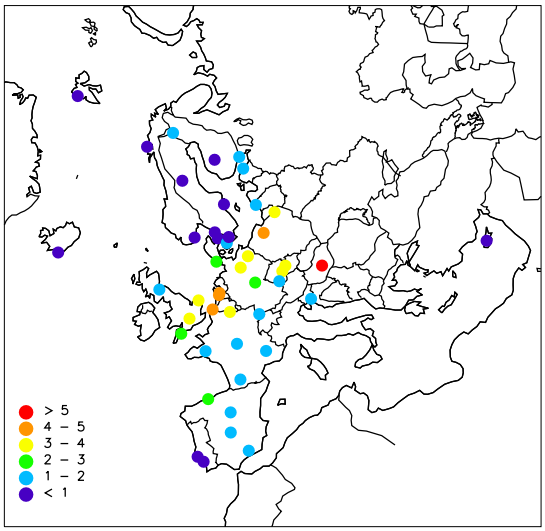


***Fig. 1.3.*** *Pb in aerosol, ng/m$^3$*

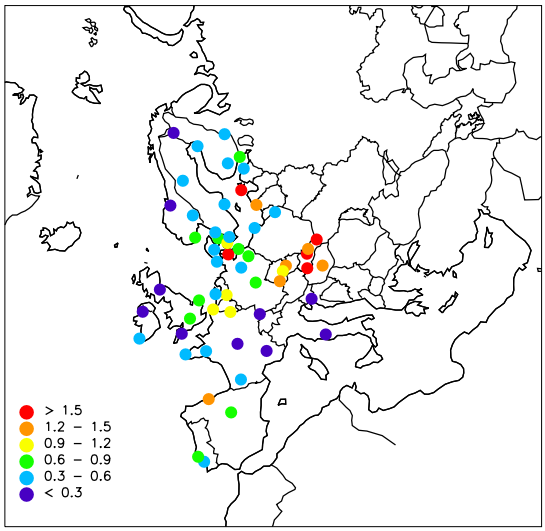


***Fig. 1.4.*** *Pb in precipitation, μg/L*

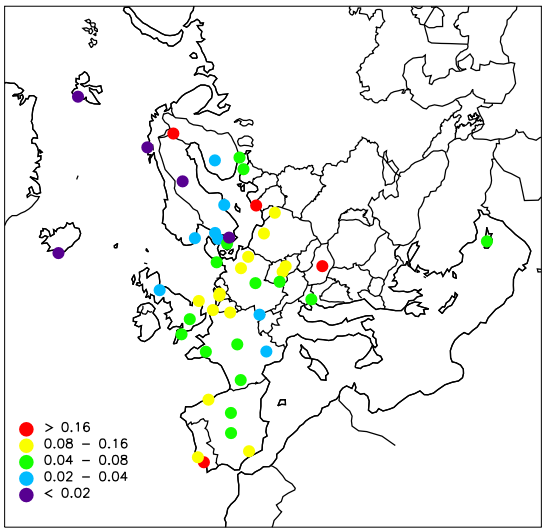


***Fig. 1.5****. Cd in aerosol, ng/m$^3$*

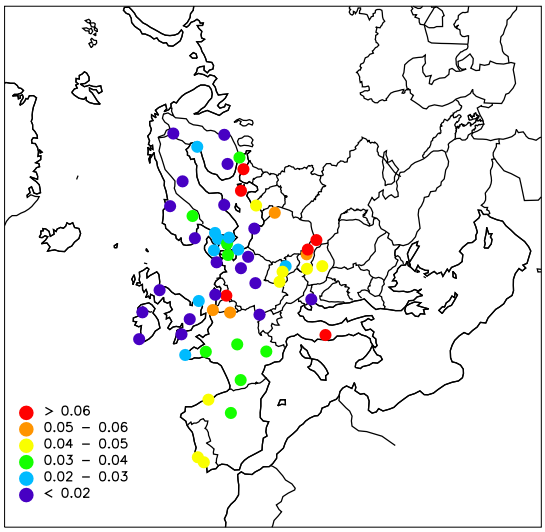


***Fig. 1.6.*** *Cd in precipitation, μg/L*

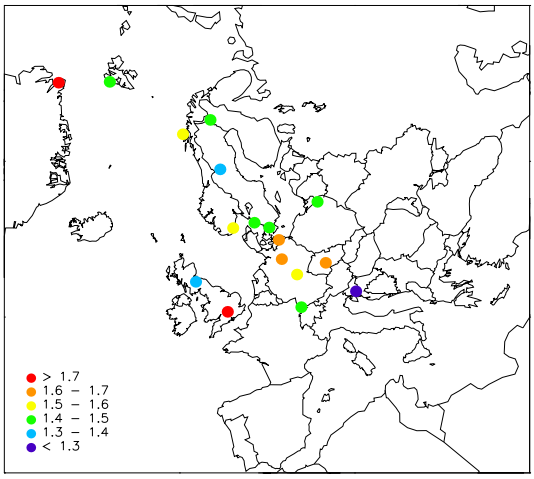


***Fig. 1.7****. Hg (g) in air, ng/m$^3$*

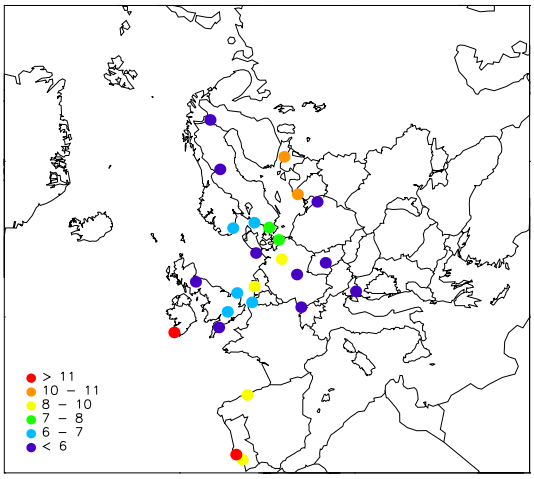


***Fig. 1.8.*** *Hg in precipitation, ng/L*

### *New reporting guidelines and standard operating procedures (SOP)*

An important measure to help support interpretation of monitoring data, is to strengthen efforts to document methodologies and data quality across EMEP sites. The EBAS database [http://ebas.nilu.no], which host data from EMEP, GAW, AMAP, CAMP, HELCOM, ACTRIS and more, has been improved to include additional metadata and information on quality assurance. To discuss these new possibilities and the increasing need for documenting the data quality, EMEP/CCC arranged a workshop in October 2016, and new reporting guidelines were agreed upon. Especially for mercury, there has been a strong need to come up with new templates, with more stringent possibilities for reporting, and to include more information of data quality and methodology. The main items which have been improved:

- ***Component name.*** *In EBAS, the component names used for different forms of mercury were not consistent, and it has been difficult to know what has actually been measured. In the new templates, there are now defined these different options:*

| Component name | Shortname | matrix | unit |
|---|---|---|---|
| total_gaseous_mercury | TGM | air | ng/m$^3$ |
| gaseous_elemental_mercury | GEM | air | ng/m$^3$ |
| gaseous_oxidised_mercury | GOM,RGM | air | pg/m$^3$ |
| Mercury | | air+aerosol | ng/m$^3$ |
| Mercury | | precipitation | ng/L |
| Mercury | PBM | aerosol,$PM_{10}$,$PM_{25}$ | pg/m$^3$ |

- ***Additional metadata.*** The data provider should now also include descriptions of the inlet (if heated and soda lime trap), maintenance information, and which standard pressure and temperature have been used for conversion.
- ***QA measure.*** This can be an on-site or off-site intercomparison, round-robin or an on-site audit. In previous years, this information was only stored separately from the database, but this information can and should now be included together with the relevant data series, and thus will also be exported to those using the data.
- ***Methodology and Standard Operating Procedures (SOPs).*** SOPs for online monitor measurements of mercury and for measurements in precipitation have recently been developed by the Global Mercury Observation System (GMOS). These SOPs are also recommended for the EMEP network, and the manuals are made available from the data submission portal [http://ebas-submit.nilu.no/Standard-Operating-Procedures].

The reporting templates and instruction on how to submit data are found at the http://ebas-submit.nilu.no. CCC has developed the submission tool [http://ebas-submit-tool.nilu.no], which the data submitters should use to check their files, and the files should be submitted via submission tool unless a special agreement is mutually agreed upon.

## 1.3. Pollution levels and transboundary fluxes in 2015

Lead, cadmium and mercury air concentrations, total deposition and transboundary fluxes calculated for 2015 are described in this section. Special attention is paid to the analysis of changes of pollution levels in the EMEP region between 2014 and 2015. Evaluation of modelling results against observed data is available in Annex A.

### *Heavy metal pollution levels in 2015*

Model-based information about heavy metal pollution levels and transboundary transport in 2015 is allocated in the internet (www.msceast.org). The modelling results are based on emission data for 2015, prepared by CEIP (see section 1.1) and meteorological data of European Centre for Medium-Range Weather Forecasts (ECMWF) [*ECMWF*, 2017]. This section overviews the main peculiarities of concentrations, deposition and source-receptor relationships of lead, cadmium and mercury in the EMEP region.

Heavy metal pollution levels in the EMEP countries are caused by three groups of emission sources. They include anthropogenic emissions of considered year, wind re-suspension of dust particles containing heavy metals originated from natural sources and historical deposition, and from sources located outside the EMEP region (so-called non-EMEP sources). Contribution of these three groups of sources is calculated for each EMEP country on regular basis.

Residence time of atmospheric mercury is very long (around 0.5 – 1 year), so it can be transported over global scale. In order to take into account contribution of non-EMEP mercury emission sources, global-scale modelling of mercury levels in 2015 is carried out. Mercury air concentrations simulated over the globe (Fig. 1.9) are used as boundary conditions for regional-scale modelling over the EMEP domain.

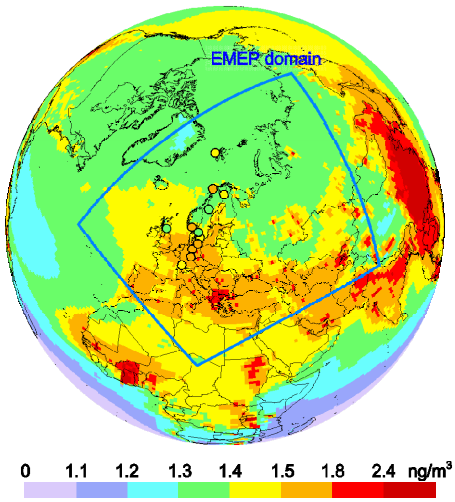


***Fig. 1.9.*** *Global distribution of $Hg^0$ concentration in 2015. Blue line depicts the boundary of the EMEP domain. Circles show EMEP measurements in the same color palette*

Annual mean air concentrations and annual total deposition fluxes of lead, cadmium and mercury are distributed over the EMEP region highly non-uniformly. Countries in the central part of Europe are characterized by the highest pollution levels. In southern Poland, northern Italy, western and south-western Germany air concentrations of lead vary from 5 to 30 ng/m$^3$, and deposition fluxes – from 1.5 to 4 kg/km$^2$/y (Fig. 1.10). Cadmium concentrations in these regions lie within 0.1 – 1 ng/m$^3$, and deposition fluxes – within 30-150 g/km$^2$/y range. Relatively high cadmium concentrations in 2015 are

noted for Russia (the central regions of European part, south-western part and southern regions of Siberia) and for the eastern part of Ukraine.

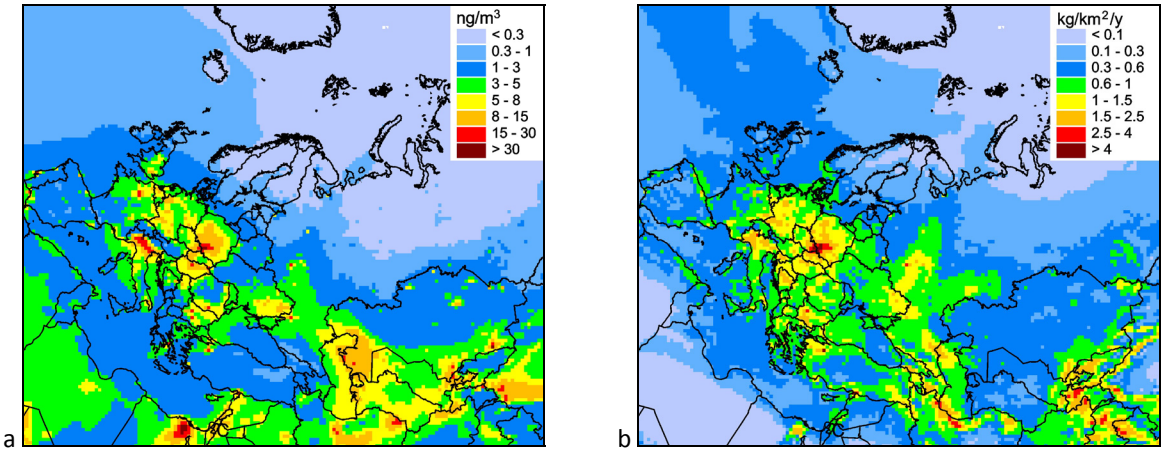


***Fig. 1.10.*** *Mean annual air concentrations (a) and total deposition (b) of lead in 2015*

Main factor responsible for air concentrations of total gaseous mercury in the EMEP region is intercontinental transport from emission sources located outside the EMEP countries. This peculiarity allows to explain why mercury concentrations in air are distributed much smoother over the EMEP region compared to concentrations of lead and cadmium. Over most part of the EMEP region the concentrations vary from 1.4 to 1.6 ng/m$^3$. Relatively high concentrations of mercury (1.6-2 ng/m$^3$) occur in the southern part of the EMEP domain and in the Mediterranean region, which is caused by the influence of natural emission from mercury geochemical belt. Besides, similar levels take place in regions with significant anthropogenic emissions (western Germany, Poland, northern Italy, Moscow region in Russia). Southern Poland, western part of Germany, northern Italy and the Balkan countries are characterized by relativity high deposition fluxes of mercury (17-40 g/km$^2$/y). Somewhat elevated fluxes (10-17 g/km$^2$/y) are also noted in some regions of the Arctic, which is explained by the effect of mercury depletion events. Nevertheless, the Arctic as a whole and desert areas of Central Asia are characterized by the lowest deposition of mercury (below 5 g/km$^2$/y).

Country-mean deposition fluxes from anthropogenic, secondary and non-EMEP sources of lead, cadmium and mercury in 2015 are calculated for each EMEP country. For example, the fluxes of lead to the EMEP countries vary from 1.6 to 0.2 kg/km$^2$/y (Fig. 1.11). The highest country-mean fluxes are noted for central Europe (Slovakia, Poland, the Czech Republic), and the lowest – in Scandinavian countries (Finland, Iceland, Norway, Sweden). Main contribution in 2015 to deposition is made by secondary sources. In 45 countries (of total 51) this contribution exceeds 50%, while the contribution of anthropogenic sources to deposition in most of countries ranges from 25% to 50%. Contribution of secondary sources to cadmium deposition is smaller than that for lead, but also considerable. In exceeds 50% in 29 countries. The role of non-EMEP sources is relatively low. In most of countries these sources contribute less than 15% of total deposition of lead and cadmium. In few countries located close to borders of the EMEP region (Kyrgyzstan, Turkmenistan, Tajikistan, Uzbekistan, Cyprus, Armenia) it exceeds 25%.

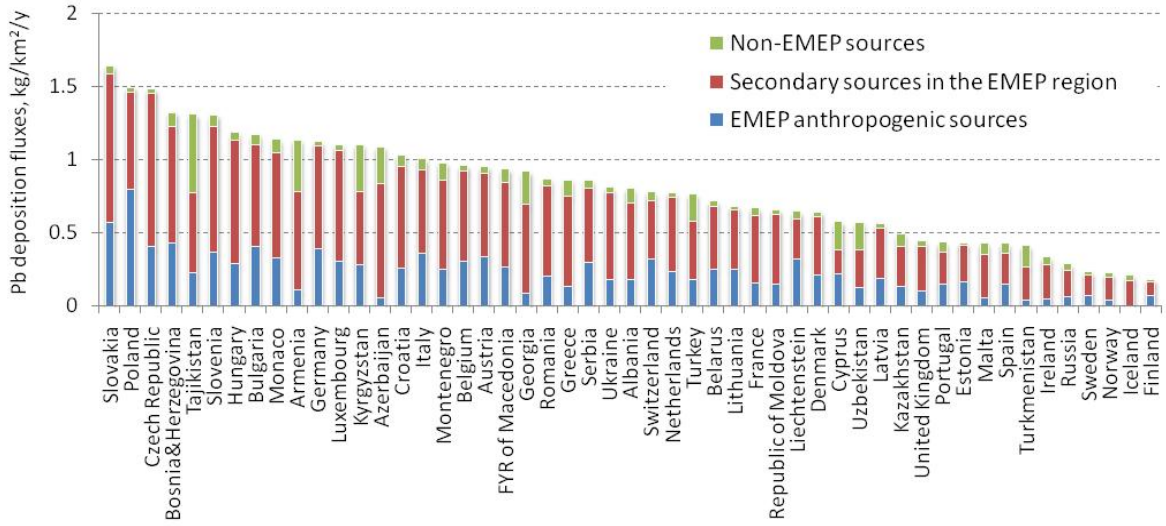


***Fig. 1.11.*** *Country-averaged deposition fluxes of lead from the European and Central Asian anthropogenic, secondary and non-EMEP emission sources in 2015*

In case of mercury the contributions of EMEP anthropogenic, secondary and non-EMEP sources to deposition in countries differ markedly from those of lead and cadmium. The main role in origin of mercury deposition in the EMEP countries belongs to intercontinental transport. The contribution of non-EMEP sources exceeds 50% in majority of countries. EMEP anthropogenic sources contribute from 1% in Iceland to almost 60% in FYR Macedonia. In 20 countries the contribution of EMEP anthropogenic sources varies from 25% to 50%. The role of secondary sources (re-emission of elemental mercury) does not exceed 1% of country-averaged deposition.

### *Transboundary transport in 2015*

Protocol on heavy metals is aimed at reduction of heavy metal pollution and targets anthropogenic emissions of lead, cadmium and mercury. Heavy metals, emitted by countries, are partly deposited within country's territories and partly transported outside country's borders. Therefore, deposition coming from EMEP anthropogenic sources is split in two parts: deposition from national sources and deposition caused by transboundary transport. Relative importance of these two components depends on a number of factors such as emission values in a country and in neighbouring courtiers, size of a country, peculiarities of meteorological conditions such as prevailing wind patterns or precipitation regime.

Information on deposition from national and foreign sources is calculated for each EMEP country. It is available in the Interment at website of MSC-E [www.msceast.org]. For example, contribution of transboundary transport to deposition of cadmium from anthropogenic sources in 2015 varies from 99% (Monaco) to 9% (Russia) (Fig. 1.12). In most of countries deposition from foreign sources exceed deposition from national sources. In 42 countries contribution of foreign sources to anthropogenic cadmium deposition exceeds 50%, and in 25 countries it exceeds 75%. For lead deposition the corresponding numbers are 39 and 23 countries, and for mercury – 33 and 18 countries. As a rule,

predominant contribution of foreign sources to deposition is noted for countries with relatively small territories (e.g., Monaco, Malta), low national emissions (e.g., Sweden, Turkmenistan, Ukraine) and located close to countries with relatively high national emissions (e.g., Slovakia bordering Poland). Relatively low contribution of foreign emission sources takes place in countries with large territory and significant national emissions (e.g., Russia, Poland, Germany). It is important to note that contribution of transboundary transport to deposition vary considerably over country's territory. Detailed information about spatial distribution of deposition from national and foreign sources in each EMEP country in 2015 is available in the Internet [www.msceast.org].

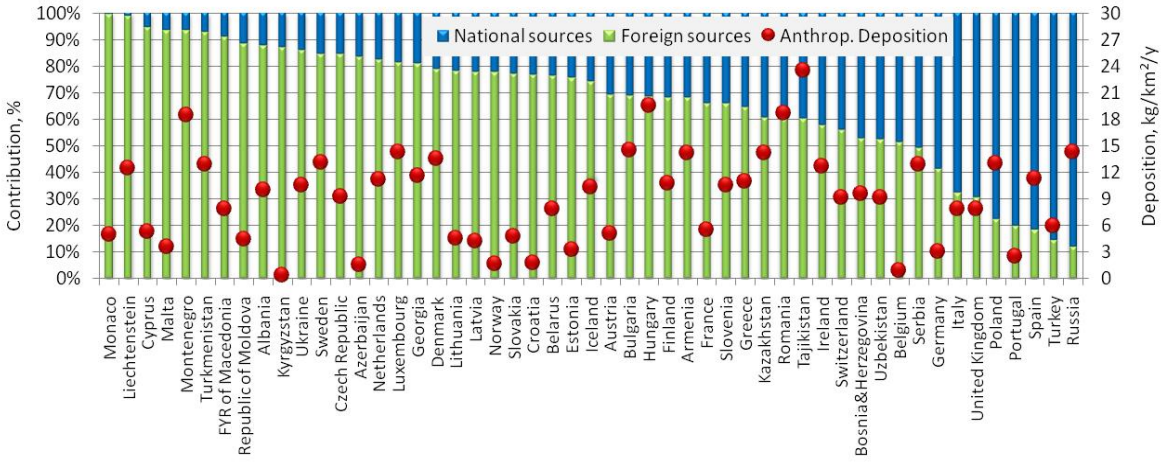


***Fig. 1.12.*** *Relative contribution of the transboundary transport and national sources to anthropogenic cadmium deposition in the European and the Central Asian countries and deposition values from anthropogenic emission sources in 2015*

Mass of heavy metals, emitted by sources of a country, can be partly deposit to the country's territory, to territories of other EMEP countries or leave the EMEP region and enter intercontinental transport. Absolute values of country-mean lead deposition of these three components as well as relative fraction of emitted mass transported outside country's territory, are exemplified in Fig. 1.13. For example, lead emission of Kazakhstan amounts to 695 t. From this mass 266 tonnes are deposited within territory of the country, and the rest (429 tonnes, or 62% of emission) is involved into transboundary transport. As much as 272 tonnes deposit to other EMEP counties, while the remaining 157 tonnes enters global transport and falls out to territories outside the EMEP countries. In most of countries major part of emitted lead and cadmium (from 60% to 90%) leaves country's territory and become involved into transboundary transport. The exception is Russia. Due to vast territory most of emitted lead and cadmium falls out within national borders, while only around 20% is transported to other countries.

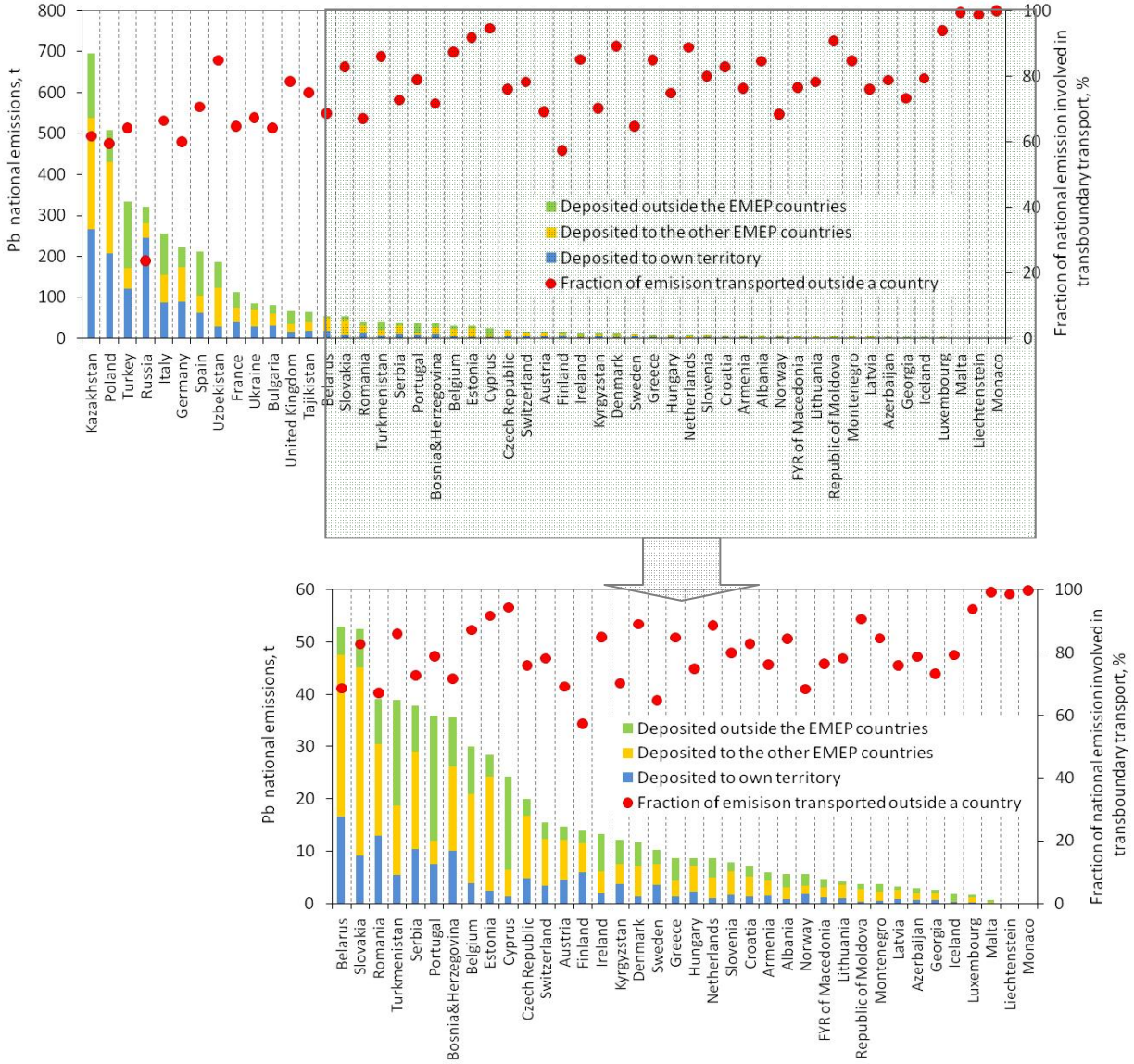


***Fig. 1.13****. Distribution of lead emitted in the EMEP countries between deposition to own territory, deposition to the other EMEP countries and deposition outside the EMEP countries in 2015. Red dots indicate relative fraction of national emissions involved into the transboundary pollution*

Attribution of mercury emission sources differs from that of lead and cadmium. Contribution of elemental form to total mercury emission in the ENEP countries ranges from 36% to 100%, and reaching around 70% on average. Thus, high fraction (80% - almost 100%) of emitted mercury is transported outside country's territory (Fig. 1.14).

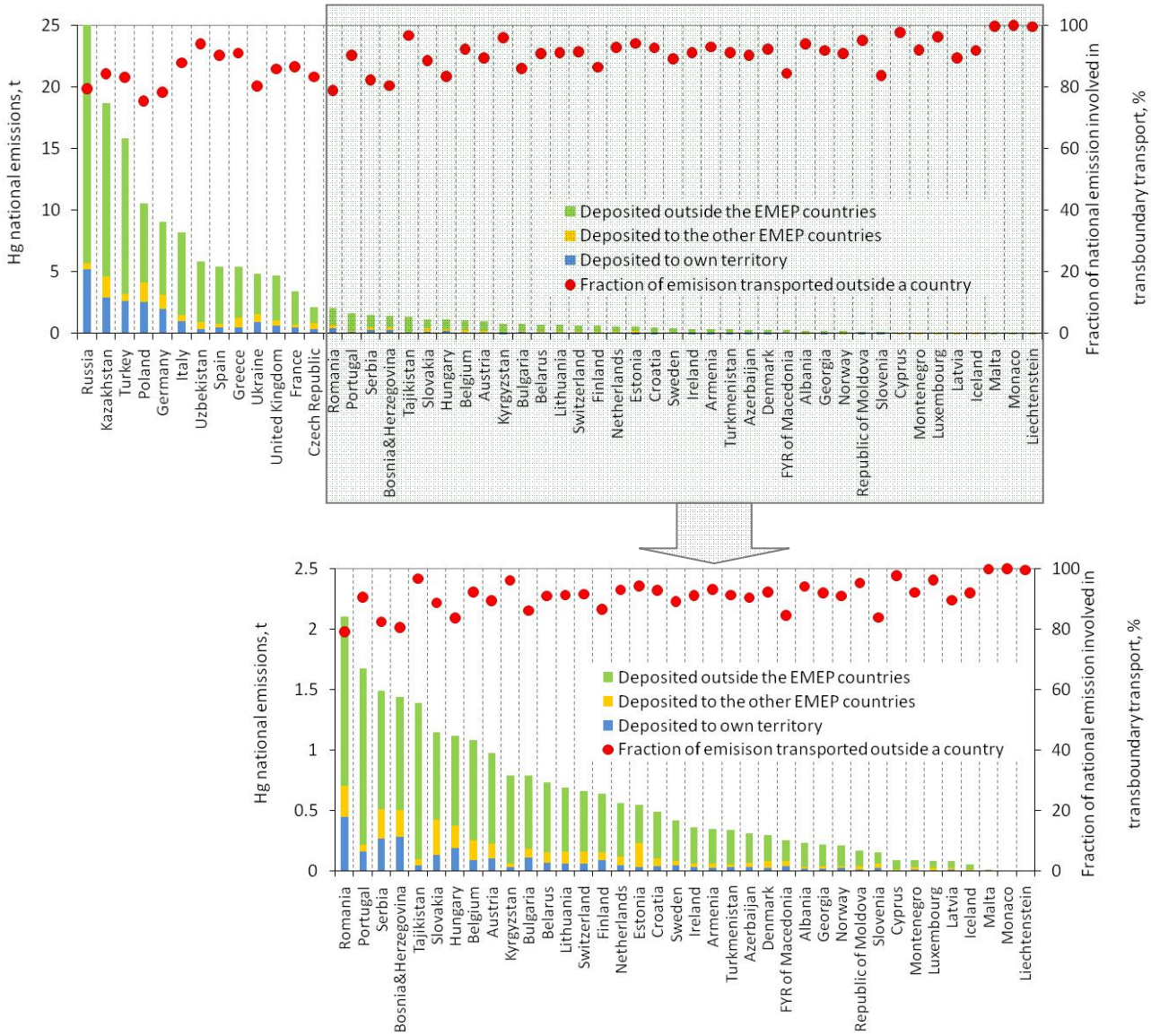


***Fig. 1.14****. Distribution of mercury emitted in the EMEP countries between deposition to own territory, deposition to the other EMEP countries and deposition outside the EMEP countries in 2015. Red dots indicate relative fraction of national emissions involved into the transboundary pollution*

### *Changes of pollution levels between 2014 and 2015*

Detailed information about lead, cadmium and mercury concentrations, deposition and transboundary fluxes in the EMEP countries is prepared annually. However, calculation results of the pollution levels for current year differ from those obtained for previous year. The differences can be caused by various reasons such as changes of reported emission data, modifications of the modelling tools, annual variability of meteorological conditions. Changes of meteorological conditions result to annual differences of wind re-suspension, which, in its turn, also induce changes of pollution levels. Comparison of meteorological conditions in 2015 with climatic mean values is overviewed in Annex B. This section is focused on analysis of changes between heavy metal pollution levels in 2015 with those calculated a year before for 2014.

Relative changes of total deposition of heavy metals in the EMEP countries between calculation results for 2014 and 2015 are calculated as difference between values for 2015 and 2014, divided by the value for 2014. Positive value of change means that deposition for 2015 is higher than the deposition for 2014, and vice versa. The changes ranged from -40% to +50% (Fig. 1.15).

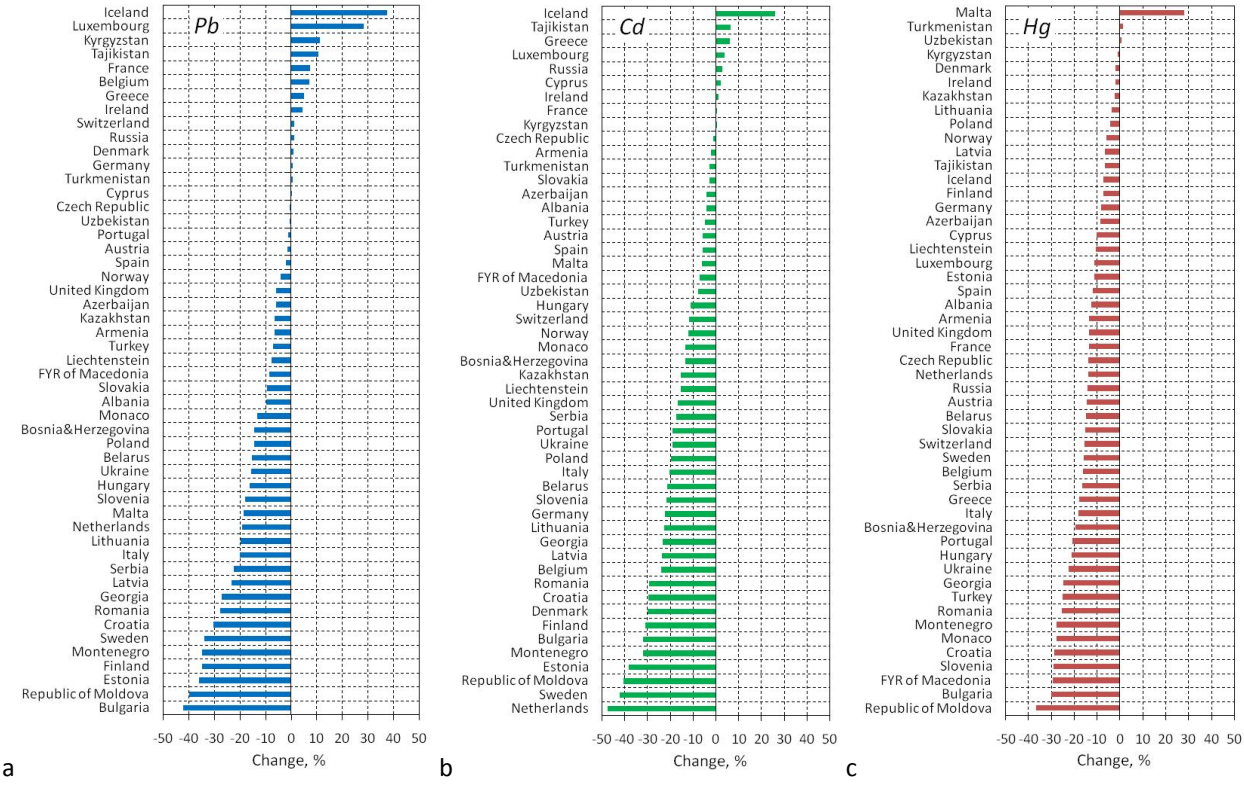


***Fig. 1.15.*** *Relative changes of lead (a), cadmium (b) and mercury (c) total deposition modelled for 2014 and for 2015*

Detailed analysis of factors which led to changes between modelling results is exemplified by deposition of lead. Most significant increase of lead deposition takes place in central regions of European part of Russia, southern regions of Russian Siberia, southern part of Balkan Peninsula (Greece) and northern coast of Norway, where relative changes exceed 50% (Fig. 1.16). Besides, marked changes (30-50%) also take place in northern France, southern Germany, south-western and central regions of Kazakhstan. Significant decline of modelled deposition takes place over vast territory including Baltic region, northern parts of Germany and Poland, north-west of Russia and Scandinavian Peninsula. The decline in this area ranges from -10% to -50%, and in some regions of Scandinavia it is even below -50%. Another vast region with similar magnitude of negative deposition change includes Italy and most part of the Balkan Peninsula. Significant relative changes, both positive and negative, also take place over the Russian Arctic, Greenland, and the Arctic Ocean. However, absolute changes in deposition in these regions are low compared to other considered areas (Fig. 1.16c).

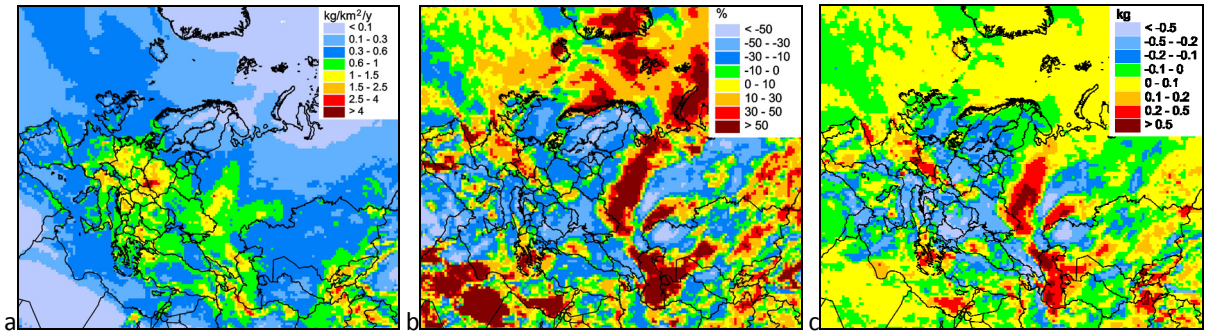


***Fig. 1.16.*** *Total deposition of lead in 2015 (a), relative (b) and absolute (c) changes of deposition modelled for 2015 and 2014*

Three factors, leading to deposition changes between calculations of 2014 and 2015, are considered: changes of anthropogenic emissions, meteorological conditions and wind re-suspension. In order to single out the effects of different factors a number of additional model calculations were carried out. The results of these calculations were compared with 'base-case run', i.e., operational modelling results for 2015.

In order to single out the effect of anthropogenic emission change model calculation with meteorological data and wind re-suspension for 2015 and anthropogenic emissions for 2014 was carried out. The relative difference between this and 'base-case' run was used to evaluate the effect of change of reported data on anthropogenic emissions.

However, the usage of the same approach to evaluate effects of two other components (changes of meteorological conditions and wind re-suspension) is difficult. Unlike anthropogenic emissions, wind re-suspension arises under combination of specific meteorological conditions, such as soil moisture (function of precipitation) and wind velocity. Since wind re-suspension strongly depends on meteorological data, the combined effect of these two components is considered. Effect of change of meteorological data alone was estimated via comparison of anthropogenic deposition, based on emissions for the same year (2015) and meteorological data for 2014 and 2015.

Maps in Fig. 1.17 demonstrate effects of anthropogenic emission changes, effect of meteorological condition changes and combined effect of meteorology and re-suspension changes. The effects are expressed as relative difference between the results of 'base-case' run and corresponding model test. Positive value of the effect supposes that a considered change favours increase of deposition from 2014 to 2015, and vice versa. Analysis of these three maps together allows identifying importance of each of the considered effects leading to deposition changes in different parts of the EMEP region.

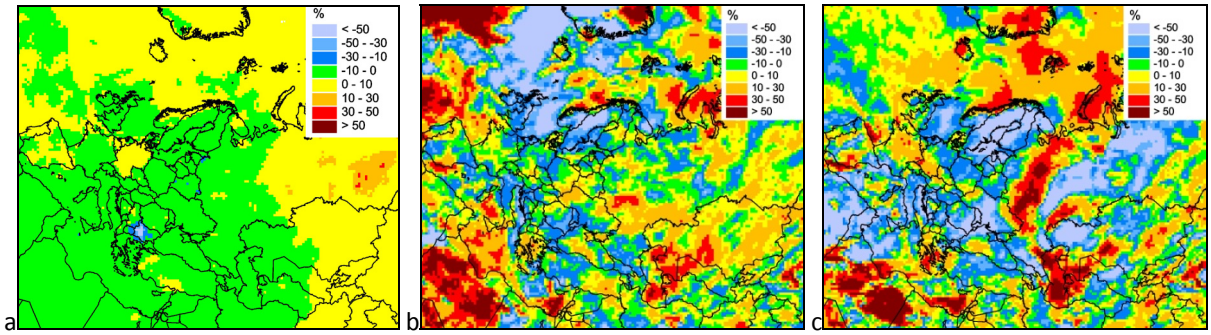


***Fig. 1.17.*** *Effects of lead deposition changes (% relative to 2015) between 2014 and 2015 caused by changes of reported anthropogenic emissions (a), meteorological conditions (b) and combined effect of meteorological data and wind re-suspension (c). Positive values mean increase of deposition from 2014 to 2015, and vice versa*

Significant deposition changes in the European part of Russia are mainly caused by combination of effects of changes in meteorological conditions and wind re-suspension (Fig. 1.17b,c). The changes of reported anthropogenic emissions have insignificant influence compared to other effects (Fig. 1.17a). In case of heavy metals main meteorological factors influencing pollution levels are precipitation amounts and atmospheric transport. Comparison of annual precipitation sums in 2014 and 2015 indicates the increase in the European part of Russia in 2015 (Fig. 1.18). Decrease of deposition in Italy and most part of the Balkan Peninsula, as well as the increase in the southern part of the Balkan Peninsula and along the northern coast of Norway can be attributed to effect of meteorology, in particular, to changes of atmospheric precipitation sums between 2014 and 2015 (Fig. 1.18). Increase of deposition in the northern part of France and southern part of Germany is explained by higher lead re-suspension flux in 2015 compared to 2014 (Fig. 1.19).

Interesting situation takes place over the large area covering the Baltic Sea, northern parts of Germany and Poland, north-west of Russia and Scandinavian Peninsula, where total deposition in 2015 are lower than that in 2014 by 30-50%, and in some regions – even more than 50% (Fig. 1.16). As follows from Fig. 1.17a, the effect of changes in reported emissions is quite low in this region (±10%) and cannot be a reason of the deposition decline.

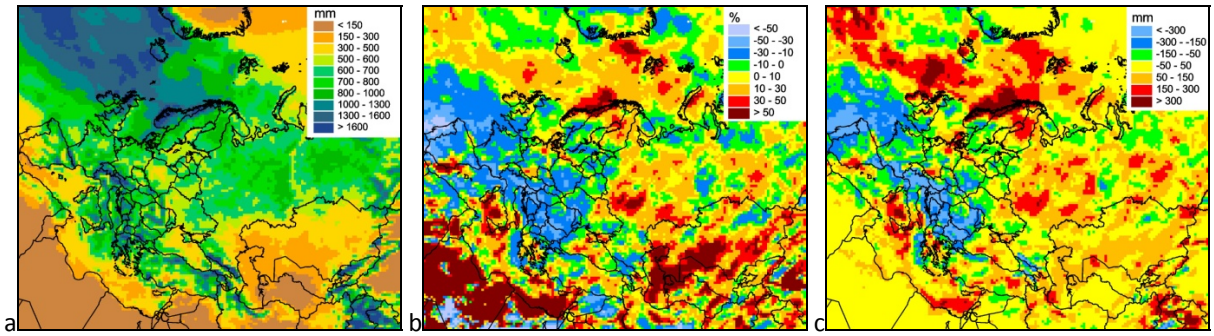


***Fig. 1.18.*** *Precipitation amounts in 2015 (a) and relative (b) and absolute (c) difference between precipitation in 2015 and 2014 (b). Positive values of the difference mean increase, and negative – decrease of precipitation in 2015 compared to 2014*

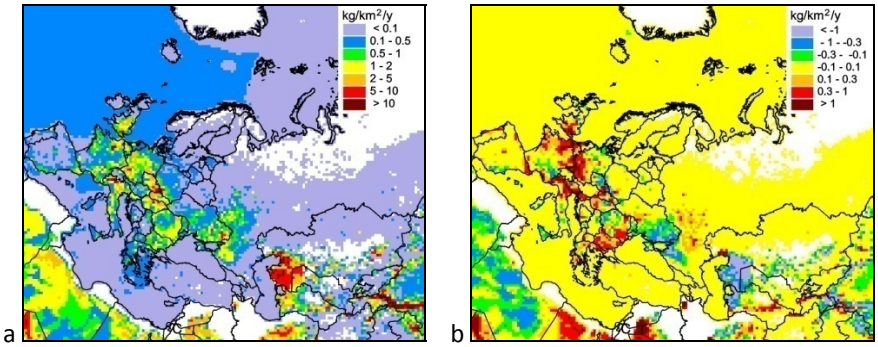


***Fig. 1.19.*** *Wins re-suspension flux of lead in 2015 (a) and difference between re-suspension fluxes in 2015 and 2014. Positive values of the difference mean increase, and negative – decrease of the flux in 2015 compared to 2014*

Change of meteorological conditions between 2014 and 2015 favours strong (-30 – -50% or even more) decline of deposition in southern part of Norway and over most part of Sweden (Fig. 1.17b). In other parts of the considered region (Finland, Baltic region, northern Poland and Germany) temperately positive or negative effect takes place. Comparison of annual precipitation sums indicates the increase from 2014 to 2015 over most part of the considered region (Fig 1.18b, c). It should favour increase of deposition, while in fact the effect of meteorological condition change is mostly negative (Fig. 1.17b). Therefore, analysis of atmospheric transport patterns in 2014 and 2015 is needed.

As follows from Fig. 1.17c, the combined effect of meteorological and re-suspension change is mainly responsible for change of overall deposition in the Baltic/Scandinavia region. Wind re-suspension flux in this region, as well as changes between 2014 and 2015 are low compared to other parts of the EMEP region (Fig. 1.19). Therefore, changes of deposition in this region is not associated with 'local' re-suspension, but may be linked with long-range atmospheric transport of re-suspended dust particles from remote regions.

Changes of atmospheric transport patterns between 2014 and 2015 are analysed considering source-receptor relationships in these two years, exemplified by Sweden, because the considered effects are the strongest for this country (Fig. 1.17b, c). In calculations for 2014 total deposition of lead amounted to 154 tonnes, and in 2015 – 102 tonnes (Fig. 1.20a). Contribution of non-EMEP sources declined insignificantly (about 4%). Much higher decline is noted for deposition from anthropogenic (national and foreign) sources (about 30%) and secondary sources (almost 40%).

Among main countries-sources of anthropogenic lead deposition in Sweden the most marked relative change is noted for Russia (-49%) and Poland (-38%) (Fig. 1.20b). According to emission data used in calculations, in 2015 Polish emissions reduced insignificantly (2%) compared in 2014. Russian emissions in European part almost has not changed, but increased significantly in its Asian part.

Secondary sources include wind-blown dust suspension from certain land-cover categories, such as bare lands and deserts, urban areas, arable lands and wind-forced suspension of marine aerosol containing heavy metals. Contributions of deposition caused by marine sources and arable lands in Sweden are comparatively low (Fig. 1.20c). Deposition caused by of re-suspension from urban areas declined by about 40%, whereas that from bare/desert lands – by and order of magnitude (almost 9-fold).

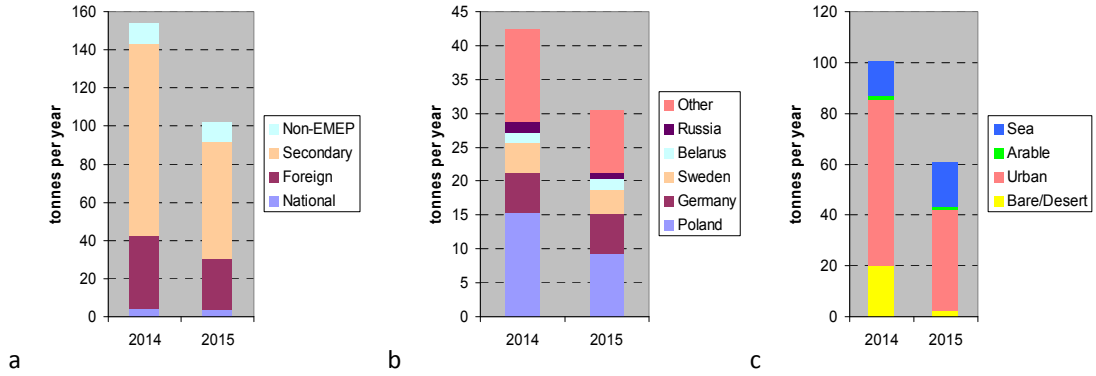


***Fig. 1.20.*** *Contribution of anthropogenic (national and foreign), secondary and non-EMEP sources to lead deposition (a), contribution of main anthropogenic sources (b) and contributions of different land-cover categories to deposition from secondary sources (c) in Sweden in 2014 and 2015*

The indicated large decreased in deposition both from anthropogenic and from secondary sources cannot be explained only by reduction of emissions in countries or the decline of wind re-suspension. Therefore, the atmospheric transport patterns have to be examined. In order to identify the role of changing atmospheric transport patterns between 2014 and 2015, deposition of lead from each EMEP country to Sweden in 2014 and 2015 was divided by corresponding country's emission. This ratio can be considered as simplified form of influence function and characterizes potential influence of a region (country) on lead deposition in Sweden. In 2015 this ratio is higher than that in 2014 for Norway, Denmark and the United Kingdom, and smaller for most countries to the south and east of Sweden (Fig. 1.21). This fact indicates at stronger potential influence from westerly atmospheric transport in 2015 compared to 2014.

Additional analysis was performed to explain changes of deposition from secondary sources (bare/desert lands). Time series of daily country-averaged deposition flux of lead, caused by wind re-suspension from bare/desert lands, to Sweden are shown in Fig. 1.22. There are two periods when the fluxes in 2014 are much higher than those in 2015: May 18-26 (days 138-146) and June 03 – 12 (days 154-163). To determine source regions, back trajectories are plotted for various Swedish locations. Examples of 5-day trajectories arriving to Swedish station SE12 (Aspvreten) demonstrate, that there is a distinct inflow of air masses from Central Asia, namely, western regions of Kazakhstan and Turkmenistan (Fig. 1.23). In these desert regions wind re-suspension is high compared to other EMEP areas (Fig. 1.19a). In 2014 re-suspension flux in these regions was much higher than that in 2015 (Fig. 1.19b). Hence, combination of higher re-suspension and specific transport patterns produced significant contribution of re-suspension from bare lands to deposition in Sweden in 2014. Lack of this combination in 2015 resulted to sharp drop of contribution to deposition from this source.

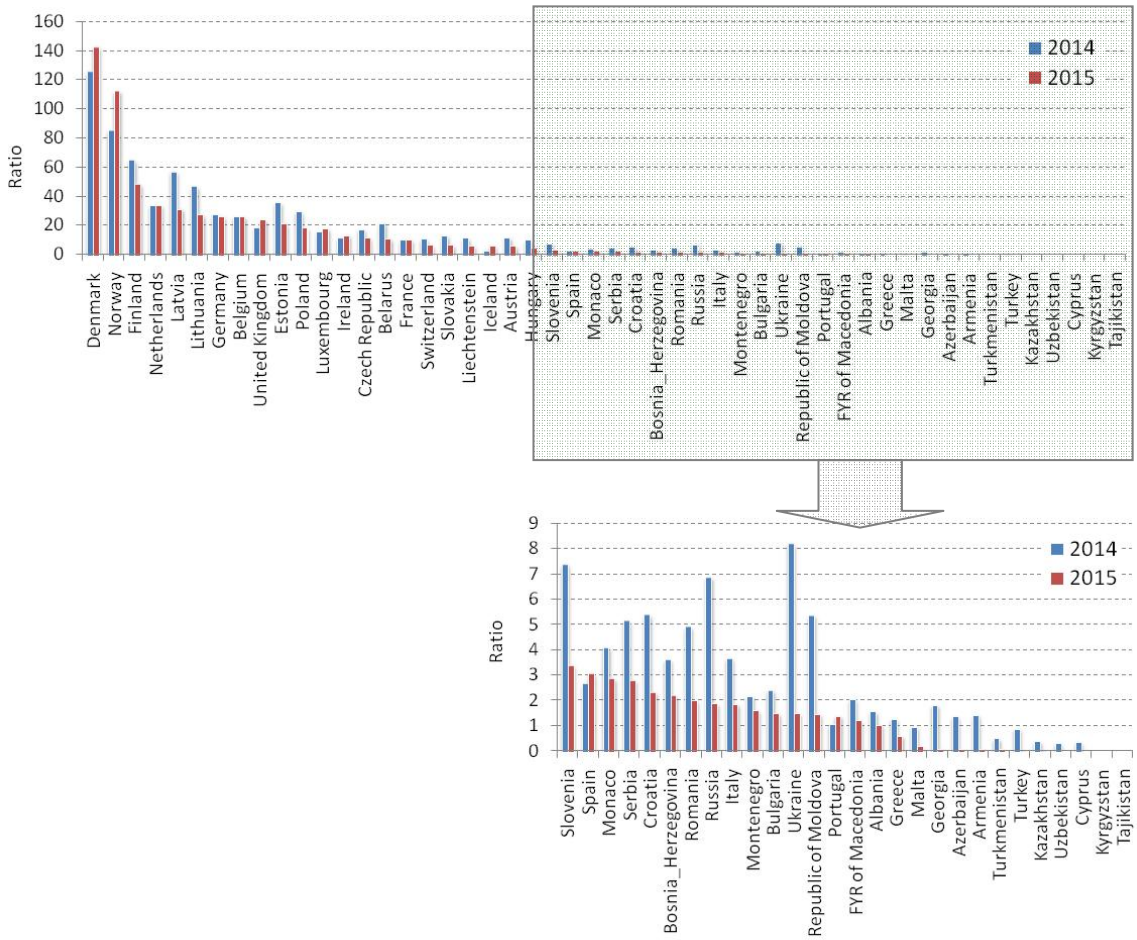


***Fig. 1.21.*** *Potential influence of foreign countries on lead deposition in Sweden in 2014 and 2015, expressed as a ratio of deposition from country's emission sources to country's emissions*

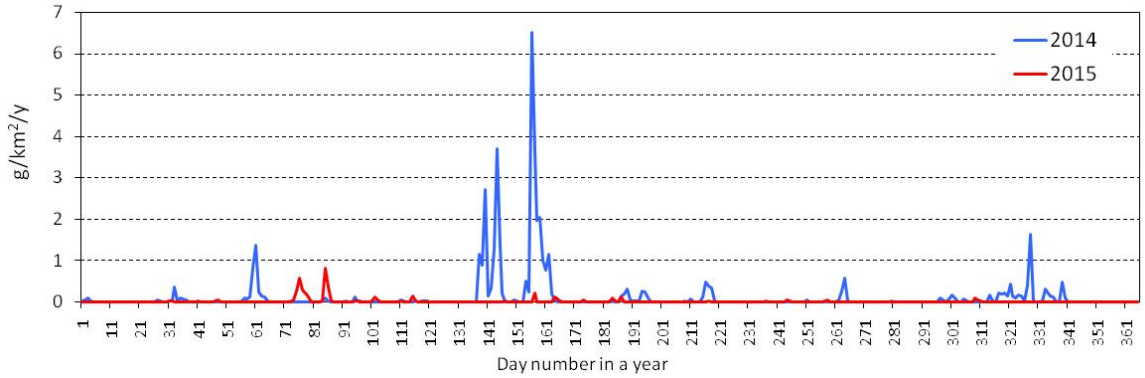


***Fig. 1.22.*** *Country-mean daily total deposition flux of lead caused by secondary sources from bare/desert lands in 2014 and 2015 in Sweden*

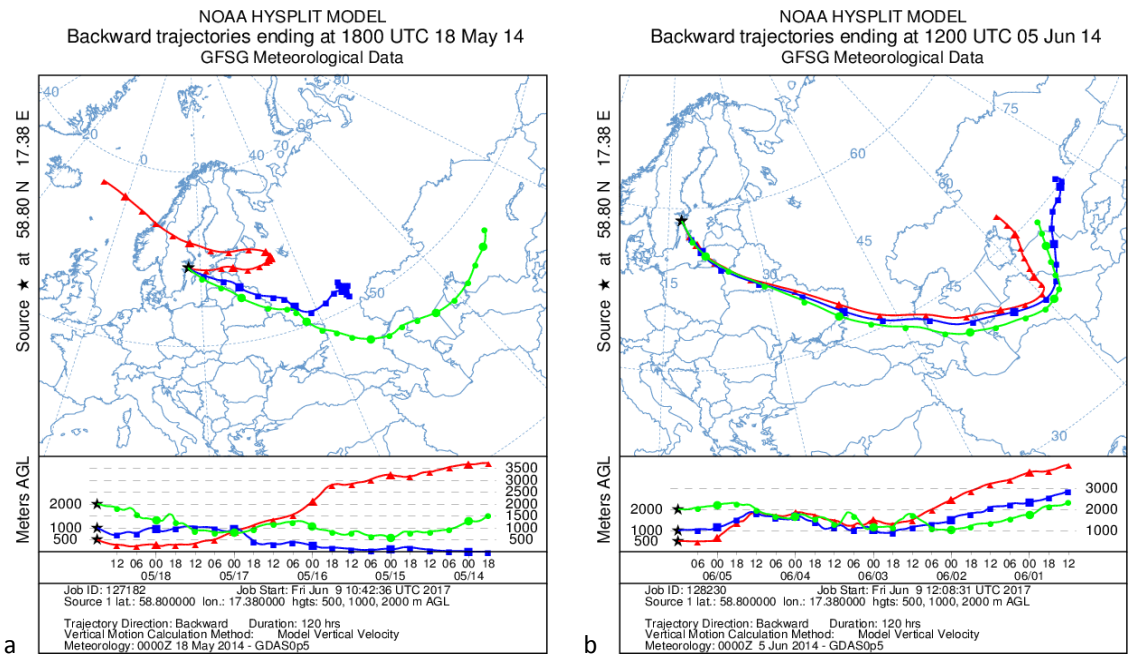


***Fig.1.23.*** *Back trajectories arriving to station SE12 (Aspvreten) in 18th of May and 05th of June 2014*

Similar combination of factors leads to increase of lead deposition in the central regions of the European part of Russia in 2015 (Fig. 1.17b,c). Period of high wind re-suspension of dust particles containing lead in western Kazakhstan and Turkmenistan coincided with episode of long-range atmospheric transport from this part of Central Asia to the European part of Russia.

***This analysis shows that wind re-suspension can significantly affect heavy metal pollution levels in the EMEP countries. In the process of transition to new EMEP grid special attention should be paid to adaptation of wind re-suspension parameterization for modelling at latitude-longitude projection and to finer spatial resolution.***

Changes of cadmium deposition are explained by the same factors as those of lead. Besides, decline of deposition between 2014 and 2015 in Belgium, the Netherlands and northern part of Germany is explained by correction of wind re-suspension flux in these countries. Comparison of modelled and observed concentrations and deposition at Belgian and the Dutch stations demonstrated overestimation of the observed levels caused by overestimated contribution of wind re-suspension [*Ilyin et al.*, 2016]. Following the approach described in [*Shatalov et al.*, 2016] cadmium re-suspension flux in these countries was reduced via correction of enrichment factor in urban areas.

***Comparison of heavy metal deposition in 2014 and 2015 demonstrated that the main factors responsible for the deposition changes in two consecutive years are changes of meteorological conditions and wind re-suspension. Therefore, even if emission data in the EMEP countries do not change significantly, deposition fluxes and source-receptor relationships can change markedly. Regular annual calculations of heavy metal levels are needed to identify and to document these changes.***

## 1.4. Arctic pollution

Following the agreement between CLRTAP and AMAP, reached at the joint meeting held in Potsdam, Germany in February 2016, MSC-E continued cooperation with AMAP in the field of analysis of heavy metal pollution level in the Arctic part of the EMEP region. In Fig. 1.24a-c deposition fluxes of lead, cadmium and mercury in the Arctic in 2015 are demonstrated.

Spatial distributions of lead and cadmium deposition fluxes are very similar. The highest fluxes – 150-500 g/km$^2$/y for lead and 8 – 20 g/km$^2$/y for cadmium - take place in the northern part of the Atlantic Ocean (Fig. 1.24a,b). Besides, particular hot spots of deposition are located in the vicinity of large anthropogenic sources on Kola Peninsula (Pb, Cd) and western Siberia (Cd). The lowest deposition fluxes are noted for Greenland and parts of the Arctic Ocean near the North Pole. In these parts of the Arctic lead deposition flux lie below 25 g/km$^2$/y, and cadmium flux – below 1 g/km$^2$/y. Spatial distribution of mercury levels differs from the distribution of lead and cadmium. Mercury deposited to snow can undergo fast photoreduction and re-emit back to the atmosphere [*AMAP,* 2011]. Therefore, unlike lead and cadmium, in case of mercury the difference between deposition and re-emission from snow (i.e., net deposition flux) is demonstrated in Fig. 1.24c. The highest values of the net deposition flux (15-25 g/km$^2$/y) are noted in the Arctic Ocean. It is explained by significant mercury oxidation and deposition during mercury depletion events. At the same time, large part of mercury deposited to snow is reduced to its volatile elemental form and re-emits to the atmosphere. Therefore, in high latitudes of the Arctic net mercury flux is relatively low (1 – 2.5 g/km$^2$/y). The lowest fluxes (below 1 g/km$^2$/y) take place in Greenland.

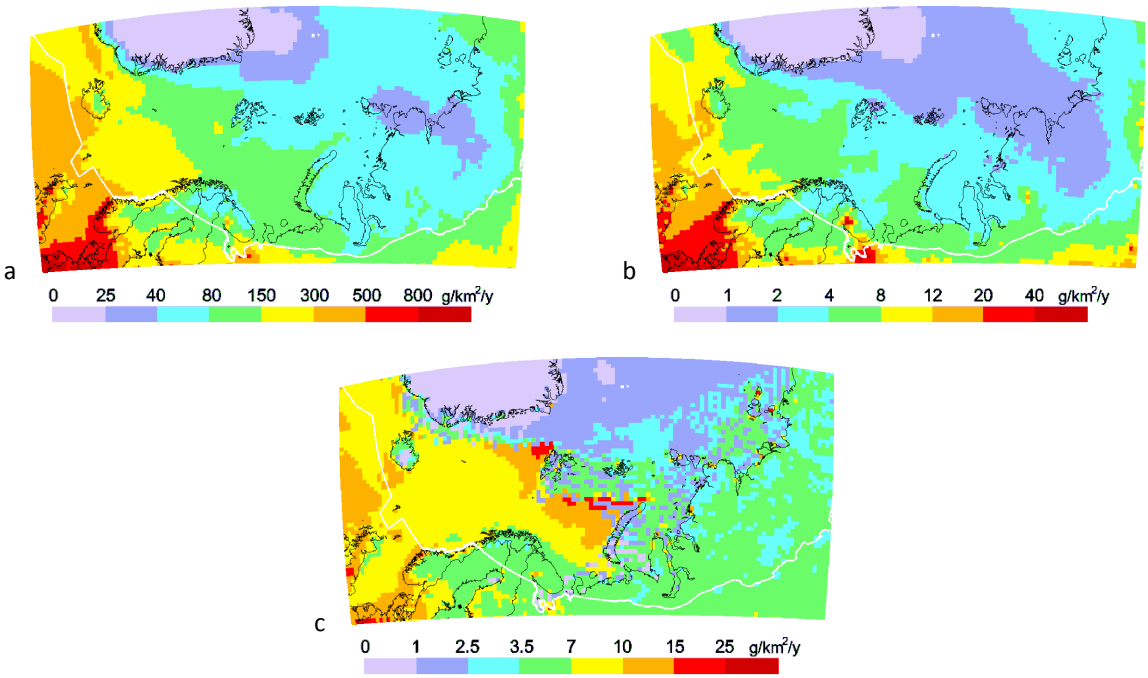


***Fig. 1.24****. Spatial distribution of annual total deposition of lead (a), cadmium (b) and net deposition flux of mercury (c) over the Arctic sector of the EMEP region in 2014. White line depicts the boundary of the AMAP domain*

Deposition of heavy metals to the Arctic is caused by EMEP anthropogenic, EMEP secondary and non-EMEP sources. Contribution of anthropogenic sources of lead makes up 11%, and of cadmium – 30% to total deposition in the Arctic (Fig. 1.25). Significant (27 – 37%) contribution is made by secondary sources, mostly by wind-blown dust containing heavy metals from urban areas and desert regions of Central Asia. It should be noted that re-suspension in not fully natural sources because re-suspended particles contain both naturally occurring metals and the metals from historical deposition from anthropogenic sources. The predominant contribution to deposition of lead and cadmium comes from non-EMEP sources. These sources include both anthropogenic sources located outside EMEP countries (e.g., in North America, eastern part of Asia) and secondary sources outside EMEP region. Mercury deposition to the Arctic is almost fully (96%) explained by the influence of non-EMEP sources. Mercury in the atmosphere has long life time, and can disperse globally after being emitted. Hence, it is worth noting that deposition from non-EMEP sources to the Arctic include also some mercury released by the EMEP sources, which flew out of the EMEP region and mixed with mercury from other sources.

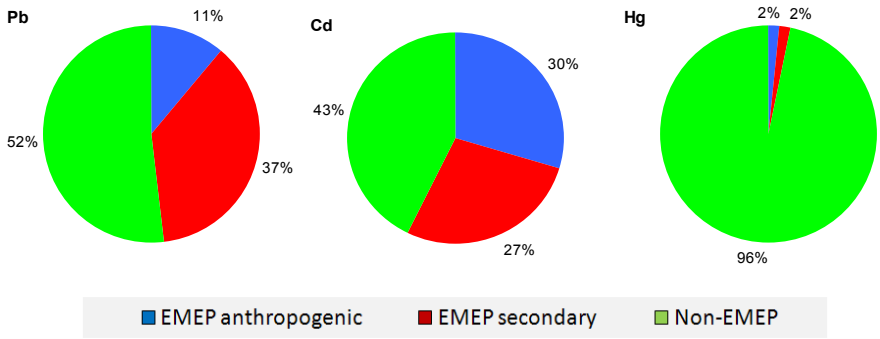


***Fig. 1.25.*** *Average contribution of different source types to annual deposition of lead (a), cadmium (b), and mercury (c) to the European and Asian terrestrial areas of the Arctic covered by the EMEP domain*

Contribution to pollution in the Arctic caused by sources of particular EMEP countries depends on a number of factors. First of all, they include emission magnitude in a country, distance from the Arctic and peculiarities of meteorological conditions (patterns of atmospheric transport and precipitation). For example, the highest total deposition of lead (around 14 tonnes) to the Arctic is made by sources of Russia (Fig. 1.26). The second position (8.6 tonnes) is taken by Kazakhstan. Although this country is remote from the Arctic, its national total emissions of lead, used in modelling, are the highest among the EMEP countries. Similar information is available for other considered heavy metals.

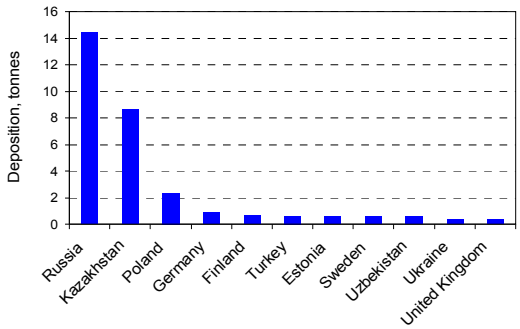


***Fig. 1.26.*** *Total deposition of lead caused by emission sources of the EMEP countries to the European and Asian terrestrial areas of the Arctic covered by the EMEP domain. Ten main countries-contributors are shown*

***Sources located outside the EMEP countries make the highest contribution to heavy metal deposition in the Arctic sector of the EMEP region. However, in order to improve model assessment of heavy metal pollution levels both in the Arctic and in other parts of the EMEP region, up-to-date data on lead, cadmium and mercury emission on the global scale is needed.***

# 2. TRANSITION OF GLEMOS MODELLING SYSTEM TO THE NEW EMEP GRID

Global EMEP Multi-Media Modelling System (GLEMOS) is an up-to-date chemical transport model used by MSC-E for the operational modelling of transboundary pollution of the EMEP countries by heavy metals and POPs. Following decisions of the Executive Body for CLRTAP [ECE/EB.AIR/113/Add.1] MSC-E undertakes significant efforts to prepare the GLEMOS system for transition of the operational modelling to the new EMEP grid. The grid changes include movement from the polar-stereographic to the regular geographic (latitude-longitude) projection of the Earth surface and increase of the grid spatial resolution. Preparatory work on transition to the new grid as well as pilot simulations and evaluation of the model performance were discussed in previous reports [*Ilyin et al.*, 2014; 2016]. This year MSC-E has continued the model update aiming to complete the transition process. The new developments include extension of the list of pollutants simulated on the new grid, preparation of additional input data for these pollutants and thorough testing of the updated modelling system. Besides, the modelling system underwent considerable structural revision aimed to prepare it for public distribution as open-source software. Current progress in update and further development of GLEMOS is discussed below.

## 2.1. Model update and further development

### *2.1.1. Adaptation of HM and POPs modules for simulations on the new EMEP grid*

The GLEMOS modelling system consists of a number of functional modules controlling the data flows and describing various physical and chemical processes (Fig. 2.1). They include the input and output systems, general modules describing dispersion processes in the environmental media (atmosphere, ocean, soil, vegetation) and modules presenting behaviour and properties of particular pollutants. The transition of the model to the new grid implies adaptation of both general and pollutant specific modules along with preparation of required input data for the new domain. The work on the model update was started with generation of various input data (meteorological fields, geophysical information, atmospheric concentrations of chemical reactants etc.) for the new grid [*Ilyin et al.*, 2014]. General modules of the model describing atmospheric transport and removal processes were adapted to the new

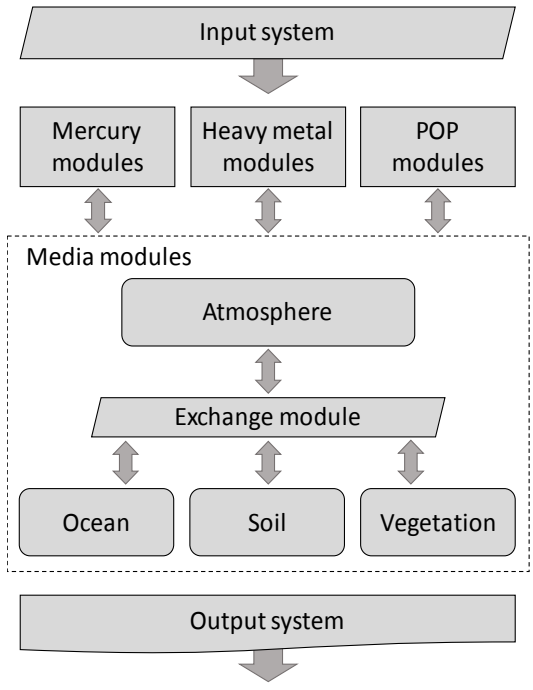


***Fig. 2.1.*** *General scheme of GLEMOS modules*

grid and tested by simulation of mercury. The pilot modelling of mercury transboundary pollution on the new EMEP grid demonstrated good model performance in comparison with measurements and with the former EMEP grid [*Ilyin et al.*, 2016].

This year other pollutant specific modules have been adapted and tested on the new grid. It relates to modelling of particle-bound heavy metals (lead and cadmium) and a selected persistent organic pollutant (benzo(a)pyren). In the case of heavy metals a number of GLEMOS modules responsible for parameterization of wind re-suspension from soil and seawater have been updated. Besides, the pre-processor of dust suspension from different surface types has been revised. A new system of preparation of the initial and boundary conditions for regional modelling has been developed based on the one-way nesting of the global scale simulations. Implementation of POP modelling on the new grid requires adaptation of the modules describing pollutants behaviour in different environmental media (atmosphere, ocean, soil and vegetation) and the mutual exchange between them. More detailed discussion of the GLEMOS update for POP modelling as well as results of pilot simulations are presented in [*Gusev et al*., 2017].

### *2.1.2. Preparation to public distribution as open-source software*

In order to support national efforts in pollution assessment on different scales it is planned to distribute the GLEMOS model for public use as open-source software. It requires revision of the model and auxiliary routines to simplify the model application and its learning curve for third-party users. For this purpose, the whole model structure was significantly updated including deep revision of the input and output systems, development of auxiliary pre-processing tools and elaboration of a set of control scripts for compilation and running the model. The revised input system allows a flexible way of preparation of geophysical information, concentration of chemical reactants, initial and boundary conditions for an arbitrary model grid. The output system provides means for configuring and controlling the model output information, which includes variety of data (2D and 3D fields, time series at monitoring sites, source-receptor matrices etc.) stored in different formats (ASCII, netCDF). The toolset of control scripts allows flexible configuring the model set-up and compilation of the model code for a particular task. It provides a choice for regular or matrix simulations of various pollutants (Pb, Cd, Hg, PAHs, PCDD/Fs, PCBs, HCB etc.) on different scales (from global to local) with arbitrary spatial resolution, switching on/off the environmental media (atmosphere, ocean, soil, vegetation) in the model set-up, choice of different process parameterizations etc.

Thus, the new release of the model prepared for public distribution (GLEMOS v2.0) contains the following components:

- GLEMOS source code (FORTRAN 95);
- A set of control scripts for compilation and running the model (c-shell);
- A set of auxiliary tools for pre-processing input data and post-processing output results;
- Technical documentation.

The updated version of the model adapted for simulation on the new EMEP grid was thoroughly tested and verified. The testing results for heavy metals are presented in Section 2.2. Detailed analysis of the model application for the selected POP (benzo(a)pyrene) is given in [*Gusev et al*., 2017].

## 2.2. Pilot simulations of Pb and Cd on the new grid

The transition of the Pb and Cd regional modelling to the new EMEP grid included modification of the GLEMOS model code and preparation of variety of input data. To test the model performance on the new grid a series of model runs were performed on a regional scale simulating Pb and Cd atmospheric dispersion in 2014 with spatial resolution 0.2°x0.2°. Simulation results were compared with results obtained on the former EMEP grid (50x50 $km^2$) and evaluated against observations. It should be noted that reported heavy metal emission data on the new grid with fine spatial resolution are not available yet. Therefore, to keep consistency between two regional simulations the gridded heavy metal emission data prepared by CEIP with spatial resolution 50x50 $km^2$ were interpolated by MSC-E into the new EMEP grid and used in the model tests. The whole set of tests was divided into two parts. The first part included model runs with anthropogenic emissions only and aimed at evaluation of the model ability to simulate transboundary transport of heavy metal pollution between the EMEP countries. The second part consisted of simulations with all types of emission sources (direct anthropogenic emissions, wind re-suspension, and non-EMEP sources) and was focused on evaluation against observations. More detailed evaluation of the model performance with finer spatial resolution (0.1°x0.1°) was performed on a national scale as a part of country-specific case studies (*Chapter 3*).

### *2.2.1. Transboundary transport of anthropogenic emissions*

Assessment of atmospheric dispersion and transboundary transport of heavy metal emissions between the EMEP countries are the primary task of the operational modelling. Therefore, the model evaluation was initially performed based on simulation of Pb and Cd transport from direct anthropogenic sources of the EMEP countries without influence of secondary sources and transport from other regions determined by boundary conditions. Results obtained on the new grid were compared with those from the regular simulations on the old grid to ensure succession of the assessment results. For the sake of brevity the comparison is illustrated by simulation of Pb implying similar results for Cd. Annual mean concentrations of Pb in the surface air simulated on the old and new grids are shown in Fig. 2.2. Both versions of the model produce very similar spatial patterns with elevated concentrations over Central and Southern Europe, Central Asia and the Middle East determined by high Pb emissions in these regions. A steep south-to-north decreasing trend of Pb concentration is also well reproduced on both grids. The model simulation on the new grid with finer spatial resolution predicts somewhat higher surface concentrations in areas with high anthropogenic emissions due to more correct reproduction of the vertical mixing. Nevertheless, the difference between two model runs is insignificant and commonly does not exceed ±30%.

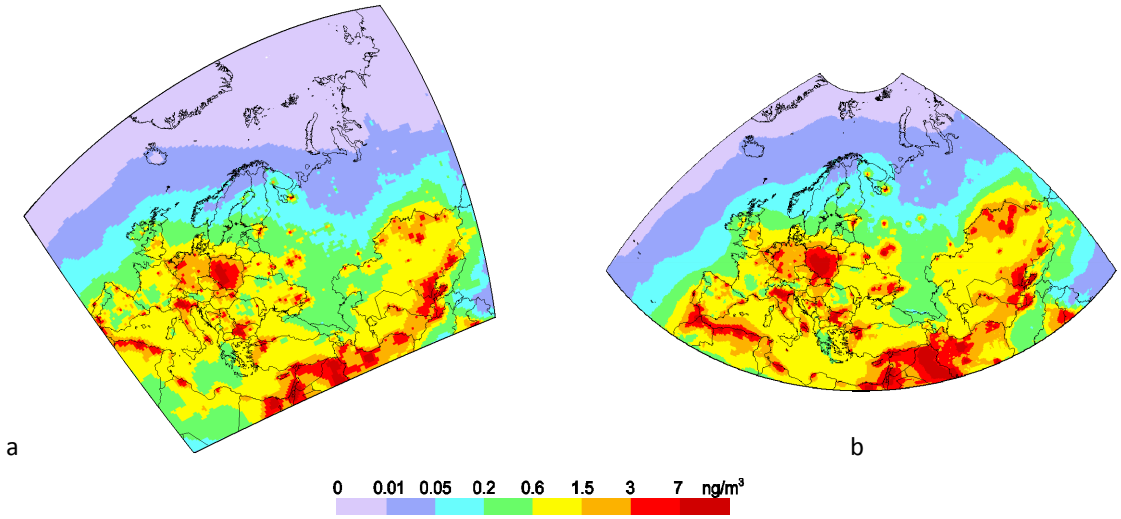


***Fig. 2.2.*** *Annual mean air concentration of Pb in 2014 from anthropogenic sources simulated over the old (a) and new (b) EMEP domains*

Figure 2.3 shows simulated maps of total (wet and dry) Pb deposition from anthropogenic sources over the old and new EMEP domains. This is the primary parameter of heavy metal pollution assessment since it characterizes the overall atmospheric load of a pollutant to the terrestrial and aquatic ecosystems and, ultimately, the impact on human health and biota. The spatial patterns of Pb deposition simulated on both grids are very similar to each other. Relatively high deposition fluxes (above 0.5 kg/km$^2$/y) are predicted in Central Europe (Poland, Germany, Slovakia), Southern Europe (Northern Italy, Bulgaria, Bosnia and Herzegovina, etc.), Central Asia (northern and southern Kazakhstan, Uzbekistan, etc.), Middle East, and at some other locations in the vicinity of emission sources. Deposition levels from anthropogenic sources quickly decrease westward and northward to open waters of the Atlantic and Arctic Oceans. The deposition pattern on the new grid looks more mosaic due to finer spatial resolution. It predicts more local 'hot spots' with elevated Pb deposition over territories of the EMEP countries, which can be at risk of heavy metal pollution.

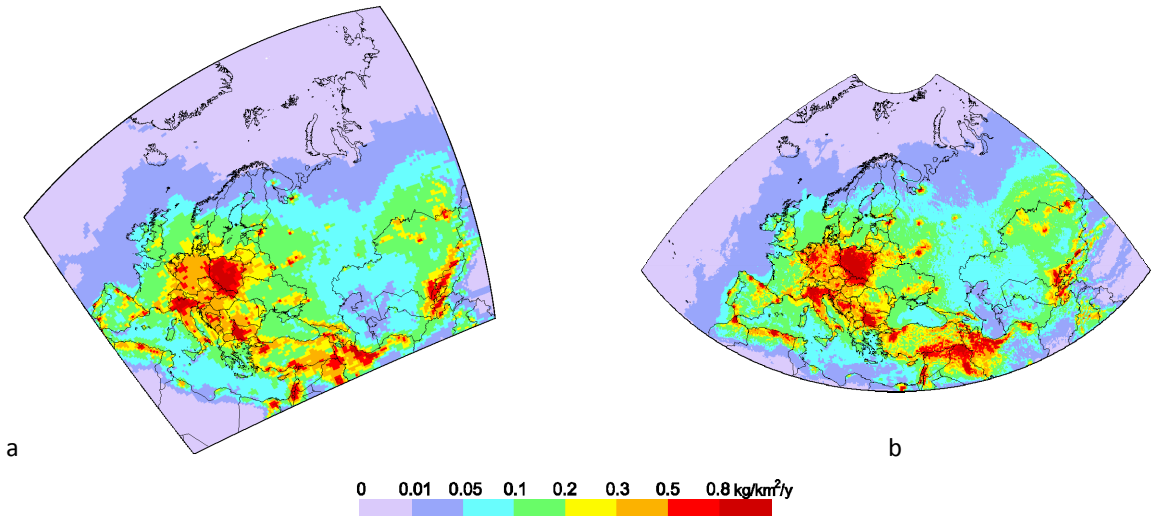


***Fig. 2.3.*** *Annual Pb deposition flux in 2014 simulated over the old (a) and new (b) EMEP domains*

Comparison of average Pb deposition to the EMEP countries from anthropogenic sources simulated on the old and new grids is presented in Fig. 2.4. In addition, average flux for each country is

specified in terms of contributions of domestic and foreign emissions to illustrate impact of transboundary transport. As seen average deposition levels differ insignificantly between the two model runs for most of the countries. In the three fourth of all countries the difference does not exceed 15%. In most cases, the difference between Pb deposition simulated on the old and new grids is determined by contribution of domestic sources. As seen from the figure, absolute contribution of foreign sources slightly differs between the two grids in the majority of countries. In contrast, the new model version simulates somewhat higher deposition from domestic sources in countries with significant emissions (e.g. Poland, Slovakia, Belgium). Updated meteorological data and increased vertical coverage of the model domain applied for simulations on the new grid allows more realistic reproduction of the vertical mixing of pollutant emissions. It leads to some increase of near-surface air concentrations and dry deposition fluxes in the vicinity of emission sources. As a result, the model application on the new grid predicts slightly smaller relative contribution of transboundary transport between the EMEP countries.

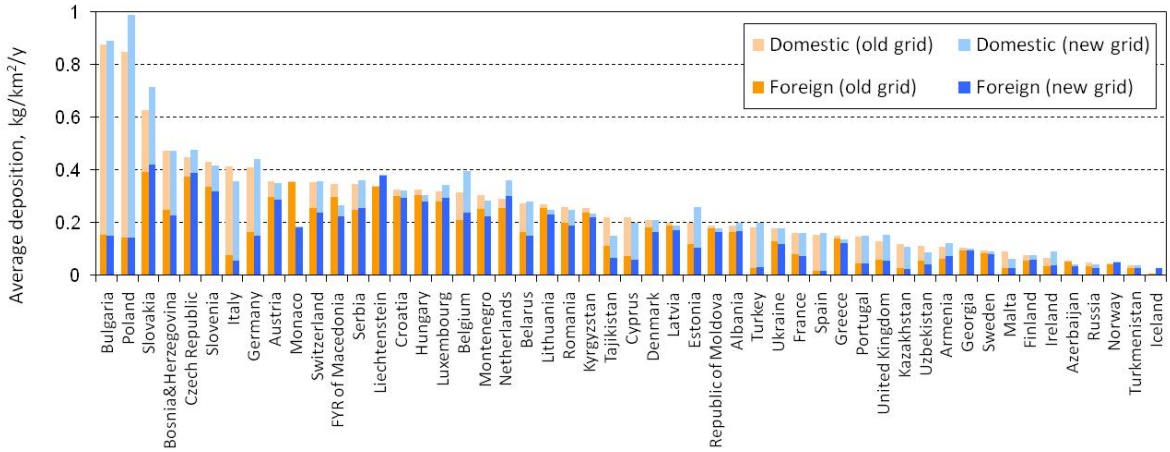


***Fig. 2.4.*** *Comparison of average Pb deposition from anthropogenic sources in the EMEP countries in 2014 simulated over the old and new domains*

### *2.2.2. Wind re-suspension of particle-bound heavy metals*

Wind re-suspension from land and aquatic surfaces can significantly contribute to heavy metal pollution in the EMEP countries [*Ilyin et al.*, 2016]. The dust pre-processor is an essential part of the GLEMOS input system. It generates the flux of windblown dust suspended from natural surfaces. These data are required for simulation the wind re-suspension of particle-bound heavy metals to the atmosphere and its contribution to transboundary pollution. Detailed description of the applied parameterizations is given in [*Gusev et al.*, 2006; 2007]. Wind suspension of mineral dust from three types of land surfaces (barren lands, urban and roadside areas, cultivated crops) and from the water surface is considered. The suspension flux is sensitive to meteorological parameters (wind, precipitation, friction velocity, etc.), characteristics of the underlying surface (land cover type, roughness, etc.) and soil type. To adapt the dust pre-processor for simulations on the new EMEP grid a variety of input data was prepared for the new domain. Datasets of the dust suspension flux with fine spatial and temporal resolution were generated and stored for simulations of heavy metal pollution in the EMEP countries.

Maps of dust suspension from aquatic and terrestrial surfaces simulated over the old and new EMEP grids are shown in Fig. 2.5. As was mentioned above transition to the new grid is accompanied by change of meteorological and land use/land cover data. It inevitably leads to changes in simulated dust suspension flux. As seen from the figure, spatial distribution and general levels of dust flux simulated on two grids is similar for Europe and adjacent land and sea areas. However, the new version of the pre-processor predicts somewhat higher dust suspension in arid areas of North Africa, Middle East, and Central Asia. It is largely determined by update of land cover data. The more recent dataset used in the new model domain (based on the MODIS satellite data) estimates larger fraction of barren lands at the Mediterranean coast of North Africa, the Syrian Desert, and the Central Asian deserts. In addition, somewhat higher sea salt aerosol emission is predicted over the Northern Atlantic.

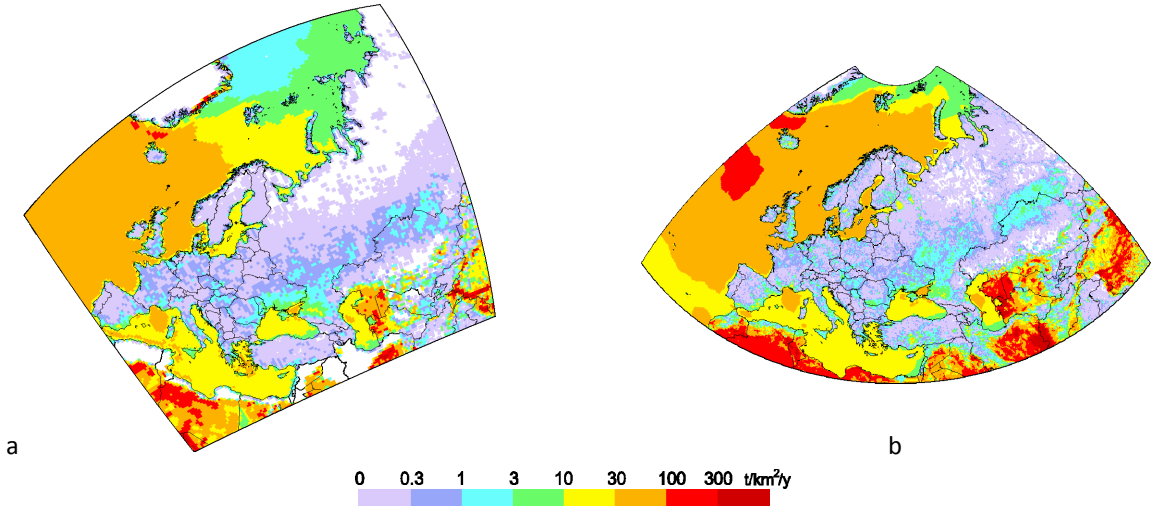


***Fig. 2.5.*** *Mineral dust (PM10) suspension from natural surfaces in 2014 simulated over the old (a) and new (b) EMEP domains*

Wind re-suspension of heavy metals is a natural process presenting emission of particle-bound metals to the atmosphere with suspended mineral dust. Heavy metal content in soil can be of natural origin and from previous atmospheric deposition of the pollutant. Therefore, soils that are significantly affected by deposition from anthropogenic sources (e.g. urban and industrial areas, road sides, etc.) can be strongly enriched with heavy meals. Estimates of heavy metal concentration in topsoil and the resulting wind re-suspension flux performed for operational EMEP calculations on the old grid are based on long-term simulations of heavy metal deposition in the EMEP domain [*Shatalov et al*., 2013]. In contrast, the current pilot estimates of wind re-suspension on the new grid were performed using a one-year simulation of heavy metal deposition in 2014 as a surrogate spatial distribution of heavy metal enrichment in topsoil. This limitation introduces additional uncertainty to the estimates of wind re-suspension flux and ultimately to the model results of heavy metal pollution levels, and should be removed in future. Comparison of heavy metal re-suspension flux simulated on the old and new EMEP grids is shown in Fig. 2.6 for Cd. Even the preliminary estimates of wind re-suspension on the new grid show good agreement with the estimates on the old grid over many territories. However, there are considerable differences in some areas caused by the uncertainties mentioned above. In particular, wind re-suspension of Cd is underestimated in some countries of Eastern and Southern Europe (e.g. Eastern Ukraine, Romania, Bulgaria) but overestimated in some

parts of Italy and the UK. There also discrepancies between the estimates on the old and new grids in Africa and Asia caused by the update of wind suspension of mineral dust in this regions.

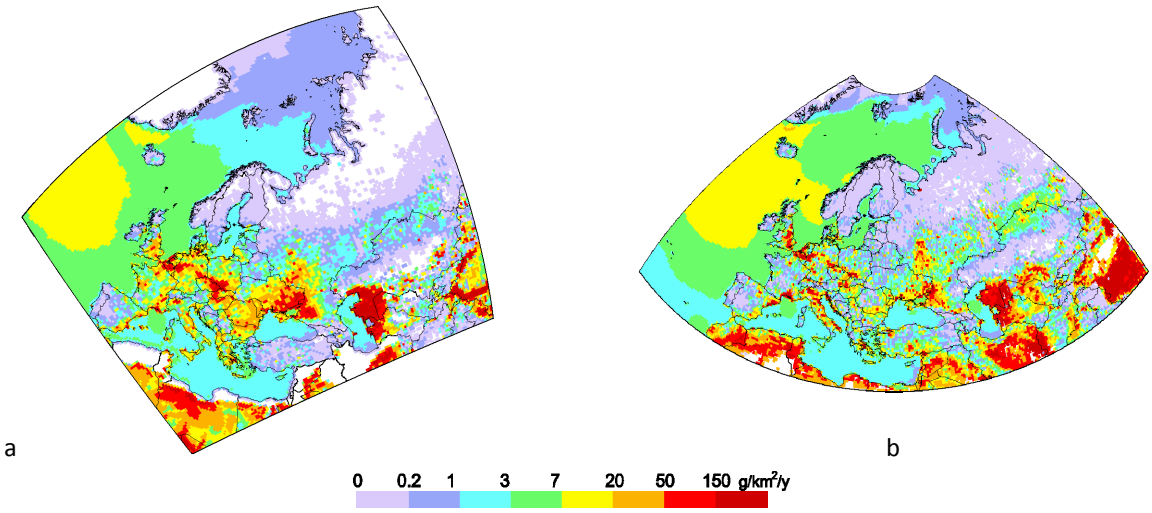


***Fig. 2.6.*** *Annual Cd re-suspension flux in 2014 simulated over the old (a) and new (b) EMEP domains*

Thus, evaluation of wind re-suspension of heavy metals of the new grid requires further refinement including estimates of long-term accumulation of the pollutants in soil from anthropogenic deposition and other factors affecting heavy metal enrichment of wind blown dust.

### *2.2.3. Evaluation of modelling results against measurements*

Full simulation of heavy metal transboundary transport and deposition of heavy metals was performed on the new EMEP grid for evaluation of the model performance against observations. It included contribution of all primary and secondary emission sources: direct anthropogenic emissions within the EMEP region, wind re-suspension and long-range transport of the pollutants from other regions defined by boundary conditions. The boundary conditions for the regional modelling were retrieved from the GLEMOS simulations on a global scale. The model evaluation results are illustrated below by the model-to-measurement comparison of Cd air concentration and wet deposition.

Annual mean concentrations of Cd in the surface air simulated on the old and new grids are shown in Fig. 2.7. Both versions of the model produce similar spatial patterns with elevated concentrations over a number of areas located in the Benelux region, southern Poland, eastern Ukraine and the centre of the European territory of the Russian Federation. The south-to-north decreasing trend from Central Europe to the Arctic is also reproduced on both grids in accordance with available observations. Besides, both model runs predict relatively low Cd concentrations in South-west Europe (France and Spain) that agrees well with measurements in this region. However, the model simulation on the new grid predicts higher concentration levels in the Mediterranean regions and over North Africa due to larger estimates of Cd wind re-suspension from arid regions as discussed earlier. The same reason determines higher concentrations predicted in Central Asia, Middle East, and over Western China.

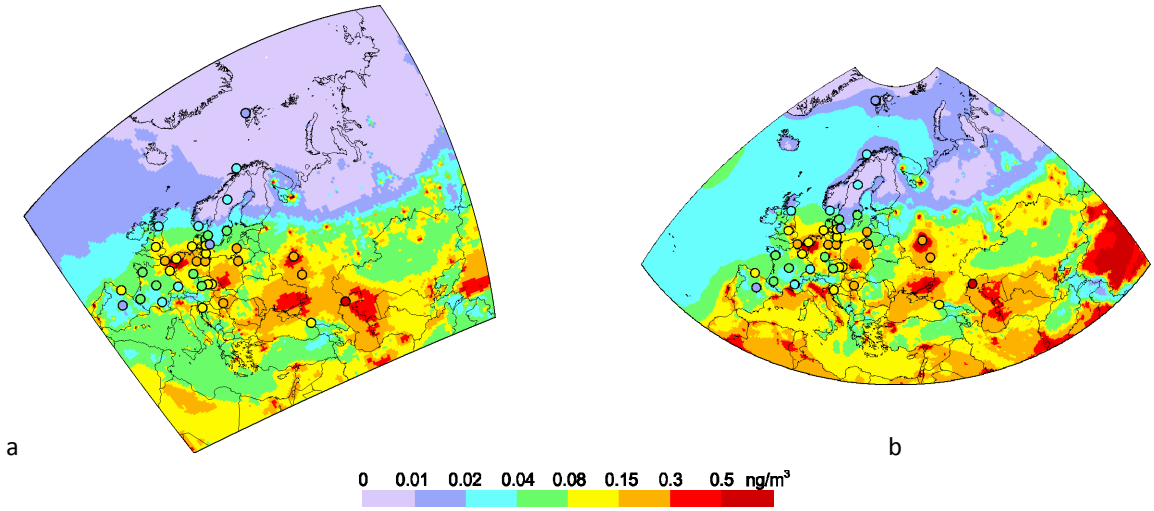


***Fig. 2.7.*** *Annual mean air concentration of Cd in 2014 simulated over the old (a) and new (b) EMEP domains. Coloured circles show Cd observations from the EMEP monitoring network*

Spatial distributions of simulated wet deposition flux for both grids are shown in Fig. 2.8. Again the model runs predict similar patterns of wet deposition in Europe. Elevated deposition fluxes are characteristics of Central Europe, the Benelux region, Northern Italy and the Balkan countries, Eastern Ukraine and the Caucasus. This is a result of combination of several factors including high local anthropogenic emissions, wind re-suspension and large precipitation amount. The simulation on the new grid provides lower wet deposition over southern Scandinavia that better agrees with observed values. Lower deposition fluxes are also predicted over the eastern territory of the Russian Federation, and in western Kazakhstan, which cannot be evaluated by measurements because of lack of heavy metal observations in these regions.

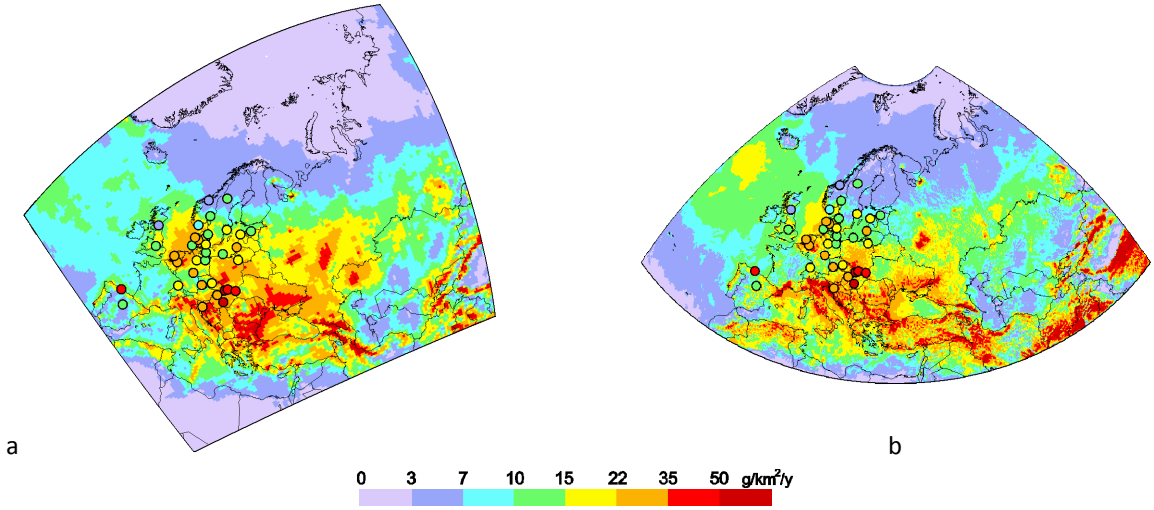


***Fig. 2.8.*** *Annual Cd wet deposition flux in 2014 simulated over the old (a) and new (b) EMEP domains. Coloured circles show Cd observations from the EMEP monitoring network*

Evaluation of the modelling results against observations from the EMEP monitoring network is presented in Fig. 2.9. The major statistics summary is given in Table 2.1. The model satisfactorily reproduces measured air concentrations of Cd on both grids (Fig. 2.9a). In most cases the difference between the model and observations does not exceed a factor of 2. The model run on the new grid provides somewhat better correlation with measurements. Both model runs demonstrates some

underestimation of observed wet deposition fluxes (Fig. 2.9b). Spatial correlation coefficient for wet deposition is slightly smaller for the new grid in comparison with the old one due to uncertainties of wind re-suspension estimates discussed in Section 2.2.2. Besides, it should be pointed out that anthropogenic emission data with fine spatial resolution is needed for improvement of the model performance for simulations on the new grid.

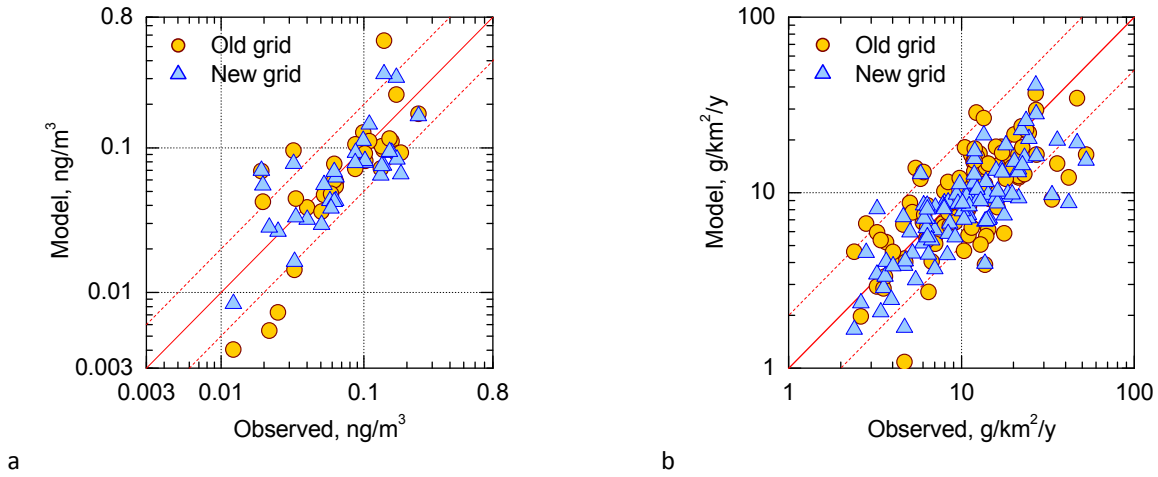


***Fig. 2.9.*** *Evaluation of annual mean air concentration (a) and wet deposition (b) of Cd in 2014 simulated over old and new EMEP domains against EMEP measurements*

***Table 2.1.*** *Statistics of the model-to-observation comparison for Cd simulations on the old and new grids*

| | Air concentration | | Wet deposition | |
|---|---|---|---|---|
| | Old grid | New grid | Old grid | New grid |
| Correlation coefficient | 0.52 | 0.59 | 0.41 | 0.36 |
| Relative bias, % | 2 | -8 | -23 | -30 |

### *2.2.4. Ecosystem-specific deposition*

Information of heavy metal deposition to various terrestrial and aquatic ecosystems is important for evaluation of adverse effects on the environment and human health. Model estimates of ecosystem-specific deposition of Pb, Cd and Hg are operationally performed by MSC-E for assessment of critical loads exceedances in cooperation with the Coordination Centre for Effects (CCE). Transition to the new grid requires testing the model performance to simulate heavy metal deposition to different land cover categories. Figure 2.10 illustrates comparison of spatial distributions of Cd deposition flux to a one of the considered land cover categories (i.e. croplands) simulated over the old and new EMEP grids. Generally, the spatial patterns are very similar to each other. Hotspots of high Cd deposition to croplands coincide in both simulations and are located in the Benelux countries, southern Poland, northern Italy, central part of the European territory of Russia, and territories adjacent to the Black sea. Relatively low deposition fluxes are predicted in Spain, France, Scandinavia, and over the eastern part of the model domain. However, there are some differences in the spatial patterns resulted from inconsistencies between input data used for simulations on different grids including meteorological and land cover data.

It should be noted that information on fraction of different land cover categories in each grid cell is critical for assessment of ecosystem-specific deposition. Transition to the new EMEP grid caused necessity to involve a new land use / land cover dataset for modelling. Currently, there is no common land use / land cover dataset adopted within EMEP and WGE that could be used by the scientific centres for model assessments and evaluation of adverse effects. ***Therefore, harmonization of the land use / land cover data is required within the Convention to avoid potential inconsistencies between different data products produced by EMEP and WGE in future.***

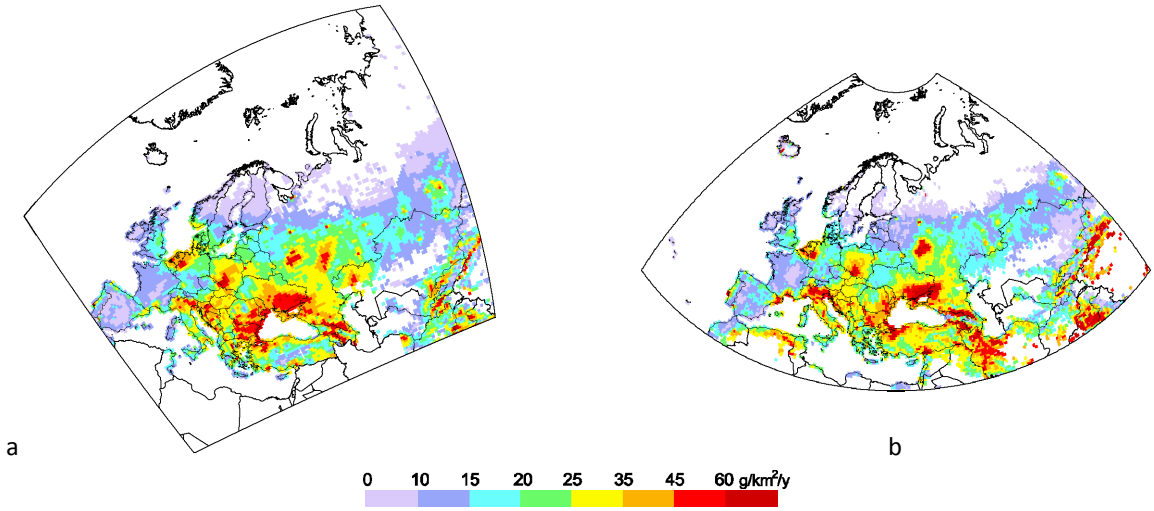


***Fig. 2.10.*** *Annual Cd deposition flux to croplands in 2014 simulated over the old (a) and new (b) EMEP domains*

Quantitative comparison of the spatial distributions of Cd deposition to croplands is shown in Fig. 2.11 in terms of probability distributions of deposition flux over the modelling domains. As seen, despite of some discrepancies in spatial patterns, the probability distributions of deposition fluxes simulated over the old and new domains are very close to each other. Both distributions have the maximum probability density at 10-20 g/km$^2$/y and slowly decreasing probabilities for higher deposition fluxes up to 60 g/km$^2$/y. Thus, the model predicts comparable ecosystem-specific deposition of heavy metal over both EMEP domains.

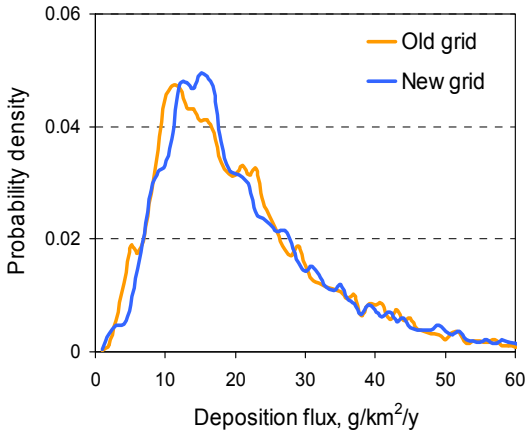


***Fig. 2.11.*** *Probability distributions of Cd deposition flux to croplands over the old and new grids*

***The pilot simulations of Pb and Cd pollution performed with GLEMOS on the new EMEP grid demonstrate good succession between the old and new model versions for assessment of transboundary transport between the EMEP countries and ecosystem-specific deposition. However, evaluation of wind re-suspension of heavy metals requires further refinement including estimates of long-term accumulation of the pollutants in topsoil. Besides, anthropogenic emission data with fine spatial resolution is needed for improvement of the model performance for simulations on the new grid.***

## 2.3. Model study of mercury chemistry and other processes in the atmosphere

Mercury dispersion in the environment is characterized by complex transformations in the atmosphere and other media as well as by inter-media exchange. In particular, oxidation and reduction chemistry significantly affects fate and transport of mercury in the atmosphere. However, there are significant gaps in the knowledge of chemical mechanisms responsible for transformations between different oxidation states of mercury and its deposition to the ground. To facilitate a better understanding of mercury atmospheric processes a multi-model study has been performed in a form of multiple simulation experiments. Four global scale models took part in the study: GLEMOS (EMEP/MSC-E), GEOS-Chem (MIT, USA), GEM-MACH-Hg (Environment and Climate Change Canada), ECHMERIT (CNR-II, Italy). The model experiments include: simulation with the standard model configuration (BASE), model run with no anthropogenic emissions (NoANT), model run with no natural and secondary emissions (NoNAT), simulations with atomic Br oxidation chemistry with two different sets of Br air concentrations (BrCHEM1 and BrCHEM2), simulation with OH-initiated oxidation chemistry (OHCHEM), simulation with $O_3$-initiated oxidation chemistry (O3CHEM). General description of the study and preliminary results were discussed in previous EMEP Status Reports [*Ilyin et al.*, 2015; 2016]. An example of the analysis and major conclusions are presented below.

Figure 2.12 shows a comparison of simulated and observed wet deposition fluxes for different model experiments. Both measured and simulated values are averaged over different groups of sites, including three groups in Europe (southern Europe, western Europe, and northern Europe), seven groups in North America, and one group per region in Asia, Australia, and the Indian Ocean. Note that the highest observed wet deposition values (30-45 ng/m$^2$/day) are associated with the southern United States, whereas the lowest values (below 10 ng/m$^2$/day) are characteristic of sites located in East Asia and in the Southern Hemisphere.

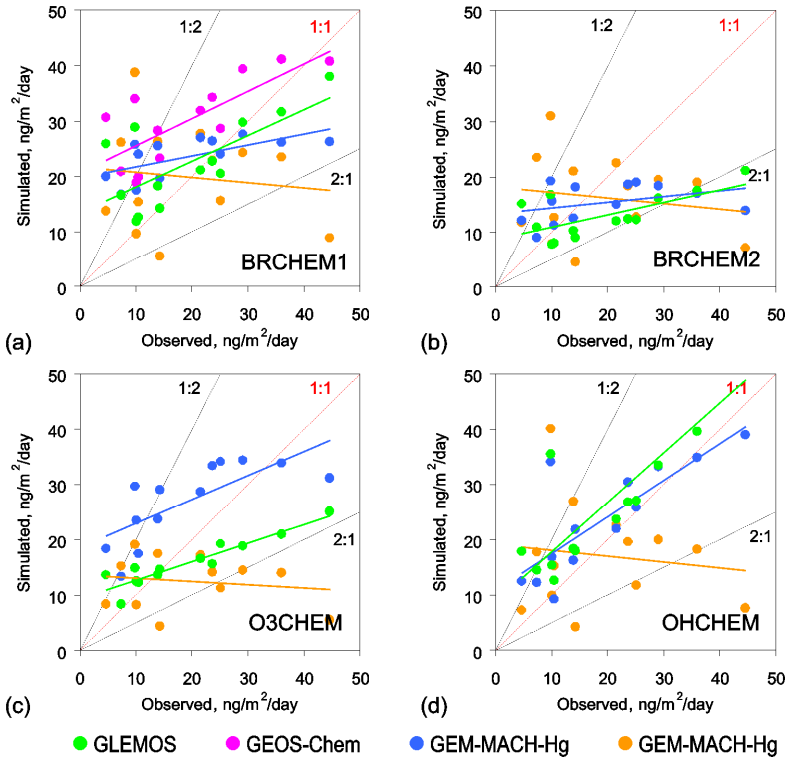


***Fig. 2.12.*** *Scatter plots of simulated vs. observed annual mean wet deposition flux in 2013 averaged over different territorial groups of sites for different model experiments: (a) BrCHEM1, (b) BrCHEM2, (c) O3CHEM, and (d) OHCHEM. Solid lines depict linear approximation. Dotted red line depicts the 1:1 ratio; dotted black lines show deviation by a factor of 2*

As shown, simulations with the Br oxidation mechanism and the first set of Br concentration data (BrCHEM1) satisfactorily reproduced observations (Fig. 2.12a). The models agreed relatively well with each other, and the model-to-measurement deviations generally did not exceed a factor of 2. However, all models overpredicted low deposition fluxes at Asian and southern sites. The overestimation of Hg wet deposition at two high-altitude Asian sites (Mt. Waliguan and Mt. Ailao) can be connected with the inability of the coarse-spatial-resolution global models to reproduce complex meteorological conditions in mountain regions. Overprediction at southern sites (Cape Grim and Amsterdam Island) can be explained by the very high Br concentrations predicted by the first dataset at temperate latitudes in the Southern Hemisphere.

Use of the same mechanism with the other Br dataset led to considerably lower wet deposition levels (Fig. 2.12b) due to use of much lower Br concentrations, particularly in the free troposphere. Hence, uncertainties in the available estimates of Br atmospheric concentration strongly affected simulation results for Hg cycling in the atmosphere. Model simulations with the $O_3$ and OH oxidation mechanisms (O3CHEM and OHCHEM) provided reasonable agreement between modelling results and measurements (Fig. 2.12c and d). Two of the three models (GEM-MACH-Hg and GLEMOS) demonstrated fairly good correlations with observations, but again tended to overestimate lower observed values. The OH oxidation chemistry provided somewhat better agreement in terms of the slope of the regression line, which was closer to the reference 1:1 line, indicating better reproduction of both low and high wet deposition fluxes.

Analysis of all the simulation experiments and comparison with variety of measurement data allowed making the following conclusions:

- The interhemispheric gradient of gaseous elemental mercury (GEM) concentration in the surface air is largely formed by the spatial distribution of anthropogenic emissions that prevails in the Northern Hemisphere. The contributions of natural and secondary emissions enhanced the south-to-north gradient, but their effect was less significant.

- Simulations with different chemical mechanisms provided somewhat different spatial GEM concentration patterns in surface air. Higher spatial correlations were obtained for the oxidation reactions with Br and OH radical, enabling better reproduction of the meridional GEM concentration profile. The reaction with $O_3$ provided poorer spatial correlation because it leveled the intercontinental GEM gradient.

- There was a general tendency to overestimate observed reactive mercury (RM) concentrations, which can be attributed to incorrect speciation of Hg emissions, the uncertainties of Hg atmospheric chemistry, and incomplete RM capture by measurements.

- Atmospheric chemistry strongly affected the RM/GEM ratio in the atmosphere. The Br chemistry provided the best agreement with observations, reproducing both general levels and seasonal variation of the RM/GEM ratio in the near-surface layer. However, the global distribution of Br concentration is highly uncertain. Model simulations with the OH chemical mechanism predicted a shift in maximum RM/GEM ratios from spring to summer, but $O_3$-initiated chemistry did not predict significant seasonal variations in Hg oxidation.

- Use of OH chemistry enabled reproduction of both the periods of maximum and minimum values and the amplitude of observed seasonal variations of mercury wet deposition. Model runs with the Br oxidation mechanism predicted a wet deposition maximum in spring, instead of in summer as observed at monitoring sites in Europe and North America. $O_3$ chemistry did not predict significant seasonal changes of wet deposition flux in these regions.

***All results of the study were published in a series of peer-reviewed papers [Travnikov et al., 2017; Bieser et al., 2017; Angot et al., 2016]. Main findings of the study will be used for further development of the modelling approaches for mercury within EMEP.***

# 3. COUNTRY-SPECIFIC STUDIES OF HEAVY METAL POLLUTION (POLAND)

This chapter is focused on main pilot results of country-specific case study of cadmium pollution levels in Poland. First of all, the chapter presents description of spatial distribution of cadmium levels in 2014 in Poland and in neighbouring countries. Besides, discrepancies between modelling results calculated with fine (0.1° x 0.1°) spatial resolution and measurement data are analyzed. Special attention is paid to the overview of the main factors affecting seasonal variability of modelled concentrations in air. Finally, main directions of further activity on the study are proposed.

## 3.1. Objectives of the study

Assessment and investigation of country-scale heavy metal pollution levels is carried out by MSC-E in close cooperation with national experts in the format of case studies for a particular country. These studies have already been carried out for Croatia, the Czech Republic, the Netherlands and Belarus. The current study is focused on evaluation and analysis of cadmium pollution levels in Poland in 2014.

According to decisions of the Executive Body for CLRTAP [*ECE/EB.AIR/113/Add.1*], atmospheric modelling under EMEP Programme has to move to new EMEP grid. The old grid describes the EMEP region with resolution 50x50 $km^2$ on stereographic projection, while the new grid is represented on latitude-longitude projection and with finer spatial resolution. Comparison of modelling results calculated on old and new grid in the EMEP region is described in Chapter 2. Country-specific study for Poland provides good opportunity to test the model ability to simulate pollution levels on the new grid with fine (0.1° x 0.1°) spatial resolution and compare the results on new and old grid at national scale.

Three main objectives are formulated for the country-specific case study of cadmium pollution in Poland. The first aim is to test the model ability to simulate pollution levels on new grid with fine (0.1° x 0.1°) spatial resolution. The second aim is analysis of factors affecting cadmium pollution levels in Poland, taking into account modelling results and national data on emission and monitoring. Finally, it is planned to provide the country's national experts with detailed information on cadmium pollution in Poland with fine spatial resolution. This information could be used by policy-makers in the field of environmental protection in the country and will include source-receptor matrices, contribution to pollution levels in national administrative regions from foreign emission sources, large point sources (LPS), key emission source categories etc.

## 3.2. Input information

Input information used for assessment of cadmium pollution levels at national scale in Poland includes emission data, monitoring data, fields of meteorological parameters, land-cover, wind re-suspension etc. Most important part of this information was provided by national experts while the rest was prepared by MSC-E. Input data is prepared for the modelling domain with resolution 0.1° x 0.1°. The domain entirely covers territory of Poland, the Czech Republic and Slovakia (Fig. 3.1). Besides, Germany, Austria, Hungary, Romania, Ukraine, Belarus, Russia, Latvia, Lithuania, Denmark and Sweden are partly included in the domain.

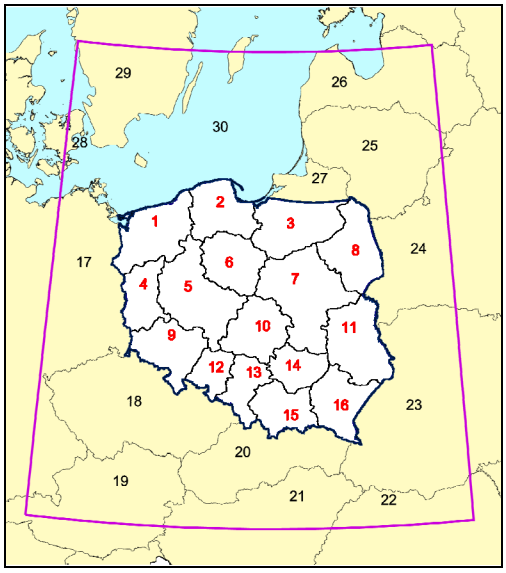


| Polish provinces (voevodships) | Other countries and regions |
|---|---|
| 1. Zachodniopomorskie | 17. Germany |
| 2. Pomorskie | 18. The Czech Republic |
| 3. Warminsko-Mazurskie | 19. Austria |
| 4. Lubuskie | 20. Slovakia |
| 5. Wielkopolskie | 21. Hungary |
| 6. Kujawsko-Pomorskie | 22. Romania |
| 7. Mazowieckie | 23. Ukraine |
| 8. Podlaskie | 24. Belarus |
| 9. Dolnoslaskie | 25. Lithuania |
| 10. Lydzkie | 26. Latvia |
| 11. Lubelskie | 27. Russia |
| 12. Opolskie | 28. Denmark |
| 13. Slaskie | 29. Sweden |
| 14. Swietokrzyskie | 30. The Baltic Sea |
| 15. Malopolskie | |
| 16. Podkarpackie | |

***Fig. 3.1.*** *Countries and Polish provinces (voevodships) covered by modelling domain with resolution 0.1° x 0.1°. Purple frame indicates boundaries of the modelling domain*

Gridded emission data of cadmium in 2014 with spatial resolution of 0.1° x 0.1° was provided by national experts from Poland. For other countries situated within modelling domain emission data, prepared by CEIP, were interpolated from 50x50km$^2$ to 0.1° x 0.1° grid (Fig. 3.2a). In addition to this, cadmium emission data from LPS (energy production, cement industry, coke and copper production) were presented by national experts (Fig. 3.2b).

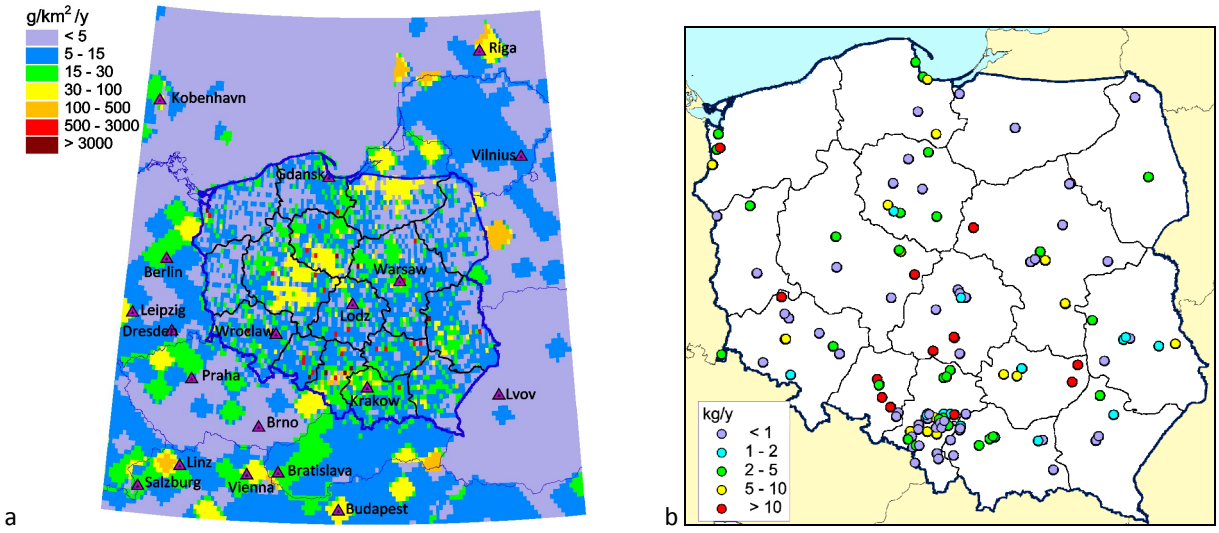


***Fig. 3.2.*** *Spatial distribution of cadmium emission in the modelling domain (a) and distribution of emissions from LPS in Poland (b)*

Information on gridded cadmium emissions in Poland from source categories was provided by national experts. Total emission values from source categories are summarized in Table 3.1. Most of cadmium (about 70%) in 2014 is emitted from sources related to category “Industry”, followed by “Other Stationary Combustion” (16.6%) and “Public Power” (5.1%).

***Table 3.1.*** *Emission of cadmium in Poland from GNFR source categories in 2014*

| Emission source category (GNFR) | Emission, t/y | Fraction of national total value (%) |
|---|---|---|
| A_PublicPower | 0.71 | 5.1 |
| B_Industry | 9.72 | 70.1 |
| C_OtherStationaryComb. | 2.30 | 16.6 |
| D_Fugitive | 0.52 | 3.8 |
| E_Solvents | 3.5E-06 | 2.6E-05 |
| F_RoadTransport | 0.43 | 3.1 |
| G_Shipping | 2.2E-03 | 1.6E-02 |
| I_Offroad | 0.08 | 0.6 |
| J_Waste | 0.09 | 0.7 |
| Total | 13.86 | 100 |

Spatial distribution of cadmium emission from two main source categories is highly different. Most significant emissions from source category B ‘Industry’ are located in particular gridcells, while over most part of the country’s territory emissions from this sector are low (Fig. 3.3a). The highest emissions are noted for Slaskie and Opolskie voevodships. Besides, relatively high emissions from this source category take place in Malopolskie, Dolnoslaskie, Lubelskie, Mazowieckie, Kujawsko-Pomorskie and Zachodniopomorskie voevodships.

Emission from source category “Other Stationary Combustion” is distributed more uniformly over the Polish territory. The highest emission fluxes are noted for the central (Wielkopolskie, Kujawsko-Pomorskie), northern (Warminsko-Mazurskie) and southern (Slaskie, Malopolskie) voevodhips of the country (Fig. 3.3b).

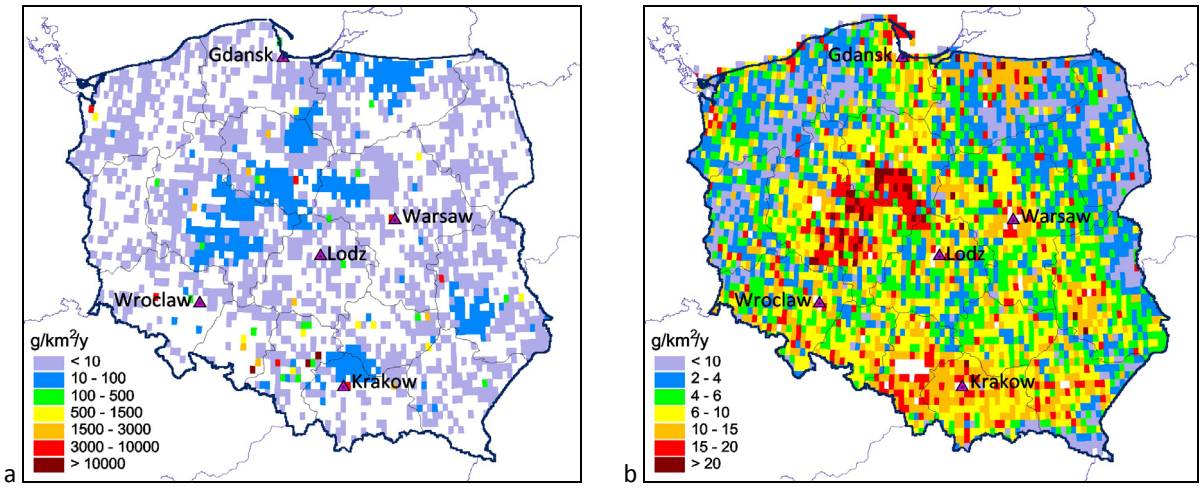


***Fig. 3.3.*** *Spatial distribution of cadmium emission in Poland from source categories “Industry” (a) and “Other Stationary Combustion” (b) in 2014. Please note that colour palettes of these two maps are different*

Another type of information necessary for the assessment of pollution level is monitoring data. Measurements of concentrations in air and wet deposition fluxes provide information about state of pollution in particular locations. Besides, monitoring information is used for evaluation of modelling results.

According to classification used within European Union, measurement stations in Europe are subdivided according to type of area where stations are located, and from viewpoint of predominant sources affecting the stations [*Larssen et al*., 1999]. Area types include urban (almost or completely built-up area), suburban (built-up area mixed with agricultural lands, woods etc) and rural. Rural stations additionally subdivided into the following categories:

- Rural-Near city (area within 10 km from the border of an urban or suburban area),
- Rural-Regional (10-50 km from major sources/source areas)
- Rural-Remote (50 km from major sources/source areas)

Subdivision of stations regarding to predominant emission sources includes the following types:

- Traffic (located in close proximity to a road and strongly influenced by traffic emissions)
- Industrial (located near single industrial sources or industrial areas)
- Background (not dominated by single emission source; representative of a wider area of at least several square kilometers)

For analysis of cadmium pollution levels in Poland in the framework of country-specific study measurements carried out at both EMEP stations and Polish national network are used. There are eight EMEP stations in the modelling domain which measurements of concentrations in air are used in the study (Fig. 3.4a). One of them is located in Poland, and the rest – in other countries (Germany, the Czech Republic, Sweden, and Latvia).

Experts from Poland provided concentrations of cadmium measured at 84 stations of national monitoring network. Among them there are three background regional, two sub-urban and 79 urban stations (Fig. 3.4b).

Information on wet deposition fluxes in the modelling domain is available from 10 EMEP stations (Fig. 3.5a). Among them two stations are located in Poland, while the others - in neighbouring countries (Germany, the Czech Republic, Slovakia, Latvia). Besides, information on wet deposition fluxes from 23 stations was also provided by national experts (Fig. 3.5b).

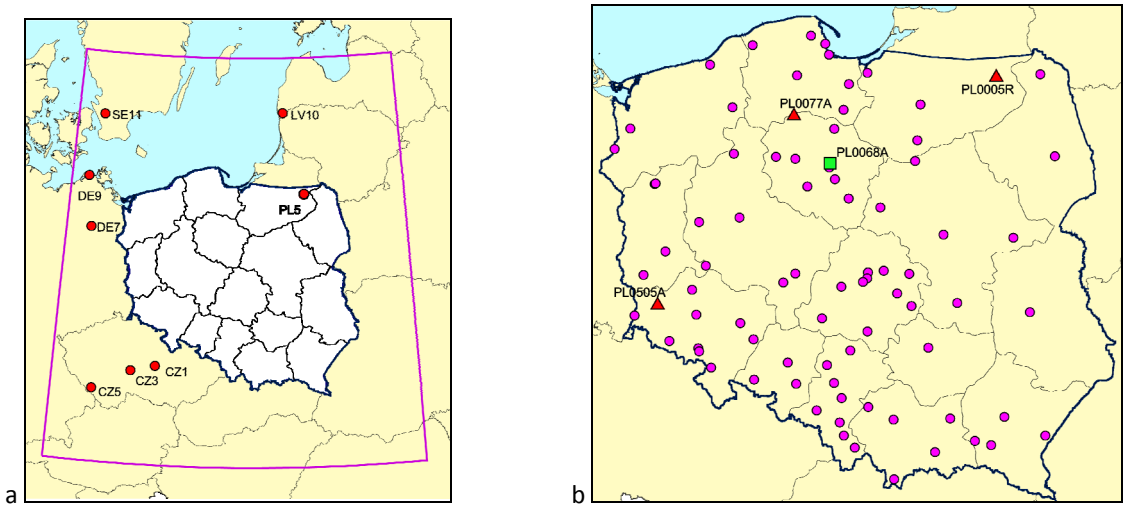


***Fig. 3.4.*** *Location of stations measuring concentrations of cadmium in air at the EMEP network (a) and national monitoring network (b). In Fig. (b) purple circles depict urban, green square – sub-urban and red triangles – background regional stations*

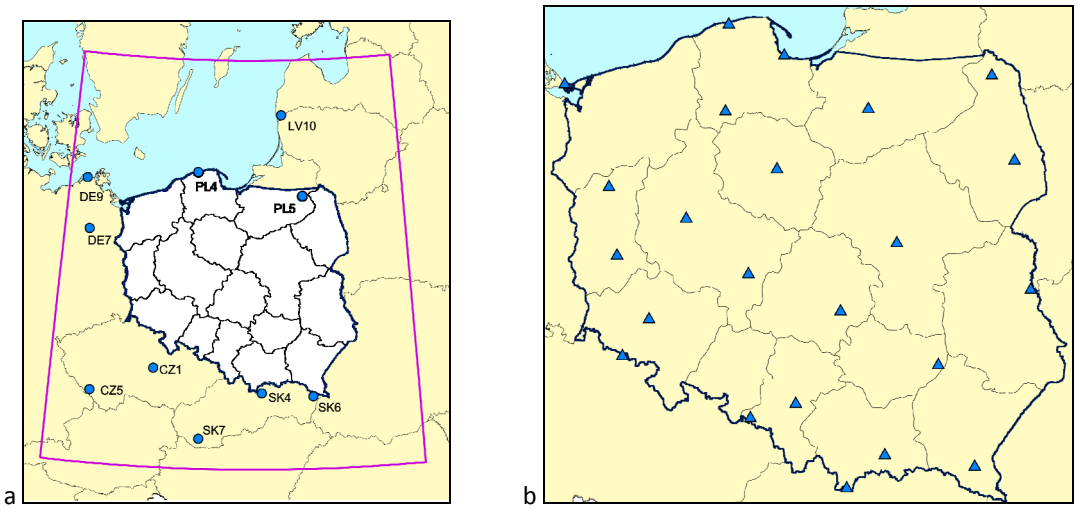


***Fig. 3.5.*** *Location of stations measuring wet deposition fluxes of cadmium at the EMEP network (a) and national Polish network (b)*

## 3.3. Analysis of transition from old to new EMEP grid at country scale

To simulate cadmium concentrations and deposition in the selected modelling domain nesting approach is used. At the first stage cadmium pollution levels are calculated in the entire EMEP region. The results of these simulations are used as boundary concentrations for modelling in the selected domain with spatial resolution of 0.1°x0.1°.

Annual mean concentrations in air calculated on new grid with fine spatial resolution are compared with the concentrations obtained on old EMEP grid. In general, spatial distribution of these air concentrations is similar. The highest levels (more than 0.5 ng/m$^3$) take place in the southern part of Poland (Fig. 3.6). These relatively high levels are explained by location of significant emission sources

in southern and south-western regions of the country. Declining gradient from southern towards the eastern, western and northern parts of Poland is reproduced by both calculations. In these parts of the country the concentrations vary from 0.1 to 0.3 ng/m$^3$. Spatial patterns of cadmium air concentrations outside territory of Poland are similar because the same emission data are used in modelling.

At the same time, there are differences between the considered spatial distributions. First of all, there is an area of relatively high concentrations in air, calculated on new grid, in the central part of Poland (Fig. 3.6a). It is explained by differences in spatial distributions of emissions, provided for old and new grid. Besides, on the map with finer spatial resolution a number of 'hot spots' of relatively high air concentrations is revealed. These 'hot spots' are not seen on the old grid map (Fig. 3.6b) because of coarser spatial resolution.

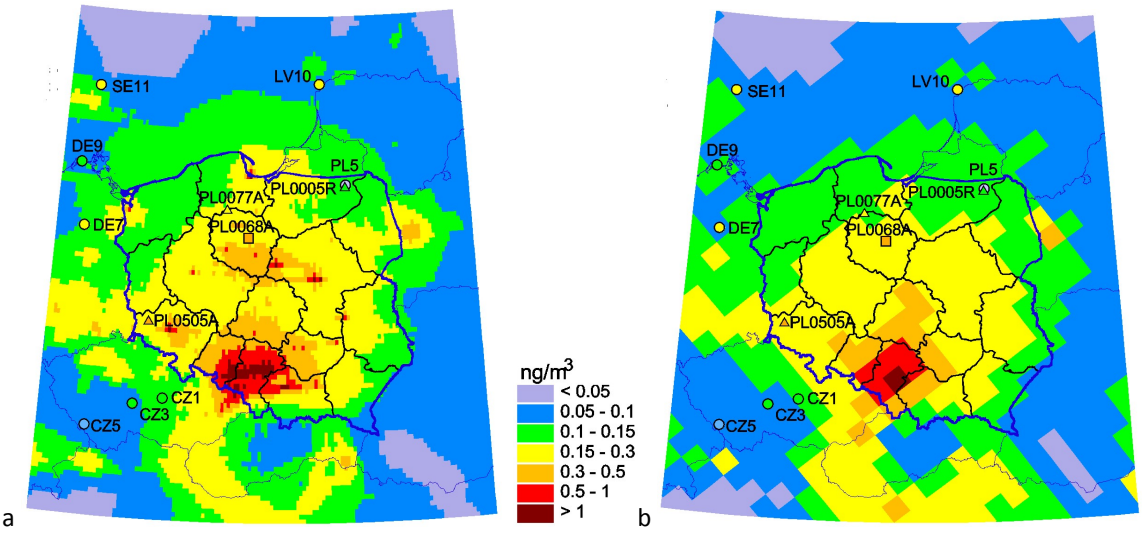


***Fig. 3.6.*** *Mean annual modelled concentrations in air on new (a) and old (b) grid and observed concentrations at EMEP (circles), regional background (triangles) and suburban (squares) stations. Measurements are shown in the same colour palette as modelled concentrations*

For evaluation of the model performance on new and old grid calculation results are compared with each other and with measured air concentrations. EMEP stations and national regional background and suburban stations are selected for the comparison.

The model performance is characterized by the following statistical indicators:

- Pearson correlation coefficient $R_{corr}$
- Mean Relative Bias (MRB)

$$MRB = \frac{(\overline{M} - \overline{O})}{\overline{O}} \cdot 100\% \qquad [3.1]$$

- Normalized root mean square error (NRMSE)

$$NRMSE = \frac{1}{\overline{O}} \cdot \sqrt{\frac{\sum_{i}^{N} (M_i - O_i)^2}{N}} \qquad [3.2]$$

- Fraction of model-measurement pairs of values differing from each other within 2-fold and 3-fold range (F2 and F3, respectively)

In formulas [3.1] and [3.2] $M_i$, $O_i$ mean modelled and observed values at i$^{th}$ station, $\overline{M}, \overline{O}$ - averaged modelled and observed values, $N$ – number of model-measurement pairs

At most of stations the modelling results obtained on new grid are closer to observed values compared to those obtained on old grid (Fig. 3.7). Air concentrations modelled at new grid have lower mean relative bias than those modelled at old grid (-23% vs. -37%) and lower NRMSE (0.37 vs. 0.52), which indicates closer agreement to observations in the selected modelling domain (Table 3.2). Spatial correlation coefficients are practically the same (around 0.9). The most significant changes of modelled concentrations are noted for Polish national stations, while at the EMEP stations the changes are small. Relatively small changes for the EMEP stations are explained by the usage of the same cadmium emission data outside territory of Poland.

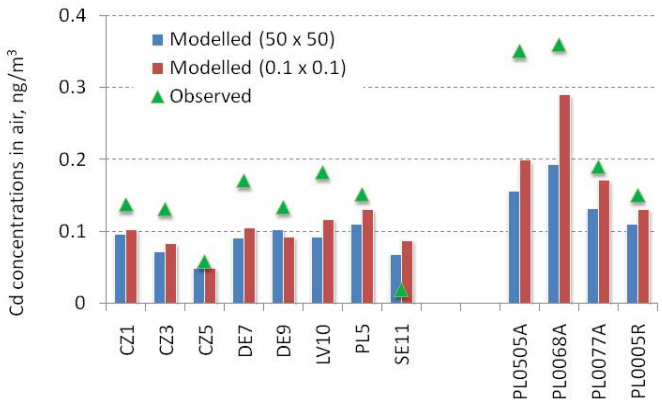


***Fig. 3.7.*** *Annual mean modelled (50x50 km$^2$, 0.1°x0.1°) and observed concentrations of cadmium at the EMEP and national Polish background regional and suburban stations*

***Transition from old (50x50km$^2$) to new (0.1°x0.1°) EMEP grid resulted to some improvement of quality of mean annual modelled concentrations at background regional stations in Poland and neighbouring areas.***

***Table 3.2.*** *Statistical indices of comparison between modelled and observed concentrations of cadmium in air*

| Statistical indicator | 50 x 50 km$^2$ | 0.1°x0.1° |
|---|---|---|
| MRB, % | -37 | -23 |
| Rcorr | 0.91 | 0.89 |
| NRMSE | 0.52 | 0.37 |
| F2, % | 83 | 92 |
| F3, % | 92 | 92 |

## 3.4. Analysis of factors affecting cadmium levels in Poland

Transition from old to new grid resulted to improvement of modelled air concentrations compared to the observed levels. However, the overall underestimation of measured air concentrations remains. Comparison of monthly mean modelled and observed air concentrations demonstrates that at most of stations modelled and observed air concentrations are close in warm period. However, in cold period the model underestimates the observed levels (Fig. 3.8).

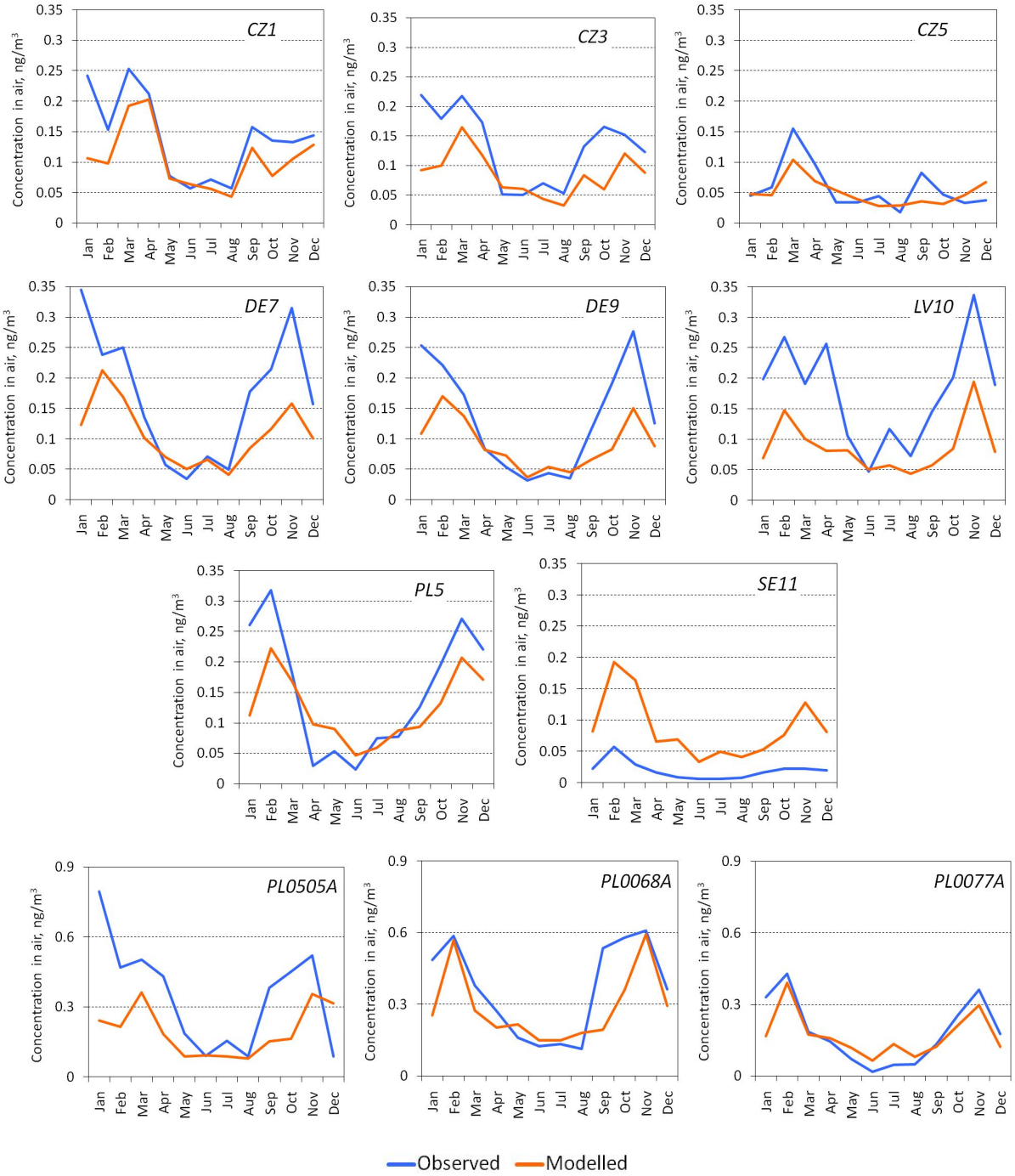


***Fig. 3.8.*** *Monthly mean modelled and observed concentrations of cadmium in air in 2014 at EMEP and national (background regional and suburban) Polish stations*

Seasonal changes of cadmium pollution levels could be caused by various reasons. First of all, a number of meteorological parameters undergo seasonal changes. In particular, significant seasonal changes are typical for turbulent vertical exchange within atmospheric boundary layer. In warm season height of atmospheric boundary layer and turbulent mixing is larger than that in cold period. Stronger exchange leads to decline of near-surface concentrations. In cold period the situation is opposite. Cooling of the underlying surface favours origin of near-surface inversions and suppression of vertical mixing, which results to increase of pollutant concentrations in the surface air.

Monthly mean modelled concentrations in air at background monitoring stations are compared with heights of atmospheric boundary layer. At most of stations the concentrations and heights of atmospheric boundary layers are anticorrelated. For example, at national station PL0068A the correlation coefficient for monthly mean values is -0.84 (Fig 3.9). In these calculations seasonal changes of cadmium emissions are not considered. Therefore, this result demonstrates that the modelled near-surface air concentrations are influenced by seasonal variability of meteorological conditions. However, taking into account monthly changes of meteorological parameters alone is insufficient to reproduce the observed seasonal variability of air concentrations.

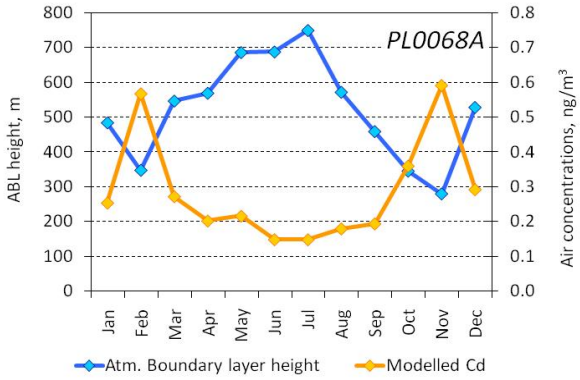


***Fig. 3.9.*** *Monthly mean values of atmospheric boundary layer height and cadmium concentrations in air at national Polish station PL0068A*

Seasonal variability of emission data is another factor influencing temporal variations of air concentrations. In order to evaluate sensitivity of modelling results to seasonal changes of emissions, a set of model test calculations was carried out. In the base case calculations no variations of emissions is taken into account. In test calculations three scenarios were considered with prescribed amplitude of total emission of 30%, 50% and 70%.

Scenario-based concentrations of cadmium have higher levels in cold period and lower – in warm period compared to the base-case calculations. The increase of concentrations in cold period reaches 50%, and the decline in warm period - 60% relative to base case values (Fig. 3.10). At some stations the increase of monthly-mean concentrations favours to reach observed levels (e.g., at station PL5). At other stations the scenario-based air concentrations even exceed observed levels in cold period (e.g., PL0068A, PL0077A). However, at the majority of stations the increase in cold period is insufficient, and the observed levels remain significantly underestimated. At the same time, modelled air concentrations in warm period become lower than the observed ones. Therefore, to reach better agreement between monthly mean values of modelled and observed levels, magnitude of emission in cold season has to be even higher, while in warm period – comparable with that used in base case calculations.

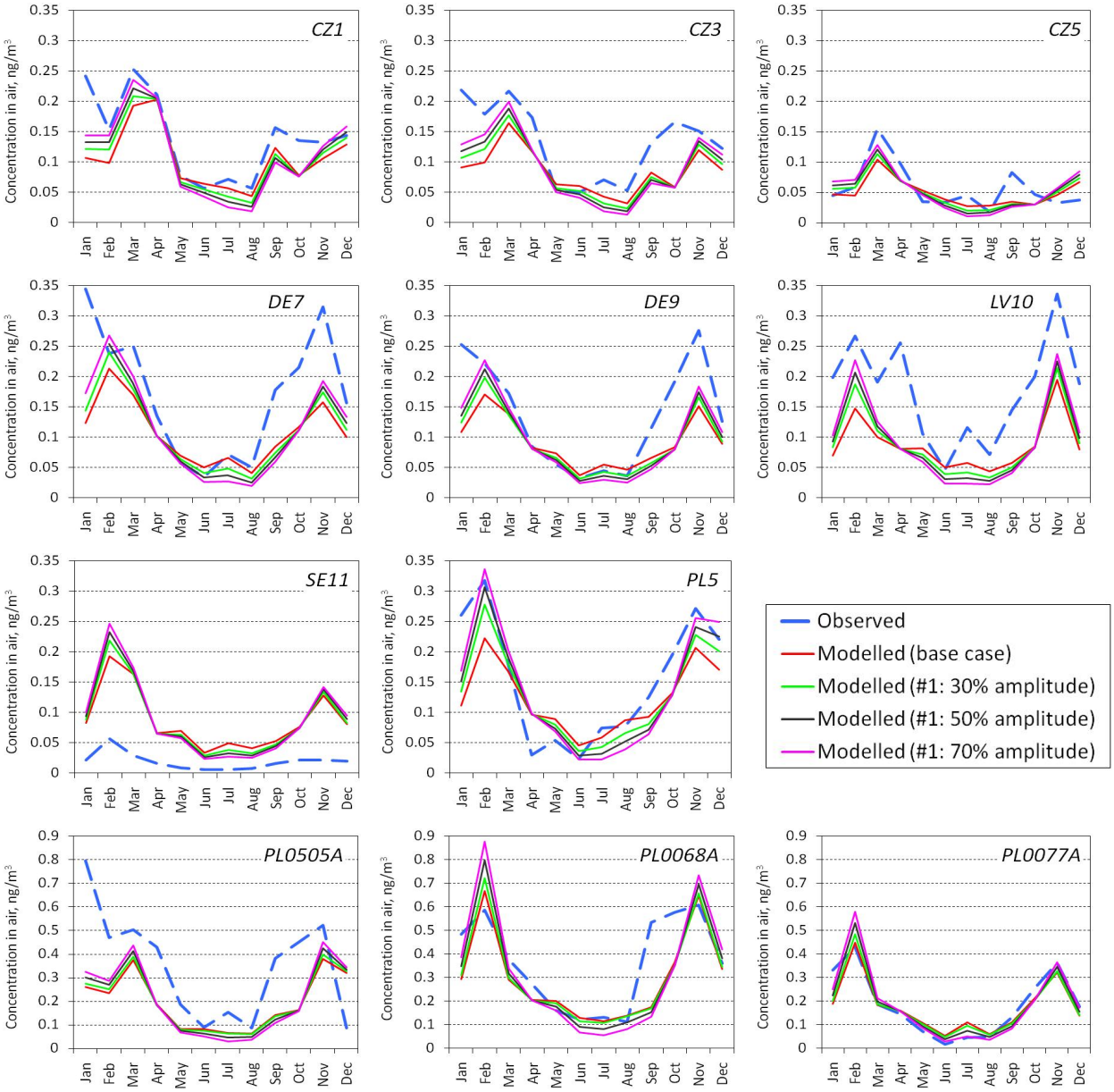


***Fig. 3.10.*** *Monthly mean cadmium air concentrations observed at Polish background regional and EMEP stations and modelled using scenarios of emission seasonal variability*

In the described model tests the assumption about seasonal changes are applied to total emission. However, real seasonal variability depends on peculiarities of economic activity. Therefore, seasonal changes of emission should be applied to emission source categories. For example, in the LOTUS/EUROS model emissions from transport and industry categories are assumed to have low seasonal changes, while emissions from residential combustion have distinct maximum in winter and minimum in summer [*Bieser et al.*, 2011] (Fig. 3.11). In the work of [*Aulinger et al.*, 2011] variability of emission caused by residential combustion depends on temperature of ambient air.

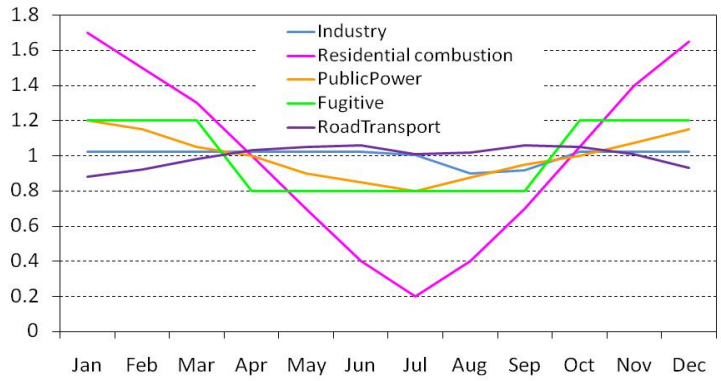


***Fig. 3.11.*** *Monthly factors applied to emission source categories, used in LOTUS/EUROS model*

Available emission inventories contain information about contribution of emission source categories to total emission values. According to the data provided by national experts as much as 70% of total national cadmium emission in Poland is caused by industry, while around 17% - by residential heating (Table 3.1). Following CEIP data [*CEIP*, 2017], in other countries which fully or partly located in the modelling domain, the contribution of emission from residential combustion sector ranges from 0% (Russia, Ukraine) to almost 90% (Romania) (Fig. 3.12). However, for the model domain as whole, the contribution of residential combustion sector to total cadmium emission is not very high (21%).

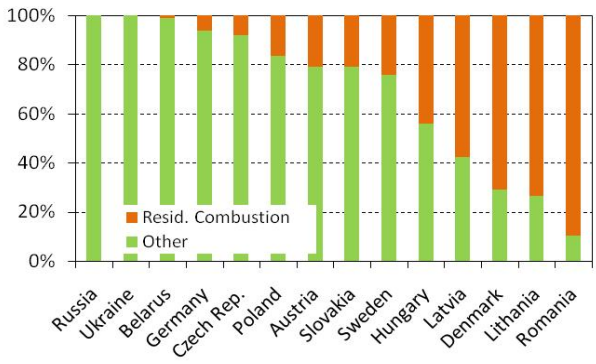


***Fig. 3.12.*** *Relative contribution of residential combustion sector to total emissions in countries located in the selected modelling domain*

Emission from residential combustion sector, reported in different years, varies considerably. According to reporting in 2014, its annual emission value in Poland varied from 18.4 to 26.5 tonnes in the period from 2005 to 2012 [*CEIP*, 2017]. However, the values reported in current year (2017) varied from 2.1 to 2.9 for the same period [*CEIP*, 2017]. Thus, the reported emission from residential combustion sector dropped by on order of magnitude (8 – 9 fold). Emissions from other sectors have not changed significantly (Fig. 3.13). Most likely that this rapid change of emissions is caused by methodological reasons. Therefore, emission of cadmium from source category 'residential combustion' may contain significant uncertainties.

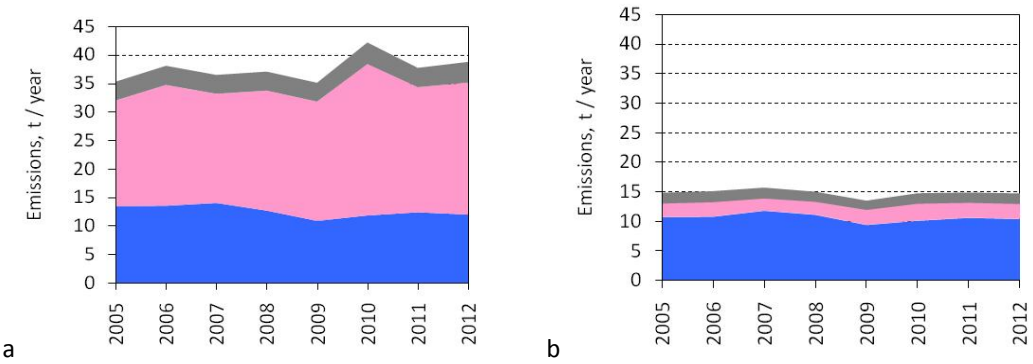


***Fig. 3.13.*** *National total emission of cadmium in Poland according to reporting in 2014 (a) and 2017 (b)*

On the base of information on sectoral composition of cadmium emissions and seasonal coefficients, used in LOTUS/EUROS model, emission data for modelling were prepared. In spite of high amplitude of emissions from residential combustion sector, overall seasonal changes of cadmium emissions in Poland are relatively low (Fig. 3.14a). Ratio between maximum (January) and minimum (August) total emissions is only 1.4. It can hardly help to reproduce observed seasonal changes of air concentrations. Taking into account sharp change in reporting emissions from this sector, additional set of emissions was prepared with the 5-fold increase of emissions from residential combustion. In the second set the ratio between maximum (January) and minimum (July) emissions is 2.6 (Fig. 3.14b). As seen, significant distinction between these to emission sets is seen for cold period, while the values in warm period do not change much.

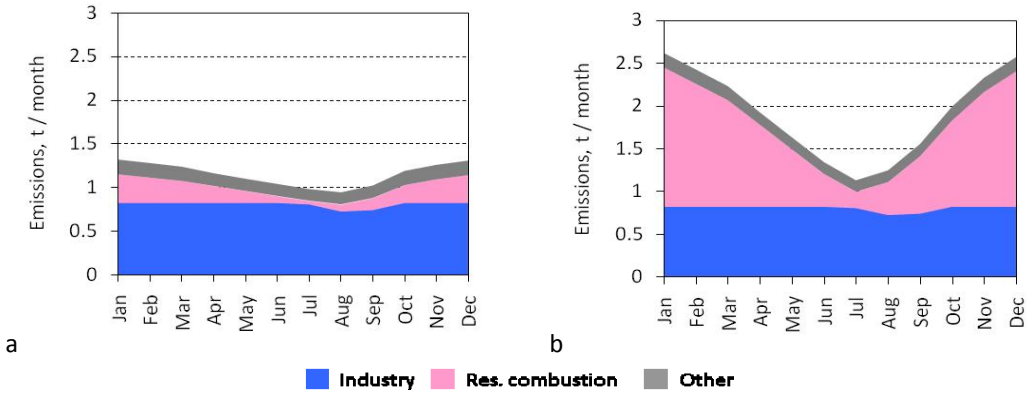


***Fig. 3.14.*** *Seasonal changes of cadmium emission data in Poland with original (a) and 5-fold increased (b) contribution of emission from residential combustion sector*

The experiment demonstrated that the use of increased emission from 'residential combustion' sector favours significant reduction of discrepancies between modelled and measured cadmium levels in cold period, while in warm period the modelled levels do not change much (Fig. 3.15). However, more detailed research on contribution of this sector to pollution levels is needed. Model simulations aimed at identifying contribution of different source categories of national and foreign emissions to pollution levels in various regions of Poland are needed. Besides, alternative approaches based on analysis of measurement data of wide range of pollutants (other heavy metals, acidifying

compounds, particulate matter etc.) at urban and background regional stations can be applied [*Lenschow et al*., 2001].

***Further improvement of cadmium emission data, in particular, from residential combustion source category, will favour better quality of pollution levels assessment***

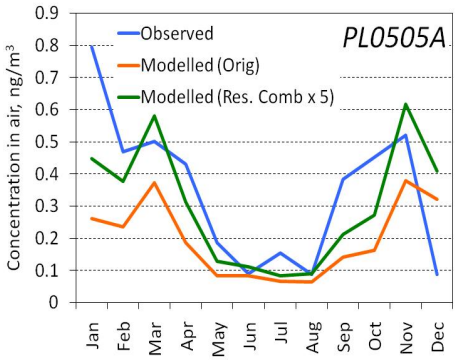


***Fig. 3.15.*** *Monthly-mean air concentrations of cadmium, modelled using different emissions form source category 'residential combustion' and observed at station PL0505A*

The third considered factor affecting seasonal variability of cadmium levels is episodic transboundary transport from polluted regions. In order to trace this effect, time series of measured and modelled concentrations at Polish stations are compared, and back trajectories are analyzed for particular episodes. For example, at the EMEP Polish station PL5 observed cadmium high peak weekly-mean concentrations occur in the beginning of February, end of October and middle of December (Fig. 3.16). However, there are also periods when the model underestimates the observed concentrations. For example, it takes place in the middle of January and middle of November.

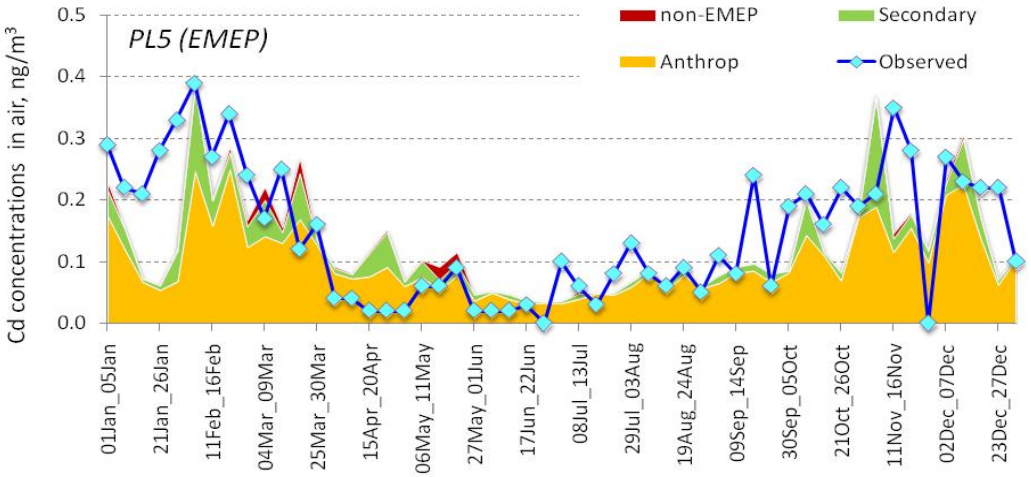


***Fig. 3.16.*** *Time series of modelled and observed concentrations of cadmium at the EMEP station PL5 (Diabla Gora) in 2014*

Online HYSPLIT model [*Stein et al*., 2015] is used to generate back trajectories for the considered periods. Frequencies of the trajectory's presence in each grid cell were calculated. In periods from 4$^{th}$ to 10$^{th}$ of February and from 9$^{th}$ to 15$^{th}$ of December, when the model catches the observed high cadmium concentrations, air masses to the station are coming through western or south-western parts of Europe and passing through central and southern Poland (Fig. 3.17a, b). However, when air masses are arriving from countries in the eastern part of the EMEP region, the modelled concentrations are significantly lower than the observed ones (Fig. 3.17c, d). Therefore, cadmium

emission data available for these countries need more detailed analysis in cooperation with national experts, CEIP and modelling community. ***For improvement of model assessment of cadmium pollution levels in the EMEP countries more work on emission data in Eastern Europe is needed.***

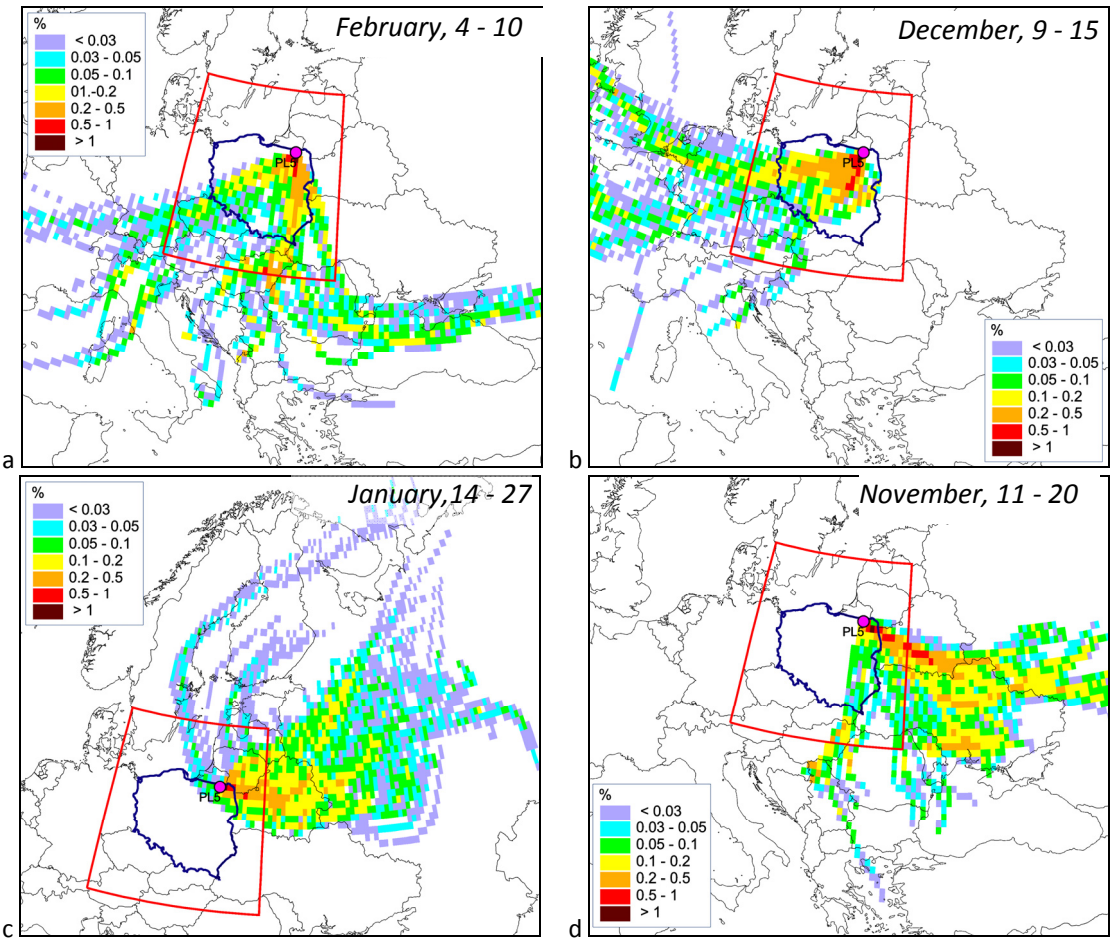


***Fig. 3.17.*** *HYSPLIT-based back trajectories (expressed as frequencies of trajectory presence in grid cells) for the EMEP station PL5 (Diabla Gora) for the periods with low (a,b) and significant (c,d) discrepancies between modelled and observed concentrations of cadmium in air*

## 3.5. Evaluation of modelling results at urban stations

There are about 80 stations measuring concentrations of cadmium in air at urban locations. Although the model is not designed to reproduce pollution levels in cities, calculated air concentrations with resolutions for these locations are compared with the observed levels. Modelled concentrations underestimate measured concentrations in air at urban stations (Fig. 3.18). It is not surprising because even at spatial resolution of 0.1°x0.1° the model cannot take into account all peculiarities of meteorological conditions and distribution of emission sources within the model gridcells. However, it is interesting to note, that at some stations, in particular at those located in Warsaw (PL0214A), Gdansk (PL0052A) and Plock (PL0389A), the overestimation of observed levels takes place (Fig. 3.19).

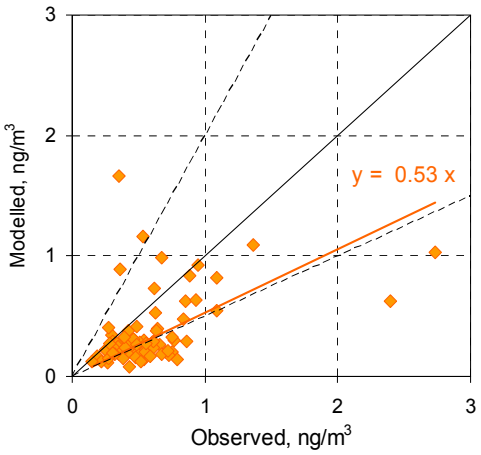


***Fig. 3.18.*** *Scatter plot of modelled (0.1°x0.1°) and observed cadmium concentrations in air at urban stations for 2014. Dashed lines indicate factor of two range*

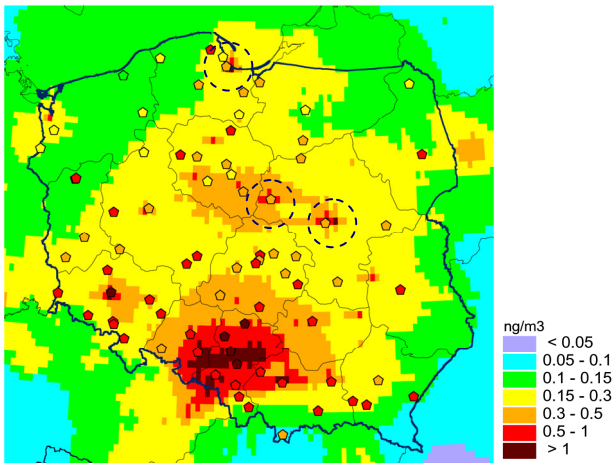


***Fig. 3.19.*** *Modelled (field) and observed (pentagons) concentrations of cadmium in air. Spatial resolution of calculated values is 0.1°x0.1°. Dashed circles indicate location of Warsaw, Gdansk and Plock*

Modelled concentrations in air strongly depend on magnitude and spatial distribution of emission values. For example, station PL0214A, located in Warsaw, is situated in the model grid cell with high cadmium emission. This emission is mostly caused by power station located in the same grid cell (Fig. 3.20). Therefore, the modelled concentration in this grid cell is also high (Fig. 3.21). When coarser resolution is used, the emissions are less spatially concentrated and thus averaged grid cell concentrations are more smoothed. It is possible to conclude, that results of modelling with fine spatial resolution are highly sensitive to spatial distribution of emission data. Further it is planned to organize more detailed investigation of cadmium levels in cities.

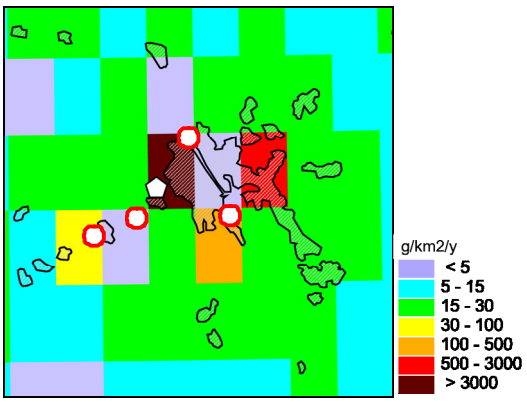


***Fig. 3.20.*** *Cadmium emission in Warsaw city and neighbouring areas. Pentagon indicates location of measurement station PL0214A, red circles – power stations*

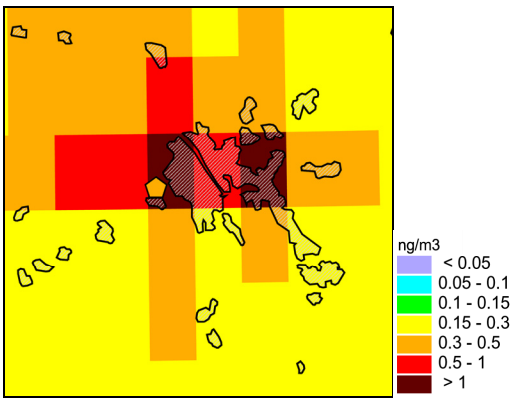


***Fig. 3.21.*** *Mean annual concentrations of cadmium in and around Warsaw city. Pentagon indicates location of measurement station PL0214A*

## 3.6. Future activities

Case study of cadmium air pollution levels in Poland will continue. Further activity in this field will include a number of main tasks. Firs of all, much attention will be paid to analysis of emission sectors and their effect on modelling results. The model tests demonstrate that the modelling results are sensitive to seasonal changes of emission from residential combustion category. However, the described simplified emission scenarios cannot allow to reach observed levels at most of stations. Hence, more sophisticated scenarios should be elaborated.

The analysis of modelling results presented in this chapter is focused on air concentrations. However, there are data on wet deposition fluxes observed both at EMEP and Polish national stations. It is planned to involve information on wet deposition in the analysis of pollution levels in Poland and in evaluation of the model performance.

Finally, it is planned to prepare country-specific information on pollution levels with fine spatial resolution. This information can be helpful for policy-makers for development of national strategies to protect the environment. This information will include transboundary deposition between provinces, contribution to pollution levels from emission source categories and from large point sources.

The results of the study will be summarized in the joint report. Besides, it is planned to produce summary report focusing on main outcomes of country-specific studies taken place for the recent several years.

# 4. COOPERATION AND DISSEMINATION OF INFORMATION

## 4.1. Parties to the Convention

### *4.1.1. Italy*

National Agency for New Technologies, Energy and the Environment of Italy (ENEA) regularly (once in five years) carries out modelling of atmospheric pollution levels of a wide range of pollutants over territory of Italy. These simulations are performed with the usage of Italian national model MINNI developed by ENEA. Results of these simulations are used by the authorities of the country to improve national environmental and human health protection policy.

In accordance with the agreement between ENEA and MSC-E model calculations of air concentrations of heavy metals (Pb, Cd, Hg, As, Ni, Cr, Cu, Zn, Se) were performed over the EMEP domain for 2015. 3D concentrations with spatial resolution of 50x50 $km^2$ and temporal resolution of 6 hours for the agreed area were produced (Fig. 4.1). For mercury concentrations of three forms (elemental, particulate, and gaseous oxidized forms) were prepared. It is planned that these calculation results are used as boundary conditions for MINNI model. The work was carried out under financial support of ENEA.

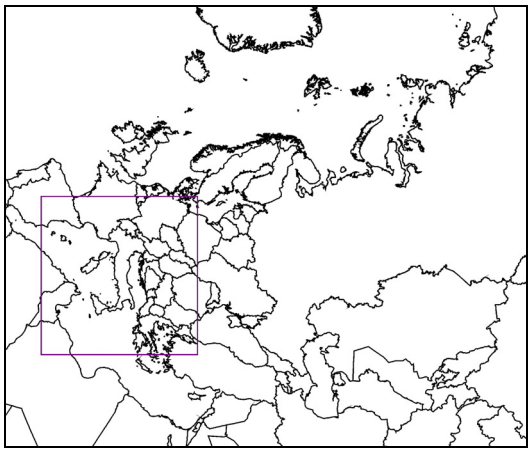

***Fig. 4.1**. EMEP modelling domain and agreed area for Italy*

Modelling of atmospheric transport of heavy metals includes contributions to pollution levels from anthropogenic and secondary emissions within the EMEP domain, and transport from sources located outside the EMEP domain. Gridded emission data in the EMEP region is received from the EMEP Centre on Emission Inventories and Projections (CEIP) [http://www.emep-emissions.at/ceip/]. Emission data, used in modelling for 2015, are based on inventories for 2014, because the data for 2015 were not available in the CEIP database at the moment of the model calculations. Speciation of mercury emissions is based on global-scale mercury emission data for 2010 prepared under UNEP [*AMAP/UNEP*, 2013].

Secondary emission sources of heavy metals are represented by wind re-suspension of dust particles containing heavy metals (Pb, Cd, As, Ni, Cr, Zn, Cu, Se) and natural emission and re-emission of mercury. The modelling approaches to simulate natural emission of mercury and wind re-suspension

of lead and cadmium are documented in the MSC-E reports [*Travnikov and Ryaboshapko,* 2002*; Ilyin et al.,* 2007]. Similar approach was applied for parameterization of re-suspension of other particulate heavy metals (As, Ni, Cr, Zn, Cu, Se).

Model calculations of considered pollutants were carried out over the EMEP domain, while air concentrations were extracted for the agreed area, which included Italy and some neighbouring territories. Modelling results were verified by comparing calculated air concentrations with the levels observed in 2015. The observed air concentrations were derived from EMEP/CCC database (EBAS). It should be noted that at the moment of verification measurement information available in EBAS for 2015 was limited, because some of the countries did not report measurements from their stations. Besides, the stations are located mostly in the central and northern Europe and only few Spanish sites are situated in the agreed domain. Possible alternative data of the EU database AirBase were also not available for 2015.

Results of the verification of modelled air concentrations are summarized in Table 4.1. The statistical indexes, used in the verification, were as follows: mean relative bias (MRB), Pearson's correlation coefficient ($R_c$), Normalized root mean square error (NRMSE) and a share of model-measurement pairs of values differing from each other within 2-fold and 3-fold range (expressed as F2 and F3, respectively).

As seen from the table, the model is capable of calculating air concentrations of heavy metals with reasonable quality: MRB for different pollutants is within ±20% range, and spatial correlation coefficient varies from 0.56 (Ni) to 0.97 (Pb). Statistical indices for Se are not representative because they are based only on measurements from two stations. It is important to note, that quality of modelling results for so-called second-priority metals (As, Ni, Cu, Cr, Zn) is similar to that for metals targeted by the Protocol (Pb, Cd, Hg).

***Table 4.1.*** *Statistical indexes of comparison between modelled and observed concentrations in air of the considered pollutants*

| Pollutant | MRB(%)* | $R_c$** | NRMSE*** | F2 (%) | F3 (%) | N |
|---|---|---|---|---|---|---|
| **Heavy metals** | | | | | | |
| Pb | 9.3 | 0.97 | 0.28 | 81.3 | 100.0 | 16 |
| Cd | 18.7 | 0.80 | 0.85 | 73.3 | 93.3 | 15 |
| Hg | -7.5 | 0.74 | 0.11 | 100.0 | 100.0 | 9 |
| As | -17.4 | 0.78 | 0.46 | 68.8 | 87.5 | 16 |
| Ni | 0.7 | 0.56 | 0.79 | 75.0 | 100.0 | 16 |
| Cr | -15.7 | 0.74 | 0.54 | 69.2 | 84.6 | 13 |
| Cu | -0.6 | 0.72 | 0.76 | 63.6 | 81.8 | 11 |
| Zn | -19.5 | 0.83 | 0.80 | 37.5 | 43.8 | 16 |
| Se | 0.0 | 1.0 | 0.0 | 100.0 | 100.0 | 2 |

* mean relative bias, ** Pearson's correlation coefficient, *** Normalized root mean square error

More detailed information on verification of modelling results for each metal was submitted to ENEA.

Special attention was paid to analysis of spatial distribution of concentrations in air of second priority metals and model performance for these metals. Similar spatial distributions of mean annual air concentrations are noted for arsenic, nickel and chromium. For example, in the EMEP region relatively high (0.3-3 ng/m$^3$) calculated concentrations of arsenic are noted for regions where powerful emission sources are located, such as Poland, Slovakia, Italy, the United Kingdom, east of Ukraine and areas in central part of Russia (Fig. 4.2a). Besides, in the agreed area relatively high concentrations caused by significant contribution of secondary sources take place in the south-eastern part of Greece, south of France and Northern Africa (Fig. 4.2b). In addition to this, in case of chromium relatively high levels are also noted for central and southern regions of the European part of Russia.

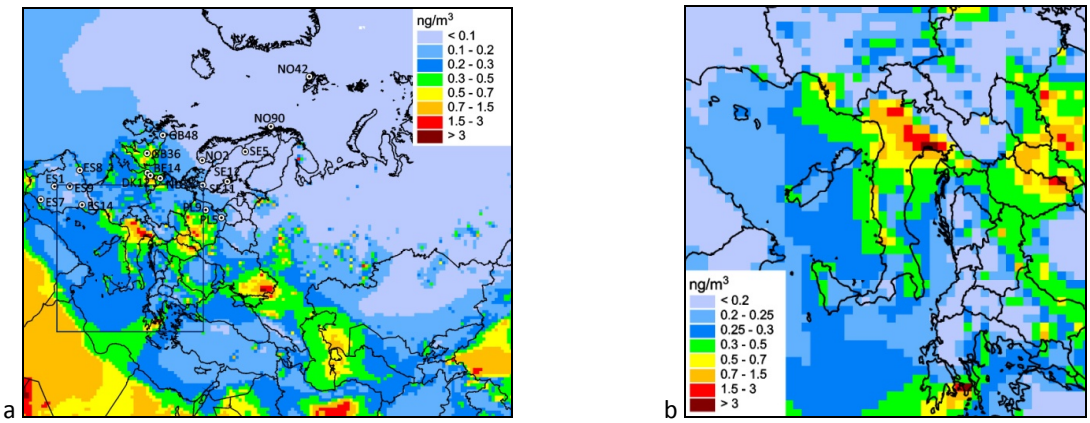


***Fig. 4.2**. Spatial distribution of annual mean concentrations of arsenic over EMEP domain (a) and over the region for MINNI modelling (b) in 2015*

Unlike arsenic, nickel and chromium, spatial distribution of air concentrations of zinc and copper has specific peculiarities. The most significant emissions and, consequently, pollution levels of zinc and copper take place in Germany (Fig. 4.3).

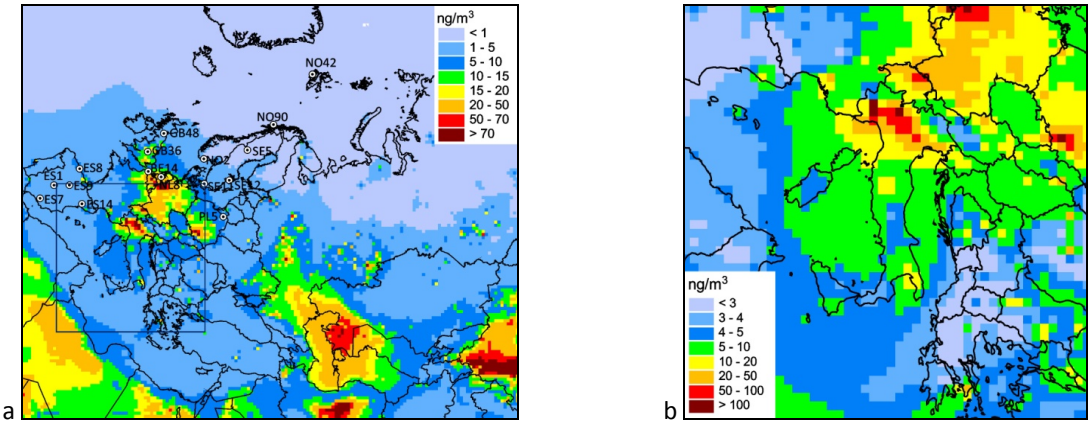


***Fig. 4.3**. Spatial distribution of annual mean concentrations of zinc over EMEP domain (a) and over the region for MINNI modelling (b) in 2015*

Data from 16 EMEP stations measuring arsenic in air in 2015 are involved into verification of the modelling results. Mean relative bias is about -17% which means some underestimation of the

observed levels by the model in area covered by monitoring stations (Table 4.1). The most significant underestimation takes place for stations DK12, PL5, SE5, SE12 and the Norwegian stations (Fig. 4.4). For other stations the bias between observed and modelled levels lies within ±40%. Spatial correlation coefficient is about 0.8, which indicates that spatial variability is captured by the model.

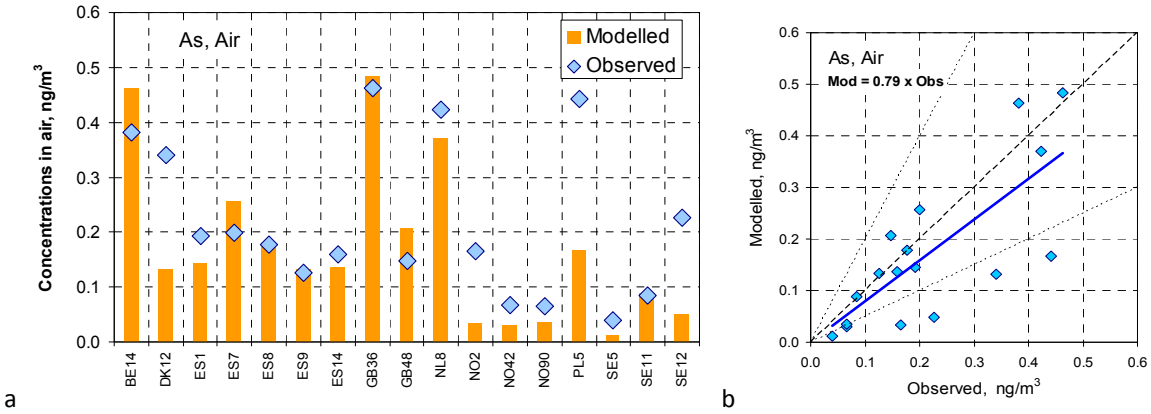


***Fig. 4.4.*** *Annual mean modelled and observed concentrations of arsenic in air in 2015 at individual stations (a) and their scatter plot (b). Dashed line mean 1:1 ratio, and dotted lines mean 2-fold range*

For 2015 data on measured air concentrations are available from 16 stations. Average level of concentrations was predicted by the model with bias about 1% (Table 4.1). However, spatial correlation is not so high compared to other metals (0.56). It is explained by 3-fold underestimation of the levels observed at Spanish station ES7 (Fig. 4.5). If this station is ignored, the correlation coefficient would be 0.79. Some overestimation of Ni levels at stations SE14, PL5 and PL9 is caused by overestimated influence of anthropogenic component of air concentrations.

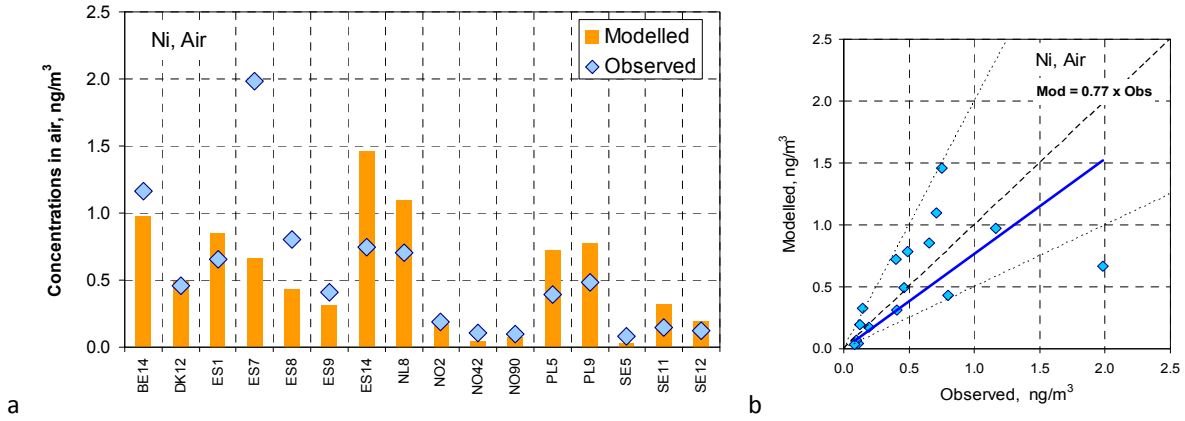


***Fig. 4.5.*** *Annual mean modelled and observed concentrations of nickel in air in 2015 at individual stations (a) and their scatter plot (b). Dashed line mean 1:1 ratio, and dotted lines mean 2-fold range*

Observed air concentrations of chromium in 2015 are available from 13 EMEP stations. Measured concentrations were somewhat (-16%) underestimated by the model (Table 4.1). The underestimation is caused mostly because of outlying measured values at station NO2, where the

modelled value is 8-fold smaller than the observed one (Fig. 4.6). For most of other stations the bias between modelled and observed levels remains with ±50%.

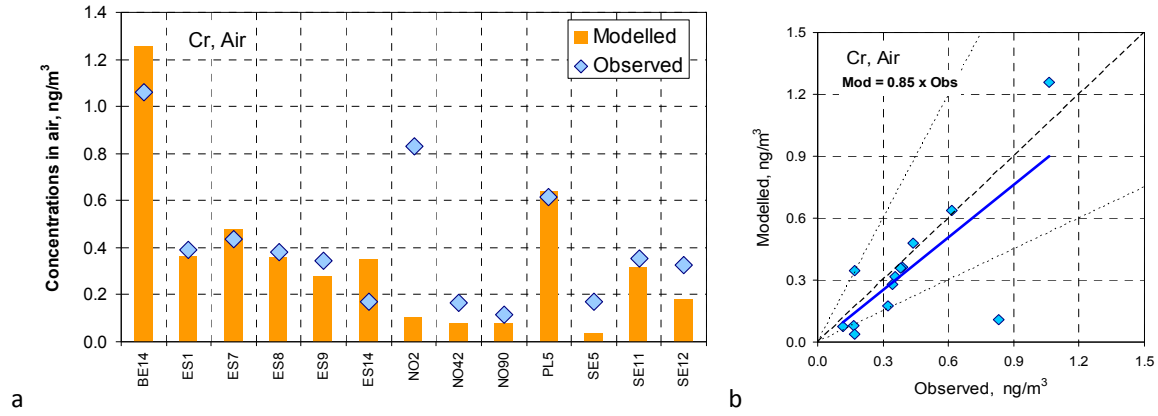


***Fig. 4.6.*** *Annual mean modelled and observed concentrations of chromium in air in 2015 at individual stations (a) and their scatter plot (b). Dashed line mean 1:1 ratio, and dotted lines mean 2-fold range*

Data from 16 stations are involved into comparison of modelled and observed levels of zinc. On average the model underestimates observed zinc levels by about 20%. However, spatial differences in modelling performance are significant. Relatively good agreement between modelled and observed concentrations is seen for stations in the United Kingdom, Sweden and Benelux region (Fig. 4.7). At the same time large differences are noted for Spanish, Norwegian and Polish stations. For comparison, measured levels in 2014 at German stations vary from 6.3 to 18.4 ng/m$^3$, in France – from 7.2 to 16.1 ng/m$^3$. The corresponding median values are 13.6 and 9.5 ng/m$^3$. The only measured value for station in Slovenia is 8.1 ng/m$^3$.

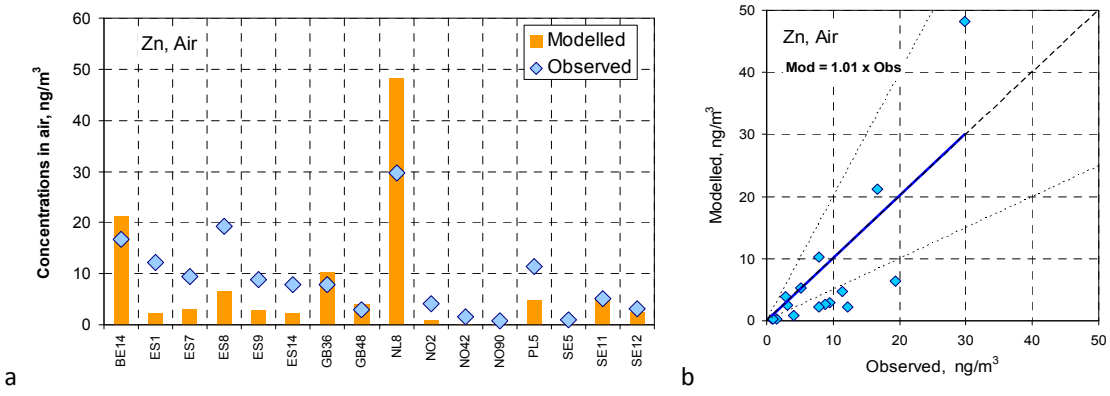


***Fig. 4.7.*** *Annual mean modelled and observed concentrations of zinc in air in 2015 at individual stations (a) and their scatter plot (b). Dashed line mean 1:1 ratio, and dotted lines mean 2-fold range*

Large differences in emission spatial distribution are reflected in distribution of calculated air concentrations in Europe: high concentrations in Germany and Poland are contrasting to low levels in Spain, France, southern and south-eastern parts of Europe. It is likely that the reason of these differences is connected with emission inventories in European countries. For example, according to the data provided by CEIP, around 90% of zinc emission in Germany is caused by automobile tyre and

brake wear, while in other countries the role of this sector is much smaller. In order to identify reasons of mentioned discrepancies between modelled and observed levels of zinc, more detailed investigation is needed.

Information on measured concentrations of copper in air in 2015 is available from 11 stations. On average, the model managed to reproduce the concentrations: the mean relative bias is about -1% and spatial correlation coefficient is 0.72 (Table 4.1). However, the relative differences between modelled and observed levels at particular stations vary significantly. The model underestimates observed levels at stations ES9, GB36 and Norwegian stations (Fig. 4.8). Some overestimation can be mentioned for station BE14, which is likely caused by overprediction of effect of secondary emissions in Benelux region. More than 90% of calculated concentration at station SE11 is contributed by anthropogenic sources. Therefore, significant (4-fold) overestimation at this station is likely explained by uncertainties of anthropogenic emissions.

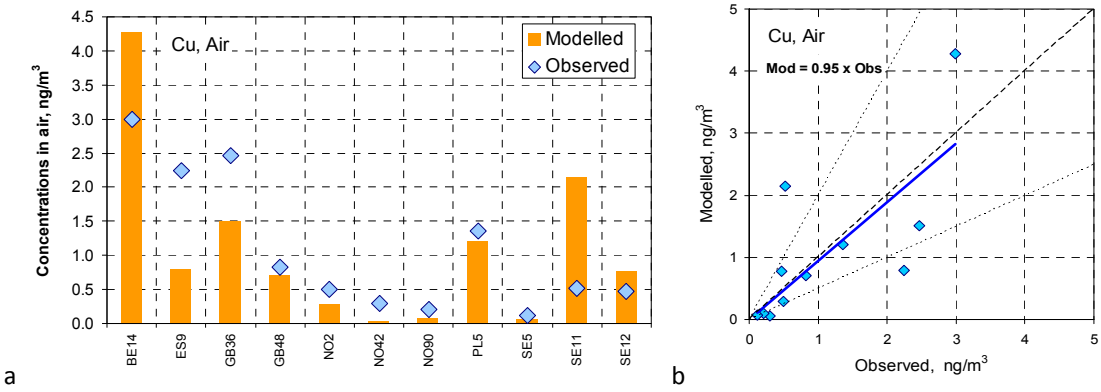


***Fig. 4.8.*** *Annual mean modelled and observed concentrations of zinc in air in 2015 at individual stations (a) and their scatter plot (b). Dashed line mean 1:1 ratio, and dotted lines mean 2-fold range*

Information on selenium measurements in the atmosphere is very limited. Only two British stations provided observed air concentrations in 2015 within the EMEP region. The model reproduced these levels with negligible mean relative bias (Table 4.1). However, it should be noted that no strict conclusions could be derived from the comparison based on the measurement data from only two stations.

In general, concentrations of second-priority metals were simulated with satisfactory accuracy: the mean relative bias is within ±20% range and spatial correlation coefficient varies from 0.6 to 0.8. However, at some particular stations the differences between modelled and observed concentrations can be significant. More detailed analysis of emission data, monitoring information and modelling approaches, carried out in cooperation between EMEP centres and national experts, could favour improvement of quality of model assessment.

Information on pollution levels of heavy metals targeted by the Protocol is regularly reported to the EMEP countries. However, pollution levels of so-called second priority metals (As, Ni, Cr, Cu, Zn, Se) can also be of interest. In particular, for air concentrations of some of these metals (As and Ni) target values are established by EU Directive 2004/107/EC. Modelling of atmospheric transport and deposition of these metals is undertaken by various groups of scientist on regional [*González et al.,* 2012, *Chen et al.,* 2013, *Dore et al.,* 2014, *Adani et al.*, 2015] and global scales [*Wai et al.*, 2016].

Information on lead, cadmium and mercury concentrations and deposition in 2015, described in Chapter 1, is supplemented with modelling results for the second priority metals. Annual mean levels of As, Ni, Cr, Cu, Zn, Se can be provided by the request.

### *4.1.2. Russia*

Assessment of heavy metal pollution levels in the EMEP region requires information about emissions, monitoring data and modelling. Coverage of the EMEP region with monitoring data as well as emission reporting by countries is not uniform. In particular, evaluation of heavy metal pollution levels in Russia is hampered by scarce monitoring data. Besides, official emissions have not been reported to CEIP during several recent years. Nevertheless, information about monitoring data on lead and cadmium air concentrations at Russian measurement stations have been presented at recent TFMM meeting held in May, 2017 in Prague, the Czech Republic. This section is focused on brief analysis of modelled and observed concentrations at Russian stations for 2014.

Background monitoring of heavy metal pollution in Russia is carried out at four stations located in biosphere reserves (BR) of European Part of Russia: Prioksko-Terrasny (PTR), Voronezhsky (VBR), Kavkazsky (KBR) and Astrakhansky (ABR). Concentrations of lead and cadmium observed at Russian stations are mostly comparable with the values observed at EMEP stations (Fig. 4.9). The exceptions are measurements of lead at Prioksko-Terrasny BR and cadmium at Astrakhansky BR, which are relatively higher than the EMEP measurements.

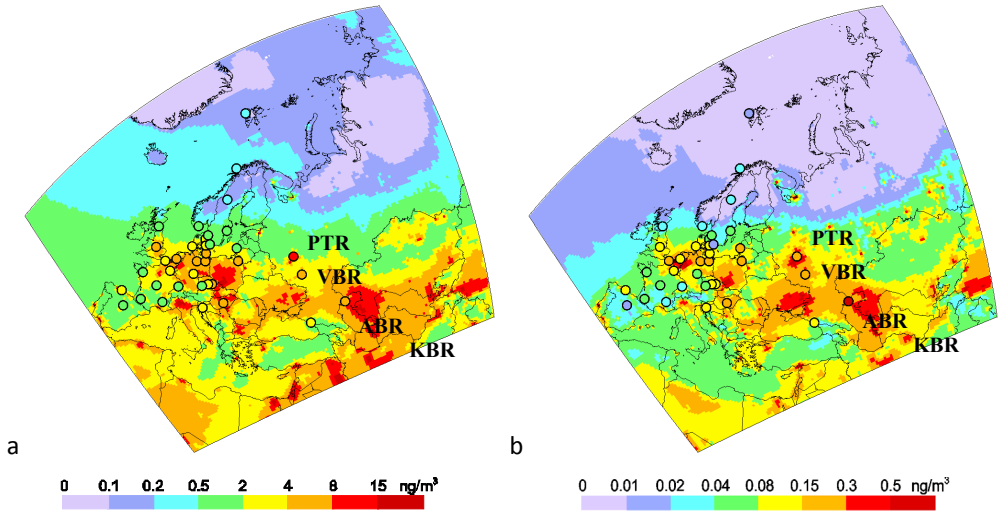


***Fig. 4.9.*** *Modelled and observed annual mean concentrations of lead (a) and cadmium (b) in the EMEP region in 2014*

Annual mean modelled concentrations of lead and cadmium in air are compared with the concentrations observed at stations of Russian monitoring network. Agreement between modelled and measured levels differs significantly among stations. At stations located in the central regions of European part of Russia, such as Prioksko-Terrasny and Voronezhsky Biosphere Reserves, the modelled concentrations of lead are below, and the concentrations of cadmium are above the observed ones (Fig 4.10). In Caucasus region (Kavkazsky Biosphere Reserve) the model tends to underestimate the observed concentrations of both lead and cadmium. In the south-eastern part of

European Russia the model produces lead levels higher than the observed, and cadmium levels lower than the observed at the station Astrakhansky Biosphere Reserve.

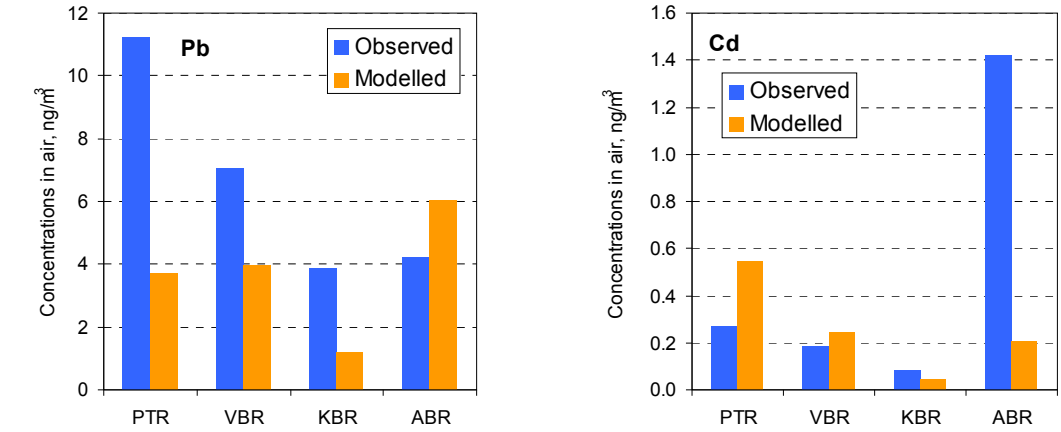


***Fig. 4.10.*** *Annual mean modelled and observed concentrations of lead (a) and cadmium (b) at stations of Russian monitoring network in 2014*

Measurements at Russian stations are carried once per three days. Time series of air concentrations with this frequency are compared in order to identify periods of higher or lower discrepancies between modelled and observed values. Besides, the modelled values are presented as a sum of contribution of anthropogenic, secondary and non-EMEP emission sources.

Observed concentrations of lead at station Prioksko-Terrasny Biosphere Reserve are the highest both among measured values of Russian and EMEP stations (Fig. 4.9a). Probably, these high levels are caused by the influence of motorway with heavy traffic, passing by the station in several kilometres. This fact can explain the significant difference between modelled and observed concentrations of lead at this station.

Time series for station Voronezhsky Biosphere Reserve are shown in Fig. 4.11. As seen, the model better reproduces lead levels in the beginning (January-April) of 2014 than in the other part of the year. For the first four month average modelled (4.7 ng/m$^3$) and observed (5.3 ng/m$^3$) levels are similar. Besides, a number of observed peak concentrations are captured by the model. From May to December the difference between average values of modelled (3.6 ng/m$^3$) and observed (7.9 ng/m$^3$) concentrations is higher. According to current model calculations, the main contribution to the observed levels at this station is made by secondary sources (87%), while the anthropogenic sources contribute 12%, and non-EMEP sources – 1%. It is important to note that in a number of episodes the model overestimates the observed levels because of predominant contribution of secondary sources.

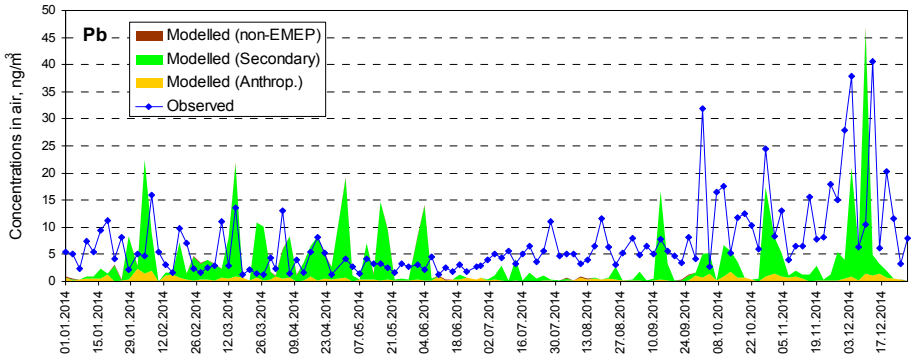


***Fig. 4.11.*** *Time series of modelled and observed concentrations of lead in air at station Voronezhsky Biosphere Reserve*

Opposite situation is noted for cadmium concentrations at station Prioksko-Terrasny Biosphere Reserve. At this station modelled concentrations exceed the observed ones two-fold. The main contribution to modelled levels is made by anthropogenic emission sources (Fig. 4.12), and secondary sources contribute less than 10% to the annual mean calculated concentrations. A number of observed peak concentrations are captured by the model, e.g., for the periods of the middle of September and middle of October. Both the model and observations demonstrate peak concentrations on January, 22, but the model exceeds the observed levels more than 4-fold.

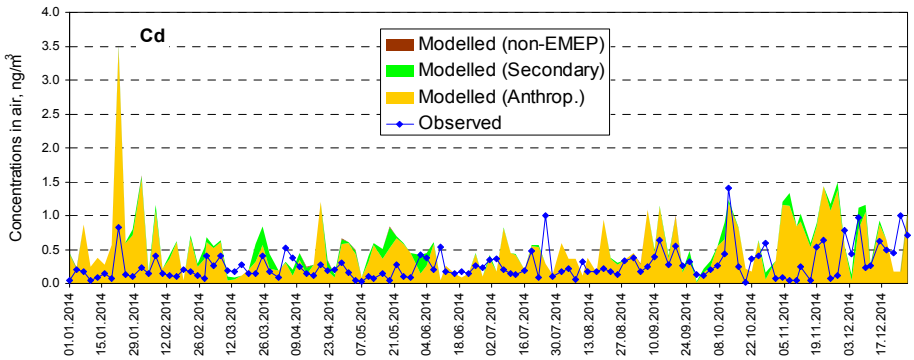


***Fig. 4.12.*** *Time series of modelled and observed concentrations of cadmium in air at station Prioksko-Terrasny Biosphere Reserve*

According to the available gridded emission data, there are few grid cells with large cadmium emission within distance of 50 – 100 km from the station (Fig. 4.13a). Analysis of back trajectories demonstrates that high modelled concentrations are associated with episodes of air mass passing over these areas of large emissions. For example, in the period from 01$^{st}$ – 28$^{th}$ of November the modelled concentrations are higher than the observed ones by an order of magnitude (Fig. 4.13). In this period the back trajectories arrive to the station mostly from the south-western or south-eastern direction, i.e., from regions with high emission values (Fig. 4.13b).

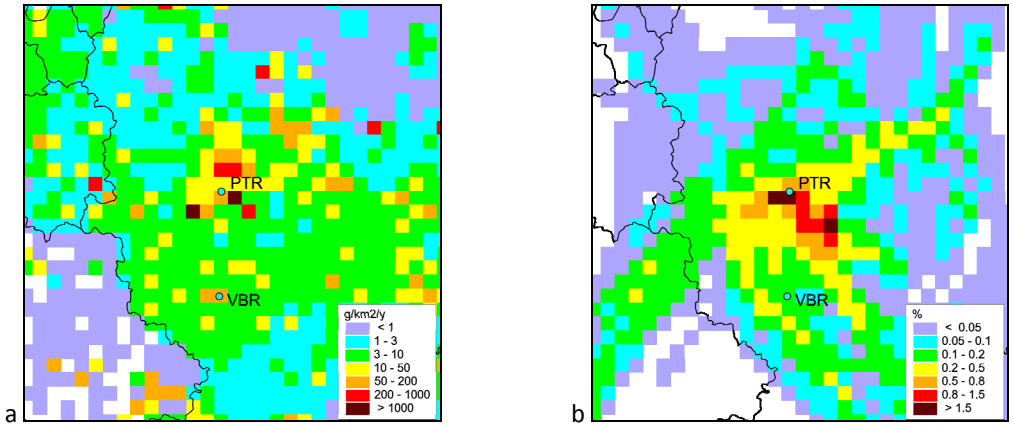


***Fig. 4.13.*** *Annual emission of cadmium (a) and HYSPLIT-based back trajectories (expressed as frequencies of trajectory presence in gridcells) for station Prioksko-Terrasny Biosphere Reserve for 01st – 28th of November*

Unlike other Russian stations, modelled concentrations of lead at station Astrakhansky Biosphere Reserve are higher than the observed levels. There are several episodes, when the modelled concentrations are much higher than the observed ones, e.g., in the middle of February, April, May, in the beginning of December (Fig. 4.14). Some of these peaks correspond to the observed concentrations. These peaks are caused by influence of wind re-suspension of lead from regions of Central Asia.

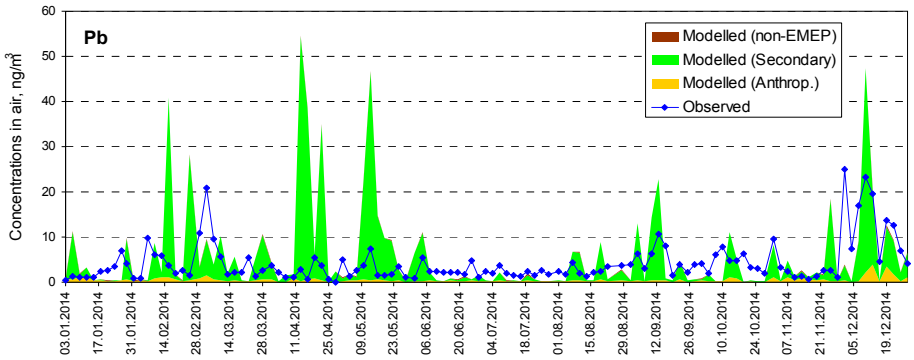


***Fig. 4.14.*** *Time series of modelled and observed concentrations of lead in air at station Astrakhansky Biosphere Reserve*

Observed cadmium concentrations in air at the station Astrakhansky Biosphere Reserve are the highest among other available measured concentrations at Russian stations. These levels are not typical for measurements in background regions either in Russia or in other European countries (Fig. 4.10). These levels may be caused by influence of unaccounted emission sources or monitoring issues.

Brief analysis lead and cadmium levels demonstrated that for a number of episodes modelled and observed concentrations agree relatively well, while in other episodes the discrepancies between modelled and observed values are considerable. The analysis revealed that the noted discrepancies can be caused by various reasons. First of all, anthropogenic emissions of heavy metals from Russia

are not officially reported to CEIP. Lack of national emission data may cause uncertainties in the emission data used in the modelling. It, in turn, can lead to underestimation or overestimation of the observed levels. Another reason is evaluation of re-suspension of heavy metals from desert regions of Central Asia. In Chapter 1 it is demonstrated that secondary sources may significantly affect pollution levels in the EMEP courtiers. Transition from old to new EMEP grid will require adaptation of wind re-suspension scheme of heavy metals. Detailed measurement data from Russian stations can be very important for further evaluation of re-suspension fluxes in the Central Asian region. Finally, quality of measurement data at some stations may need special attention.

Cooperation between the EMEP centres (MSC-E, CEIP, CCC) and national experts from Russia is needed to tackle the identified issues. In particular, special country-specific study aimed at investigation and assessment of heavy metal pollution levels in Russia can facilitate deeper understanding of factors affecting pollution levels in Russia.

## 4.2. Subsidiary bodies of the Convention

### *4.2.1. Task Force on Measurements and Modelling*

In the framework of cooperation with TFMM MSC-E of EMEP took part in 18th meeting of the Task Force held in May 2016 in Prague, the Czech Republic. TFMM was informed about progress in transition of MSC-E atmospheric transport model to new EMEP grid and about pilot results of country-specific case study on assessment of cadmium pollution levels in Poland.

In particular, it was shown that heavy metal pollution levels in the EMEP region, calculated on old and new EMEP grid are very similar in European part of the EMEP region. Major differences in spatial distribution of pollution levels modelled on old and new grid are noted for the southern regions of the EMEP domain and explained by differences in land-cover data used in modelling. Harmonization of land-cover data used by the EMEP centres for modelling and by WGE for evaluation of the effects was suggested.

Pilot results of model calculations of cadmium deposition fluxes and air concentrations with fine spatial resolution in Poland were presented. It was shown that modelling results agreed reasonably well with the observed concentrations measured at the EMEP and national Polish stations. Analysis of discrepancies between modelled and measured levels revealed underestimation of the observed levels in cold seasons. Main reasons responsible for seasonal changes of pollution levels were analyzed (Chapter 3.). Plans of further activity on country-specific study for Poland were demonstrated.

The following issues can be discussed between the EMEP Centres and scientific community at the next meeting of TFMM:

- Modelling of suspension of wind-blown dust and harmonization of land-cover data in operational work under the Convention.
- Approaches to compare “grid cell-averaged” modelled concentrations and deposition against “point” measured values

### *4.2.2. Working Group on Effects*

Heavy metals are toxic pollutants known for their adverse effects on human health and biota. Laboratory and experimental research established a link between heavy metal concentrations in the environment (soils, water) and their concentrations in tissues of living organisms. At certain concentrations in the environment (critical limits) the corresponding concentration in human body or tissues of other organisms may lead to harmful effects [*de Vries et al*., 2015]. Ecotoxicological effects of heavy metals include injuries of plant leaves, hampered growth of vegetation and changes of physiologic and microbiological conversion processes [*Hettelingh et al*., 2015]. Accumulation of cadmium in human body negatively affects kidney and bones, while lead and mercury are well-known neurotoxins [*WHO*, 2007]. Deposition fluxes, at which critical limit concentrations in the media are reached, are referred to as critical loads.

The critical loads approach is widely used for assessment of adverse effects of various pollutants on terrestrial and aquatic ecosystems in Europe [*De Vries et et al*., 1994; *Kuylenstierna et al.*, 1998; *Reinds et al*., 2008; *Holmberg et al*., 2013; *De Vries et al*., 2015] and other regions [*Hettelingh et al*., 1995; *Kuylenstierna et al*., 2001; *Bouwman et al*., 2002]. Recently, it was successfully applied for risk assessment of heavy metal (cadmium, lead and mercury) pollution on a regional scale within the EMEP region [*Hettelingh et al*., 2015]. The assessment was based on a collaborative work of the Coordination Centre for Effects (CCE) and MSC-E. This year MSC-E has continued the co-operation with CCE on evaluation of critical loads exceedances for heavy metals on regional and hemispheric scales.

## EMEP region

In spite of large (around 80%) decline of lead deposition over the recent two decades, the fraction of ecosystem area where lead levels exceeded critical loads is still significant (about 20%) [*de Wit et al*., 2016; *Slootweg et al*. 2007]. At the same time measurements of heavy metal concentrations at ICP-IM sites demonstrates that lead content in forest soils tends to increase for the period from 1990 to 2013 [*Bringmark et al*., 2013].

Ecosystem-specific deposition of lead, cadmium and mercury is calculated annually for the EMEP region and individual EMEP countries to support work of the effect community. All variety of information is available at the MSC-E website (www.msceast.org). An example of simulated lead deposition to arable lands and forests in 2015 is shown in Fig. 4.15. As seen the highest lead deposition to both types of land cover is predicted in Central Europe (southern Poland), Southern Europe (northern Italy and the Balkans), and the Caucasus, where deposition fluxes exceed 1 kg/km$^2$/y for arable lands, and 2.5 kg/km$^2$/y for forests. Over the most part of Scandinavia and northern Russia the fluxes are below 0.2 kg/km$^2$/y.

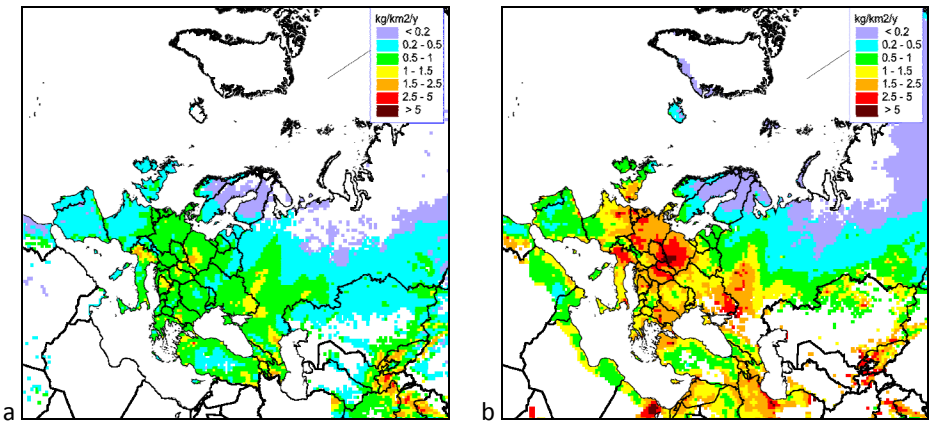


***Fig. 4.15.*** *Annual lead deposition flux to arable lands (a) and forest (b) in 2015*

***It is important to note that the most recent estimates critical load exeedances for heavy metals are outdated and relate to 2010. An update of information on heavy metal critical loads is needed for assessment of contemporary effects heavy metal pollution on biota and human health.***

## Northern Hemisphere

This year MSC-E has also started a new joint activity with CCE focused on evaluation of critical loads exceedances for mercury on a hemispheric scale. For this purpose, the centre performed modelling of mercury deposition to forests and (semi-)natural vegetation in the boreal and temperate region of the Northern Hemisphere under the current conditions (2010) and in future (2035).

Contemporary levels of mercury deposition were simulated using the global emissions inventory for 2010 [*AMAP/UNEP*, 2013]. Besides, a number of mercury emission scenarios for 2035 were considered in the study [*Pacyna et al.*, 2016]. They include the 'Current Policy' scenario (CP 2035) assuming that governmental policies and measures existing in 2010 have been adopted, including those that have not been fully implemented; the 'New Policy' scenario (NP 2035) assuming that policy commitments and plans announced by countries worldwide to reduce greenhouse gas emissions, as well as phase out fossil-energy subsidies, were fully implemented; and the 'Maximum Feasible Reduction' scenario (MFR 2035) set out a target of all counties reaching the highest feasible reduction efficiency in each emission sector. General discussion of the scenarios and forecasts of mercury pollution levels on global and regional scales were discussed in previous EMEP Status Reports [*Ilyin et al*., 2015; 2016].

Figure 4.16 illustrates the model assessment of mercury deposition flux to forests of the Northern Hemisphere in 2010 and in 2035 according to the selected emission scenarios. As seen, in 2010 mercury atmospheric load to forests in major part of Europe and North America varies within the range of 15-25 g/km$^2$/y (Fig. 4.16a). Similar deposition levels are predicted over tropical forests of Africa and South America. Considerably higher fluxes are characteristics of some areas in Central and Southern Europe (35-50 g/km$^2$/y) as well as in South Asia and East Asia (above 80 g/km$^2$/y). Relatively low mercury deposition was estimated for boreal forests of Scandinavia, Northern Russia and Canada (5-15 g/km$^2$/y).

Similar spatial pattern was simulated for mercury deposition to forests in 2035 according to the 'Current Policy' scenario (Fig. 4.16b). However, it is expected that deposition will decrease in Europe and North America as well as increase in South and East Asia due to appropriate emission changes in these regions. In contrast, the NP 2035 scenario predicts significant deposition reduction in all regions of the Northern Hemisphere except for South Asia, where some increase of deposition to forests is still expected. The maximum decrease of mercury atmospheric load to forests is simulated in accordance with the MFR 2035 scenario. In this case deposition flux evenly decreases in all regions of the Northern Hemisphere and rarely exceeds the value of 25 g/km$^2$/y.

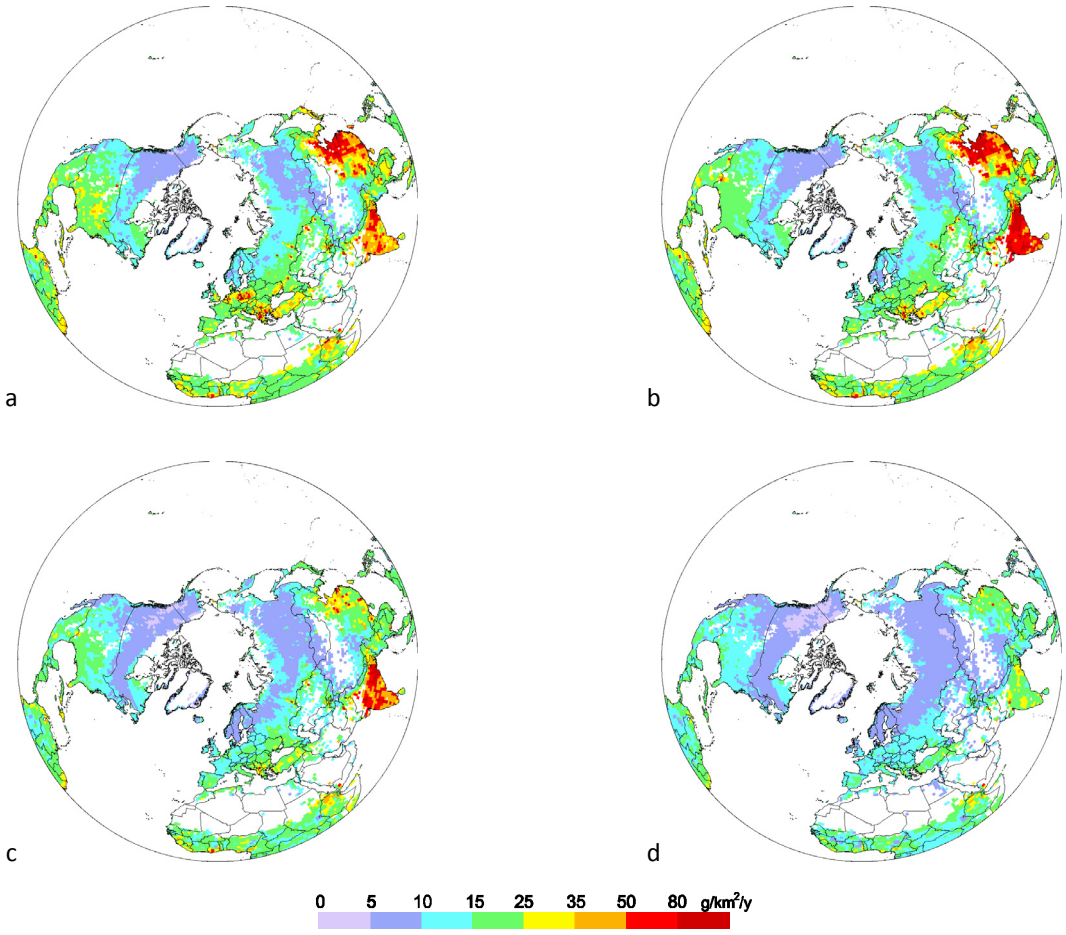


***Fig. 4.16.*** *Mercury deposition flux to forests in the Northern Hemisphere in 2010 (a) and in 2035 according to different emission scenarios: (b) – CP 2035; (c) – NP 2035; (d) – MFR 2035*

Quantitative characteristics of changes of mercury deposition to forest between 2010 and the future scenarios are given in Fig. 4.17 in the form of probability distribution of deposition fluxes over the whole forested territories of the Northern Hemisphere. The probability density corresponding to the current conditions (2010) is characterized by bi-modal distribution with the major maximum at 10 g/km$^2$/y and the secondary maximum at 18 g/km$^2$/y (Fig. 4.17a). The former corresponds to deposition over large territories of boreal forests of Scandinavia, Northern and Eastern Russia and Canada; the latter characterized deposition to temperate forests of Europe and North America as well as tropical forests of Africa and South America.

As it was mentioned above the CP 2035 scenario does not expect significant changes of mercury deposition (Fig. 4.17b). Decrease of deposition fluxes in Europe and North America leads to slight shift of the secondary peak to smaller values. The increase of forest areas with high deposition (above 50 g/km$^2$/y) in South and East Asia is not seen as it falls beyond the scope of the plot. Deposition changes according to the NP 2035 scenario with respect to 2010 appear on the graph by shifting both peaks toward smaller values, 8 and 15 g/km$^2$/y, respectively (Fig. 4.17b). Besides, forest areas where mercury deposition exceeds 20 g/km$^2$/y reduce considerably. The MFR 2035 scenario is characterized by even larger shift of the peaks (7 and 13 g/km$^2$/y) and limitation of mercury deposition flux by 30 g/km$^2$/y over all forests of the Northern Hemisphere (Fig. 4.17c).

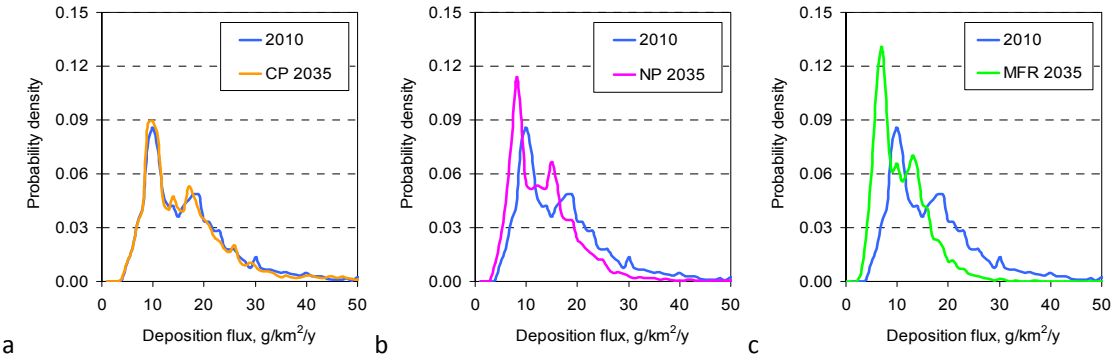


***Fig. 4.17.*** *Probability distribution of mercury deposition flux to forests of the Northern Hemisphere in 2035 in comparison with 2010 according to different emission scenarios: (a) – CP 2035; (b) – NP 2035; (c) – MFR 2035*

***This collaborative work will be continued next year. Results of the study can be used both for risk assessment of mercury pollution in the EMEP region and to support international efforts to protect human health and the environment from the adverse effects of mercury on a global scale.***

## 4.3. International organizations

### *4.3.1. UN Environment*

Global concern over mercury pollution resulted in development of the Minamata Convention on Mercury a legally-binding multilateral environmental agreement that was adopted by governments in 2013 and will enter into force in August 2017 [http://www.mercuryconvention.org/]. To support the negotiation process the United Nations Environment Programme (UN Environment) coordinated preparation of a series of Global Mercury Assessments (GMA) [*UNEP*, 2002; *AMAP/UNEP*, 2008; *AMAP/UNEP*, 2013; *AMAP/UNEP*, 2015]. EMEP participated in all the assessments sharing information on mercury pollution and coordinating activities on global scale modelling.

A new Global Mercury Assessment 2018 (GMA 2018) is now under development in accordance with the request of the UN Environment Governing Council (Decision 27/12). MSC-E takes part in the assessment coordinating work of an international group of experts focused on modelling of mercury pollution on global and regional scales. The expert group includes modelling teams from different scientific institutions of Europe and North America: Helmholtz-Zentrum Geesthacht (HZG, Germany), Institute of Atmospheric Pollution Research (CNR-IIA, Italy), Massachusetts Institute of Technology (MIT, USA), Environment and Climate Change Canada (ECCC, Canada), National Oceanic and Atmospheric Administration (NOAA, USA), Lamar University (LU, USA). The research co-ordination work of MSC-E for GMA 2018 is funded by the Arctic Monitoring and Assessment Programme as a part of a bi-lateral contract.

The part of GMA 2018 focused on assessment of mercury fate and transport in the atmosphere consists of both review of recent studies on model assessment of mercury pollution and new model estimates of mercury intercontinental transport involving an updated global inventory of mercury anthropogenic emissions. The literature survey of recent modelling studies consider various aspects of mercury pollution on global and regional scales including new findings in atmospheric chemistry

and other processes governing mercury cycling in the atmosphere, estimates of mercury transport between continents and regions, evaluation of historical trends and future scenarios, and peculiarities of mercury pollution in different regions such as Europe, North America, East Asia and the polar regions.

Atmospheric chemistry plays a key role in the fate of mercury in the atmosphere defining its long-range transport potential and deposition to the ground. Despite decades of intensive studies by international scientific community, the nature and details of mercury oxidation and reduction chemistry remain very uncertain. A number of recent studies continue investigation of chemical mechanisms involving both theoretical methods [e.g. *Auzmendi-Murua et al*., 2014; *Dibble et al.,* 2012, 2014; *Jiao and Dibble*, 2015, 2017; *Dibble and Schwid*, 2016] and chemical transport models [e.g. *Kos et al.,* 2013; *Weiss-Penzias et al*., 2015; *Shah et al.,* 2016; *Travnikov et al*., 2017; *Bieser et al.,* 2017; *Horowitz et al.,* 2017]. A thorough discussion of possible oxidation and reduction mechanisms as well as associated uncertainties is given by *Ariya et al.* [2015]. Other important processes of mercury transport and fate, which include dry and wet deposition as well as air-surface exchange, were also addressed in the recent studies [*Zhang et al.,* 2012; *Wright and Zhang*, 2015; *Zhang et al.,* 2016; *Nair et al*., 2013; *Holmes et al*., 2016; *Kaulfus et al*., 2017; *Fu et al.,* 2016; *Wang et al*., 2016; *Wright et al*., 2016].

Evaluation of historical trends of Hg atmospheric concentration and deposition to other environmental media is important because it helps understanding how legacy of previous anthropogenic emissions affects the present-day Hg pollution levels and future environmental responses to expected emission control measures. Long-term changes of mercury content in the environment since pre-industrial times were investigated in a series of studies, which applied a multi-media box model coupling the atmosphere, ocean, and terrestrial reservoirs [*Amos et al*., 2013; 2014; 2015]. More recent trends of mercury deposition over two last decades in Europe, North America and other regions were also evaluated in a number of modelling studies [*Soerensen et al.,* 2012; *Muntean et al*., 2014; *Colette et al*., 2016; *Zhang et al.,* 2016]. Future changes of Hg atmospheric concentration and deposition to the ground as a result of changes in anthropogenic emissions, land use and land cover as well as climate change were also investigated [*Lei et al.,* 2014; *Pacyna et al*,. 2016; *Zhang et al.,* 2016].

A variety of regional scale models was applied to investigate peculiarities of mercury pollution in different geographical regions. The studies were focused on evaluation of model performance, assessment of pollution levels, and combined model-measurement analysis in Europe [*Gencarelli et al.*, 2014; *Bieser et al*., 2014; 2017; *Gencarelli et al*., 2016], North America [*Myers et al*., 2013; *Megaritis et al*., 2014; *Grant et al.,* 2014; *Cohen et al*., 2016], East Asia [*Chen et al*., 2014; *Zhu et al.*, 2015; *Wang et al.*, 2016], as well as in the Arctic and Antarctica [*Fisher et al.,* 2013; *Dastoor and Durnford*, 2014; *Chen et al*., 2015; *Zhang et al*., 2015; *Dastoor et al*., 2015; *Angot et al.*, 2016].

A new multi-model study of mercury pollution on global and regional scales was initiated to support GMA 2018 with new modelling results. It will be based on updated mercury emissions inventory for 2015 that is developed within the framework of GMA 2018. The simulations program of the study was discussed and accepted by the participating modelling groups at the web conference held in

June 2017. The work on the model assessment has been started and will be continued next year. Results of the study will be included to the final version of GMA 2018.

***Co-operation with UN Environment broaden dissemination of the experience as well as scientific and policy oriented information generated within the Convention and improves visibility of the Convention on the international scene. On the other hand, it supports pollution assessment within EMEP by variety of data (including emission inventories and observations).***

### *4.3.2. Helsinki Commission*

In framework of cooperation with Helsinki Commission (HELCOM), MSC-E performs regular evaluation of airborne pollution load of heavy metals to the Baltic Sea. This work is carried out in accordance with the Memorandum of Understanding between the Baltic Marine Environment Protection Commission (HELCOM) and the United Nations Economic Commission for Europe (UN ECE) and is based on the long-term EMEP/HELCOM contract.

This year this activity was focused on the evaluation of cadmium and mercury pollution of the Baltic Sea. In particular, long-term variations of cadmium and mercury deposition fluxes to the Baltic Sea were estimated for the period 1990-2014. Source apportionment of deposition and verification of modelling results against measurements was made for 2014. Results of the assessment are available in a form of Joint report of EMEP Centres for HELCOM [*Bartnicki et al*., 2016] and several indicator fact sheets, published on the HELCOM website [http://www.helcom.fi].

Anthropogenic emissions of the HELCOM countries dropped substantially from 1990 to 2014 (by 39% for cadmium and 48% for mercury). In 2014 the largest contributors to heavy metal emissions of the HELCOM area were Russia, Poland, and Germany. The share of emissions from these countries in total emissions of heavy metals in the Baltic Sea region exceeded 90%.

Model simulations of pollution indicate substantial decline of annual total atmospheric deposition of cadmium and mercury to the Baltic Sea from 1990 to 2014. The drop of cadmium deposition during this period is more significant (54%) comparing to mercury deposition (24%) (Fig. 4.18a). Temporal changes of heavy metal pollution in different parts of the Sea are not homogeneous. Particularly, significant decrease of cadmium deposition is noted for the Bothnian Bay and the Gulf of Finland (68% and 64%). For mercury more significant changes took place in the Sound and the Kattegat (55% and 37%).

The rate of deposition decrease was higher in the early 1990-s, however after 2000 it became smaller or almost levelled off. Annual depositions to the Baltic Sea in 2014 were higher comparing to 2013 by 33% for cadmium and 9% for mercury, which can be explained by inter-annual changes of meteorological conditions, in particular, variability of atmospheric transport.

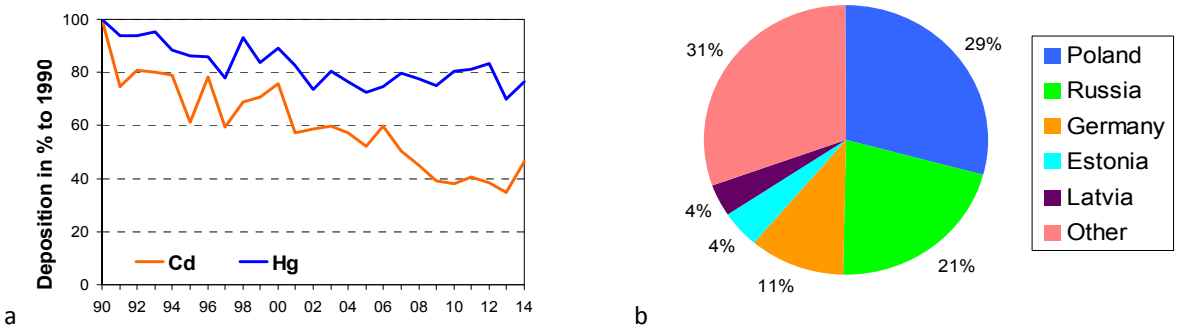


***Fig. 4.18.*** *Relative changes of annual atmospheric deposition of cadmium and mercury to the Baltic Sea in the period 1990-2014 (a) and contribution of emission sources from the EMEP countries to total anthropogenic deposition to the Baltic Sea in 2014 (b)*

Spatial trends in cadmium deposition in the Baltic Sea region in 2014, are analysed in [*Bartnicki et al.*, 2016]. Higher levels of deposition are estimated for southern and western parts of the region, while its northern part is characterized by relatively lower deposition fluxes. Similar pattern of deposition can also be noted for observed cadmium deposition fluxes.

Anthropogenic emission sources of HELCOM countries contributed to annual deposition over the Baltic Sea in 2014 about 27% for cadmium and 14% for mercury. Among the HELCOM countries the most significant contribution to cadmium and mercury deposition to the Baltic Sea was made by Poland, Russia, and Germany (Fig. 4.18b). Along with anthropogenic emission sources significant contribution to cadmium and mercury deposition (more than 50%) was made natural emissions, re-suspension with dust, sources located outside the HELCOM counties, and re-emission.

# 5. MAIN CHALLENGES AND DIRECTIONS OF FUTURE RESEARCH

The Status Report covers various aspects of heavy metal pollution assessment within EMEP in 2017 including evaluation of pollution levels and transboundary transport of heavy metals, model development associated with transition to the new EMEP grid, cooperation with the EMEP courtiers, CLRTAP subsidiary bodies, and international organization. Main challenges of the assessment revealed in the report and future research directions are summarized below. These topics are also reflected in the proposals for the EMEP workplan for 2018-2019 and the updated Mandates of the EMEP Centres (Annex C).

- Heavy metal monitoring data are available with good coverage in the western, central and northern parts of Europe, whereas in the eastern parts of Europe and Central Asia the monitoring network is scarce. Therefore, more sites with continuous measurements in these regions are needed, and especially for mercury where there is also a need for more sites in southern Europe. For mercury measurement there is also a special need to improve the data quality, both regarding monitors and manual methods. It is due time to organize a new field and laboratory intercomparison, in cooperation with other networks like AMAP and GMOS. Further, there are new methods developed, both advanced online instrumentation for heavy metals (i.e. XRF) as well as passive sampler for mercury. EMEP/CCC and TFMM should look into these new developments when discussing the new monitoring strategy beyond 2019.

- The pilot simulations of heavy metal pollution performed with GLEMOS on the new EMEP grid demonstrate good model performance in comparison with measurements and results obtained on the former EMEP grid. However, final transition of the operational EMEP modelling to the new grid requires additional testing and developments. In particular, wind re-suspension of heavy metals requires further refinement including estimates of long-term accumulation of the pollutants in topsoil. Besides, harmonization of the land use / land cover data on the new grid is required within the Convention to avoid potential inconsistencies between different data products produced by EMEP and WGE in future.

- Country-specific case studies of heavy metal pollution demonstrated significant potential revealing uncertainties and improving quality of model assessment both on a national scale and for the whole EMEP region. These pilot studies will be continued for a number of countries (Poland, United Kingdom, Russia) using detailed national emission and monitoring data. It is planned to perform assessment of heavy metal pollution on a country scale, evaluation of pollution levels in high-emission or high-impact (e.g. urban) areas applying data fusion approaches, and analysis of factors affecting quality of modelling assessment with fine spatial resolution. Major results and experience obtained during the whole period of the country-scale case studies will be overviewed in a summary report.

- Completeness and reliability of emissions data are among the key factors affecting quality of model assessment of pollution levels. Detailed analysis of heavy metal pollution on a country scale involving both modelling results and measurements revealed potential uncertainties of heavy metal emissions from some source categories (e.g. residential combustion). Besides, the need to revise emissions data for Eastern Europe was demonstrated. Therefore, the work on

improvement of reported heavy metal emissions data should be continued to reduce uncertainties of model assessment. In addition, an up-to-date estimate of heavy metal emissions on a continental or global scale are needed to properly take into account the contribution of sources located outside the EMEP region.

- The critical loads approach is successfully applied for risk assessment of heavy metal pollution on a regional scale within EMEP based on a collaborative work of CCE and MSC-E. However, the most recent estimates critical load exeedances for heavy metals are significantly outdated. An update of information on heavy metal critical loads is needed for assessment of contemporary effects of heavy metal pollution on biota and human health. Additionally, a joint work of CCE and MSC-E on critical loads analysis for mercury on a hemispheric scale will be continued to support international efforts to protect human health and the environment from the adverse effects of mercury on a global scale.

- Global Mercury Assessment 2018 (GMA 2018) is now under development in accordance with the request of the UN Environment Governing Council. MSC-E will continue participation in the assessment. In particular it will co-ordinate a multi-model study of mercury pollution on global and regional scales focused on evaluation of intercontinental transport and source apportionment of mercury deposition in different regions. Results of the study will be included to the final version of GMA 2018.

- Based on the CLRTAP 2016 Assessment Report the *Ad hoc* Policy Review Group [ECE/EB.AIR/WG.5/2017/3] recommended significant further work on heavy metals improving the analysis of long-term trends in secondary emissions and the capacity for quantifying intercontinental transport via multi-compartment modelling. Therefore, development of the GLEMOS modelling system will be continued with particular focus on mercury multi-media dispersion. The research will include analysis of the key factors affecting mercury accumulation in and exchange between the environmental media as well as evaluation of mercury secondary emissions and their contribution to pollution of the EMEP countries.

# REFERENCES


Aas W, Nizzetto P.B. [2017] Heavy metals and POP measurements 2014, Norwegian Institute for Air Research. EMEP/CCC-Report 3/20167

Adani M., Mircea M., D'Isidoro M., Costa M.P. and Silibello C. [2015]. Heavy Metal Modelling Study over Italy: Effects of Grid Resolution, Lateral Boundary Conditions and Foreign Emissions on Air Concentrations. *Water Air Soil Pollut*. (2015) 226:46

AMAP [2011] AMAP assessment 2011: mercury in the Arctic. Oslo, Norway: Arctic Monitoring and Assessment Programme (AMAP); (pp. xiv +193).

AMAP/UNEP [2008] Technical Background Report to the Global Mercury Assessment. Arctic Monitoring and Assessment Programme / UNEP Chemicals Branch. 159 pp. http://www.unep.org/chemicalsandwaste/LinkClick.aspx?fileticket=gwLbyNhGtn8%3d&tabid=3593&language=en-US. Accessed on June 28, 2016.

AMAP/UNEP [2013] Technical Background Report for the Global Mercury Assessment 2013. Arctic Monitoring and Assessment Programme, Oslo, Norway / UNEP Chemicals Branch, Geneva, Switzerland. vi + 263 pp. (http://www.amap.no/documents/download/1265. Accessed on June 16, 2017).

Amos H.M., D.J. Jacob, D. Kocman, H.M. Horowitz, Y. Zhang, S. Dutkiewicz, M. Horvat, E.S. Corbitt, D.P. Krabbenhoft, and E.M. Sunderland [2014] Global biogeochemical implications of mercury discharges from rivers and sediment burial, *Environ. Sci. Technol*., 48(16), 9514–9522.

Amos H.M., Jacob D.J., Streets, D.G. , and Sunderland E.M. [2013] Legacy impacts of all-time anthropogenic emissions on the global mercury cycle, *Global Biogeochemical Cycles* **27**(2), 410--421.

Amos H.M., Sonke J.E., Obrist D., Robins N., Hagan N., Horowitz H.M., Mason R.P., Witt M., Hedgecock I.M., Corbitt E.S., and Sunderland E.M. [2015] Observational and Modelling Constraints on Global Anthropogenic Enrichment of Mercury, *Environ. Sci. Technol.* 49(7), 4036--4047.

Angot H., Dastoor A., De Simone F., Gårdfeldt K., Gencarelli C. N., Hedgecock I. M., Langer S., Magand O., Mastromonaco M.N., Nordstrøm C., Pfaffhuber K. A., Pirrone N., Ryjkov A., Selin N. E., Skov H., Song S., Sprovieri F., Steffen A., Toyota K., Travnikov O., Yang X., and Dommergue A.[ 2016] Chemical cycling and deposition of atmospheric mercury in polar regions: review of recent measurements and comparison with models, *Atmos. Chem. Phys*., 16, 10735-10763, doi:10.5194/acp-16-10735-2016.

Ariya P.A., Amyot M., Dastoor A., Deeds D., Feinberg A., Kos G., Poulain A., Ryjkov A., Semeniuk K., Subir M. & Toyota K. [2015] Mercury Physicochemical and Biogeochemical Transformation in the Atmosphere and at Atmospheric Interfaces: A Review and Future Directions, *Chemical Reviews* 115(10), 3760-3802.

Aulinger, A., Matthias, V., and Quante, M. [2011] An approach to temporally disaggregate Benzo(a)pyrene emissions and their application to a 3D Eulerian atmospheric chemistry transport model, Water Air Soil Pollution. March 2011, Volume 216, Issue 1, pp 643–655

Auzmendi-Murua I., Castillo Ál. & Bozzelli J.W. [2014] Mercury Oxidation via Chlorine, Bromine, and Iodine under Atmospheric Conditions: Thermochemistry and Kinetics, *The Journal of Physical Chemistry A* 118(16), 2959-2975.

Bartnicki J., Gusev A., Aas W., Benedictow A. [2016] Atmospheric Supply of Nitrogen, Cadmium, Mercury, Benzo(a)pyrene and PBDEs to the Baltic Sea in 2014. Summary Report for HELCOM. MSC-W Technical Report 1/2016.

Bieser J., Aulinger A., Matthias V., Quante M., and Builtjes P. [2011]. SMOKE for Europe – adaptation, modification and evaluation of a comprehensive emission model for Europe. *Geosci. Model Dev.,* 4, 47–68.

Bieser J., De Simone F., Gencarelli C.N., Hedgecock I.M., Matthias V., Travnikov O., Weigelt A. [2014] A diagnostic evaluation of modelled mercury wet deposition in Europe using atmospheric speciated high-resolution observations, *Environ. Science and Pollution Research* 21 (16).

Bieser, J., Slemr, F., Ambrose, J., Brenninkmeijer, C., Brooks, S., Dastoor, A., DeSimone, F., Ebinghaus, R., Gencarelli, C. N., Geyer, B., Gratz, L. E., Hedgecock, I. M., Jaffe, D., Kelley, P., Lin, C.-J., Jaegle, L., Matthias, V., Ryjkov, A., Selin, N. E., Song, S., Travnikov, O., Weigelt, A., Luke, W., Ren, X., Zahn, A., Yang, X., Zhu, Y., and Pirrone, N. [2017] Multi-model study of mercury dispersion in the atmosphere: vertical and interhemispheric distribution of mercury species, Atmos. Chem. Phys., 17, 6925-6955, https://doi.org/10.5194/acp-17-6925-2017.

Blunden J. and Arndt D. S., Eds. [2016] State of the Climate in 2015. *Bull. Amer. Meteor. Soc*., 97 (8), S1–S275, DOI:10.1175/2016BAMSStateoftheClimate.1

Bouwman A., Van Vuuren D., Derwent R. & Posch M. [2002] A global analysis of acidification and eutrophication of terrestrial ecosystems. Water Air and Soil Pollution 141, 349-382.

Bringmark L, Lundin L, Augustaitis A, Beudert B, Dieffenbach-Fries H, Dirnböck T, Grabner M-T, Hutchins M, Kram P, Lyulko I, Ruoho-Airola T, Vana M, [2013]. Trace metal budgets for forested catchments in Europe – Pb, Cd, Hg, Cu and Zn. Water, Air and Soil Pollution 224: 1502CEIP [2017]. Centre on Emission Inventories and Projections. Web-Dab EMEP data base.

CEIP [2017]. Centre on Emission Inventories and Projections. Web-Dab EMEP data base. http://www.ceip.at/ms/ceip_home1/ceip_home/webdab_emepdatabase/. Accessed on May 31, 2017.

Chen B., Stein A.F., Maldonado P.G., Sanchez de la Campa A.M., Gonzalez-Castanedo Y., Castell N., de la Rosa J.D. [2013]. Size distribution and concentrations of heavy metals in atmospheric aerosols originating from industrial emissions as predicted by the HYSPLIT model. *Atmospheric Environment*, pp. 234-244

Chen L., H.H. Wang, J.F. Liu, Y.D. Tong, L.B. Ou, W. Zhang, D. Hu, C. Chen, and X. J. Wang [2014] Intercontinental transport and deposition patterns of atmospheric mercury from anthropogenic emissions, *Atmospheric Chemistry and Physics*, *14*(18), 10163–10176, doi:10.5194/acp-14-10163-2014.

Chen L., Y. Zhang, D.J. Jacob, A.L. Soerensen, J.A. Fisher, H.M. Horowitz, E.S. Corbitt, and X. Wang [2015] A decline in Arctic Ocean mercury suggested by differences in decadal trends of atmospheric mercury between the Arctic and northern midlatitudes, *Geophysical Research Letters*, *42*(14), 6076–6083, doi:10.1002/2015GL064051.

Cohen M.D., Draxler R.R., Artz R.S., Blanchard P., Gustin M.S., Han Y., Holsen T.A., Jaffe D.A., Kelley P., Lei H., Loughner C.P., Luke W.T., Lyman S.L., Niemi D., Pacyna J.M., Pilote M., Poissant L., Ratte D., Ren X., Steenhuisen F., Steffen A., Tordon R., and Wilson S. [2016] Modelling the global atmospheric transport and deposition of mercury to the Great Lakes, Elementa, 4:000118, 10.12952/journal.elementa.000118.

Colette A. et al. [2016] Air pollution trends in the EMEP region between 1990 and 2012. EMEP: CCC-Report 1/2016, Kjeller, Norway.

Dastoor A., Ryzhkov A., Durnford D., Lehnherr I., Steffen A., and Morrison H. [2015] Atmospheric mercury in the Canadian Arctic. Part II: Insight from modelling, *Science of The Total Environment*, 509–510, 16-27, http://dx.doi.org/10.1016/j.scitotenv.2014.10.112.

Dastoor A.P. and Durnford D.A. [2014] Arctic ocean: is it a sink or a source of atmospheric mercury?, *Environmental Science and Technology*, 48, 1707-1717.

De Vries W, Hettelingh J-P. and Posch M. (eds.) [2015] Critical Loads and Dynamic Risk Assessments. Nitrogen, Acidity and Metals in Terrestrial and Aquatic Ecosystems. Springer, *Environmental Pollution*, Vol. 25.

De Vries W., Reinds G. J. & Posch M. [1994]. Assessment of critical loads and their exceedance on European forests using a one-layer steady-state model. *Water Air Soil Pollut*. 72, 357-394.

de Wit H.A., Hettelingh J-P., Harmens H. [2016]. Trends in ecosystem and health responses to long-range transported atmospheric pollutants. Norwegian Institute for Water Research, Report No. 6946-2015, ICP Waters report 125/2015. 92 p.

Dibble T.S. and Schwid A.C. [2016] Thermodynamics limits the reactivity of BrHg• radical with volatile organic compounds, Chemical Physics Letters, doi: http://dx.doi.org/10.1016/j.cplett.2016.07.065

Dibble T.S., Zelie MJ, Jiao Y. [2014] Quantum chemistry guide to PTRMS studies of as-yet undetected products of the bromine-atom initiated oxidation of gaseous elemental mercury. The Journal of Physical Chemistry. A. 118: 7847-54. PMID 25116586 DOI: 10.1021/jp5041426

Dibble T.S., Zelie MJ, Mao H. [2012] Thermodynamics of reactions of ClHg and BrHg radicals with atmospherically abundant free radicals *Atmospheric Chemistry and Physics*. 12: 10271-10279. DOI: 10.5194/acp-12-10271-2012

Dore A. J., Hallsworth S., McDonald A. G., Werner M., Kryza M., J. Abbot, Nemitz E., Dore C. J., Malcolm H., Vieno M., Reis S., Fowler D. [2014] Quantifying missing annual emission sources of heavy metals in the United Kingdom with an atmospheric transport model. *Science of the Total Environment*, 479 –480 171–180.

ECMWF [2017] European Centre for Medium-Range Weather Forecasts, http://www.ecmwf.int/en/forecasts/dataset, access: 1 July 2017.

Fisher J.A., Jacob D.J., Soerensen A.L., Amos H.M., Corbitt E.S., Streets D.G., Wang Q., Yantosca R.M., Sunderland E.M. [2013] Factors driving mercury variability in the Arctic atmosphere and ocean over the past 30 years. *Global Biogeochemical Cycles* 27: 1226-1235.

Fu X., Yang X., Lang X., Zhou J., Zhang H., Yu B., Yan H., Lin C.-J., & Feng X. [2016] Atmospheric wet and litterfall mercury deposition at urban and rural sites in China, *Atmospheric Chemistry and Physics* 16(18), 11547--11562.

Gencarelli C.N., Bieser J., Crabone F., De Simone F., Hedgecock I.M., Matthias V., Travnikov O., Yang X., Pirrone N. [2016] Sensitivity study of regional mercury dispersion in the atmosphere. *Atmos. Chem. Phys. Discuss*., doi:10.5194/acp-2016-663 (under review).

Gencarelli C.N., De Simone F., Hedgecock I.M., Sprovieri F., Pirrone N. [2014] Development and application of a regional-scale atmospheric mercury model based on WRF/Chem: a Mediterranean area investigation, *Environmental Science and Pollution Research* 21 (6), 4095-4109.

González A., Vivanco M.G., Palomino I., Garrido J.L., Santiago M. and Bessagnet B. [2012]. Modelling Some Heavy Metals Air Concentration in Europe. *Water Air Soil Pollut* (2012) 223:5227-242

Grant S.L., Kim M., Lin, P., Crist K.C., Ghosh S., and Kotamarthi V.R. [2014] A simulation study of atmospheric mercury and its deposition in the Great Lakes, *Atmospheric Environment*, 94, 164-172, 10.1016/j.atmosenv.2014.05.033.

Gusev A., I. Ilyin, L.Mantseva, O.Rozovskaya, V. Shatalov, O. Travnikov [2006] Progress in further development of MSCE-HM and MSCE-POP models (implementation of the model review recommendations) EMEP/MSC-E Technical Report 4/2006.

Gusev A., O.Rozovskaya, V. Shatalov [2007] Modelling POP long-range transport and contamination levels by MSCE-POP model. EMEP/MSC-E Technical Report 1/2007.

Gusev A., O.Rozovskaya, V.Shatalov, W.Aas, P. Nizzetto [2017] Persistent Organic Pollutants: assessment of transboundary pollution on regional and global scales. EMEP Status Report 3/2016.

Hettelingh J-P., Schütze, de Vries W., Denier van der Gon H., Ilyin I., Slootweg J. and Travnikov O. [2015]. Chapter 21. Critical loads of cadmium, lead and mercury and their excedances in Europe. Pp. 523-546. In: Critical Loads and Dynamic Risk Assessments. Nitrogen, Acidity and Metals in Terrestrial and Aquatic Ecosystems. Ed. by de Vries W, Hettelingh J-P. and Posch M. Springer, *Environmental Pollution*, Vol. 25.

Hettelingh, J.-P., Sverdrup, H. & Zhao, D. [1995] Deriving critical loads for Asia. Water Air and Soil Pollution 85, 2565-2570

HMCR [2017]. Hydrometeorological Centre of Russia. The main weather and climate features of the northern hemisphere. http://www.meteoinfo.ru/climate. Accessed on July 04, 2017

Holmberg, M., Vuorenmaa, J., Posch, M., Forsius, M., Lundin, L., Kleemola, S., Augustaitis, A., Beudert, B., de Wit, H. A., Dirnböck, T., Evans, C. D., Frey, J., Grandin, U., Indriksone, I., Krám, P., Pompei, E., Schulte-Bisping, H., Srybny, A. & Váňa, M. [2013] Relationship between critical load exceedances and empirical impact indicators at Integrated Monitoring sites across Europe. Ecological Indicators 24, 256-265.

Holmes C.D., Krishnamurthy N.P., Caffrey J.M., Landing W.M., Edgerton E.S., Knapp K.R., and Nair U.S. [2016] Thunderstorms Increase Mercury Wet Deposition, *Environmental Science & Technology* 50(17), 9343-9350.

Horowitz H.M., Jacob D.J., Zhang Y., Dibble T.S., Slemr F., Amos H.M., Schmidt J.A., Corbitt E.S., Marais E.A., and Sunderland E.M. [2017] A new mechanism for atmospheric mercury redox chemistry: Implications for the global mercury budget, *Atmospheric Chemistry and Physics Discussions*, 1-33, doi:10.5194/acp-2016-1165.

http://www.ceip.at/ms/ceip_home1/ceip_home/webdab_emepdatabase/. Accessed on May 31, 2017.

Ilyin I., O. Rozovskaya, V. Sokovykh, O. Travnikov [2007] Atmospheric modelling of heavy metal pollution in Europe: Further development and evaluation of the MSCE-HM model. EMEP/MSC-E Technical Report 4/2007.

Ilyin I., O.Rozovskaya, O.Travnikov, M.Varygina, W.Aas [2014] Heavy Metals: Transboundary Pollution of the Environment. EMEP Status Report 2/2014.

Ilyin I., O.Rozovskaya, O.Travnikov, M.Varygina, W.Aas [2015] Heavy metals: Analysis of long-term trends, country-specific research and progress in mercury regional and global modeling, EMEP Status Report 2/2015.

Ilyin I., Rozovskaya O., Travnikov O., Varygina M., Aas W. and Pfaffhuber K.A. [2016]. Assessment of heavy metal transboundary pollution, progress in model development and mercury research. EMEP Status Report 2/2016, 75p.

Ilyin I., Travnikov O., Varygina M., Vana M., Machalek P. and Hnilikova H. [2012]. Assessment of Heavy Metal Pollution Levels in the Czech Republic (EMEP case study). Joint MSC-E/CHMI Report. EMEP/MSC-E Technical note 1/2012. 56 p.

Jiao Y. and Dibble T.S. [2015] Quality Structures, Vibrational Frequencies, and Thermochemistry of the Products of Reaction of BrHg• with NO2, HO2, ClO, BrO, and IO, *The Journal of Physical Chemistry A* **119**(42), 10502-10510.

Jiao Y. and Dibble T.S. [2017] First kinetic study of the atmospherically important reactions BrHg(radical dot) + NO2 and BrHg(radical dot) + HOO, *Phys. Chem. Chem. Phys.* **xx**, xx.

Kaulfus A.S., Nair U.S., Holmes C.D., and Landing W.M. [2017], Mercury Wet Scavenging and Deposition Differences by Precipitation Type, Environmental Science & Technology, 51 (5), pp 2628–2634.

Kos G., Ryzhkov A., Dastoor A., Narayan J., Steffen A., Ariya P.A., and Zhang L. [2013] Evaluation of discrepancy between measured and modelled oxidized mercury species, *Atmospheric Chemistry and Physics*, 13, 4839-4863.

Kuylenstierna J. C. I., Hicks W. K., Cinderby S., Cambridge H., van der Hoek K. W., Erisman J. W., Smeulders S. & Wisniewski J. R. [1998] Critical loads for nitrogen deposition and their exceedance at European scale. *Environ. Pollut*. 102, 591-598

Kuylenstierna J. C. I., Rodhe H., Cinderby S. & Hicks K. [2001] Acidification in developing countries: ecosystem sensitivity and the critical load approach on a global scale. *Ambio* 30, 20-28.

Larssen S., Sluyter R. and Helmis C. [1999]. Criteria for EUROAIRNET. The EEA Air Quality Monitoring and Information network. Technical Report no. 12. EEA, Copenhagen, 43 p.

Lei H., D.J. Wuebbles, X.-Z. Liang, Z. Tao, S. Olsen, R. Artz, X. Ren, and M. Cohen [2014] Projections of atmospheric mercury levels and their effect on air quality in the United States, *Atmospheric Chemistry and Physics*, *14*(2), 783–795, doi:10.5194/acp-14-783-2014.

Lenschow P., Abraham H-J., Kutzner K., Lutz M., Preuβ J.-D. and Reichenbächer W. [2001]. Some ideas about sources of PM10. *Atmospheric Environment* 35, Supplement 1, S23-S33.

Megaritis, A. G., Murphy, B. N., Racherla, P. N., Adams, P. J., and Pandis, S. N. [2014] Impact of climate change on mercury concentrations and deposition in the eastern United States, Science of the Total Environment, 487, 299-312, 10.1016/j.scitotenv.2014.03.084.

Muntean M., Janssens-Maenhout G., Song S., Selin N.E., Jos Oliver J.G.J., Guizzardi D., Maas R., Dentener F. [2014] Trend analysis from 1970 to 2008 and model evaluation of EDGARv4 global gridded anthropogenic mercury emissions. *Science of the Total Environment* 494-495, 337-350.

Myers T., Atkinson R.D., Bullock O.R., Jr., and Bash J.O. [2013] Investigation of effects of varying model inputs on mercury deposition estimates in the Southwest US, *Atmospheric Chemistry and Physics*, 13, 997-1009, 10.5194/acp-13-997-2013.

Nair U.S., Wu Y., Holmes C.D., Ter Schure A., Kallos G., and Walters J.T. [2013] Cloud-resolving simulations of mercury scavenging and deposition in thunderstorms, *Atmospheric Chemistry and Physics*, 13, 10143-10157, 10.5194/acp-13-10143-2013.

Pacyna J.M., Travnikov O., De Simone F., Hedgecock I.M., Sundseth K., Pacyna E.G., Steenhuisen F., Pirrone N., Munthe J., Kindbom K. [2016] Current and future levels of mercury atmospheric pollution on a global scale. *Atmos. Chem. Phys*. 16, 12495-12511. doi:10.5194/acp-16-12495-2016

Reinds, G. J., Posch, M., De Vries, W., Slootweg, J. & Hettelingh, J.-P. [2008]. Critical loads of sulphur and nitrogen for terrestrial ecosystems in Europe and northern Asia using different soil chemical criteria. *Water Air and Soil Pollution* 193, 269-287

Shah V., Jaegle L., Gratz L.E., Ambrose J.L., Jaffe D.A., Selin N.E., Song S., Campos T.L., Flocke F.M., Reeves M., Stechman D., Stell M., Festa J., Stutz J., Weinheimer A.J., Knapp D.J., Montzka D.D., Tyndall G.S., Apel E.C., Hornbrook R.S., Hills A.J., Riemer D.D., Blake N.J., Cantrell C.A., and Mauldin R.L. [2016] Origin of oxidized mercury in the summertime free troposphere over the southeastern US, *Atmospheric Chemistry and Physics,* 16, 1511-1530, 10.5194/acp-16-1511-2016.

Shatalov V., Ilyin I., Gusev A. and Travnikov O. [2016] Heavy metals and persistent organic pollutants: model assessment of pollution and research activities. EMEP/MSC-E Technical Report 1/2016., 76 p.

Shatalov V., Ilyin I., Gusev A., Rozovskaya O., Sokovykh V. and Travnikov O. [2013] Heavy Metals and Persistent Organic Pollutants: Model Assessment of Pollution and Research Activities. MSC-E Technical Report 1/2013. 68 p.

Slootweg J, Hettelingh J-P, Posch M, Schütze G, Spranger T, De Vries W, Reinds GJ, Van't Zelfde M, Dutchak S, Ilyin I. [2007] European critical loads of cadmium, lead and mercury and their exceedances. *Water, Air and Soil Pollution*: Focus 7: 371–377.

Soerensen A.L., Jacob D.J., Streets D.G., Witt M.L.I., Ebinghaus R., Mason R.P., Andersson M., and. Sunderland E.M [2012] Multi-decadal decline of mercury in the North Atlantic atmosphere explained by changing subsurface seawater concentrations. *Geophys. Res. Lett*. 39(21):L21810

Stein A. F., Draxler R. R., Rolph G. D., Stunder B. J. B., Cohen M. D. and Ngan F. [2015]. NOAA's HYSPLIT Atmospheric Transport and Dispersion Modeling System. BAMS, December 2015, pp 2059-2077.

Tista M., Mareckova K. and R.Wankmueller [2017] Methodologies applied to the CEIP GNFR gap-filling 2017. Part I: Heavy Metals (Pb, Cd, Hg). Technical report CEIP 01/2017.

Tørseth K., W. Aas, K. Breivik, A. M. Fjæraa, M. Fiebig, A. G. Hjellbrekke, C. Lund Myhre, S. Solberg, and K. E. Yttri [2012]. Introduction to the European Monitoring and Evaluation Programme (EMEP) and observed atmospheric composition change during 1972–2009. *Atmos. Chem. Phys. Discuss*., 12, 1733-1820.

Travnikov O., A.Ryaboshapko [2002] Modelling of Mercury Hemispheric Transport and Depositions. MSC-E Technical Report 6/2002.

Travnikov O., Angot H., Artaxo P., Bencardino M., Bieser J., D'Amore F., Dastoor A., De Simone F., Diéguez M. D. C., Dommergue A., Ebinghaus R., Feng X. B., Gencarelli C. N., Hedgecock I. M., Magand O., Martin L., Matthias V., Mashyanov N., Pirrone N., Ramachandran R., Read K. A., Ryjkov A., Selin N. E., Sena F., Song S., Sprovieri F., Wip D., Wängberg I., and Yang X. [2017] Multi-model study of mercury dispersion in the atmosphere: atmospheric processes and model evaluation, *Atmos. Chem. Phys*., 17, 5271-5295, doi:10.5194/acp-17-5271-2017.

UNECE [2009] EMEP monitoring strategy. ECE/EB.AIR/GE.1/2009/15

UNEP [2002] Global Mercury Assessment 2002. UNEP Chemicals. 258 pp. http://www.unep.org/chemicalsandwaste/Portals/9/Mercury/Documents/final-assessment-report-25nov02.pdf. Accessed on June 28, 2016.

Wai K-M, Wu S.,, Li X., Jaffe D.A., and Perry K.D. [2016]. Global Atmospheric Transport and Source-Receptor Relationships for Arsenic. *Environ. Sci. Technol*., 2016, 50 (7), pp 3714–3720.

Wang X., Z. Bao, C. J. Lin, W. Yuan, and X. Feng [2016] Assessment of Global Mercury Deposition through Litterfall. *Environmental Science and Technology*, *50*(16), 8548–8557, doi:10.1021/acs.est.5b06351.

Weiss-Penzias P., Amos H.M., Selin N.E., Gustin M.S., Jaffe D.A., Obrist D., Sheu G.R., and Giang A. [2015] Use of a global model to understand speciated atmospheric mercury observations at five high-elevation sites, *Atmospheric Chemistry and Physics*, 15(3), 1161-1173, 10.5194/acp-15-1161-2015.

WHO [2007] Health risks of heavy metals from long-range transboundary air pollution. Copenhagen: Joint WHO/Convention task force on health aspects of air pollution, World health organization, Regional office for Europe.

WMO [2015] Annual Bulletin on the Climate in WMO Region VI - Europe and Middle East - 2015 . Ed. by Deutscher Wetterdienst. Responsible Mächel H. http://clima.meteoam.it/BollettinoWMO6R/bulletin_2015.pdf. Accessed on June 28, 2016.

Wright L.P., and Zhang L. [2015] An approach estimating bidirectional air-surface exchange for gaseous elemental mercury at AMNet sites, *Journal of Advances in Modelling Earth Systems*, 7, 35-49, 10.1002/2014ms000367.

Wright L.P., Zhang L., and Marsik F.J. [2016] Overview of mercury dry deposition, litterfall, and throughfall studies, *Atmospheric Chemistry and Physics* 16(21), 13399--13416.

Zhang L., Blanchard P., Johnson D., Dastoor A., Ryzhkov A., Lin C.J., Vijayaraghavan K., Gay D., Holsen T.M., Huang J., Graydon J.A., St Louis V.L., Castro M.S., Miller E.K., Marsik F., Lu J., Poissant L., Pilote M., and Zhang K.M. [2012] Assessment of modelled mercury dry deposition over the Great Lakes region, *Environmental Pollution*, 161, 272-283, 10.1016/j.envpol.2011.06.003.

Zhang Y., D.J. Jacob, H.M. Horowitz, L. Chen, H.M. Amos, D.P. Krabbenhoft, F. Slemr, V.L. St Louis, and E.M. Sunderland [2016] Observed decrease in atmospheric mercury explained by global decline in anthropogenic emissions, *Proceedings of the National Academy of Sciences of the United States of America*, *113*(3), 526–531, doi:10.1073/pnas.1516312113.

Zhang Y., D.J. Jacob, S. Dutkiewicz, H.M. Amos, M.S. Long, and E.M. Sunderland [2015] Biogeochemical drivers of the fate of riverine mercury discharged to the global and Arctic oceans, *Global Biogeochem. Cycles*, 29, 854–864, doi:10.1002/2015GB005124.

Zhu J., Wang T., Bieser J., Matthias V. [2015] Source attribution and process analysis for atmospheric mercury in eastern China simulated by CMAQ-Hg. *Atmos. Chem. Phys*. 5 (15).

Annex A

# EVALUATION OF MODELLING RESULTS VS. OBSERVATIONS

Modelled mean annual concentrations in air and annual sums of wet deposition fluxes of lead, cadmium and mercury are verified via comparison with available background monitoring data. The model performance is influenced by a number of factors. First of all, numerical description of natural processes responsible for atmospheric transport and deposition in a model is based on a number of assumptions and approximations. Therefore, modelling results inevitably contain some uncertainty. Model uncertainties have been evaluated in [*Travnikov and Ilyin*, 2005]. It was demonstrated that intrinsic model uncertainty (i.e., uncertainty of the model as such, without effect of emission data) of modelled deposition of heavy metals was amounted to ±30-40% for Europe as a whole. Intrinsic uncertainty for air concentrations of particulate metals (Pb, Cd) is around ±40%, and mercury - around ±20%.

Another factor affecting modelling results is emission data. Information about uncertainties of heavy metal emission data in a number of the EMEP countries is reported annually to CEIP [*CCC*, 2017]. Values of lead, cadmium and mercury emission data uncertainties range from 23% to 488%, 29% – 449% and 13%-182%, respectively (Table A.1).

***Table A.1.*** *Uncertainties (%) of the reported emission data in 2015*

| 2015 | Pb | Cd | Hg |
|---|---|---|---|
| Belarus | 192 | 266 | 111 |
| Belgium | 106 | 81 | 32 |
| Croatia | 140 | 291 | 78 |
| Cyprus | 95 | 81 | 13 |
| Denmark | 488 | 449 | 103 |
| Estonia | 184 | 134 | 182 |
| Finland | ±29 | ±29 | ±19 |
| France | 163 | 39 | 34 |
| Latvia | 60 | 70 | 68 |
| Poland | 67 | 69 | 68 |
| Sweden | 23 | 37 | 70 |
| United Kingdom | 29 | -30 to >50 | -30 to 50 |

Finally, measurement data also contain some uncertainty. These uncertainties can occur at different steps of measurement procedure such as sampling, transporting, storing, laboratory analysis. Currently information about uncertainties of laboratory analysis is updated on annual basis. This is done by regular laboratory intercomparison tests, supervised by CCC. Numerical characteristic of analytical uncertainty is relative deviation of concentration, analyzed in a laboratory, from theoretical value. In order to characterize quality of laboratory analysis, so-called Data Quality Objectives (DQO) was introduced by CCC. For heavy metals DQO are equal to ±15% of high concentrations (typical for background levels in the central and eastern parts of Europe) and ±25% for low concentrations (typical for Scandinavia). According to the recent intercomparison tests, analysis of heavy metals at most of the EMEP laboratories fits the DQO criteria [*CCC*, 2017].

Agreement between modelled and observed values is characterized by a number of statistical indices. They include Mean Relative Bias (MNB), Pearson's correlation coefficient and Normalized Root Mean Square Error (NRMSE). Besides, a share of model-measurement pairs of values differing from each other within 2-fold and 3-fold range (F2 and F3, respectively) is also considered. Statistical indices characterising agreement between modelled and observed concentrations in air and wet deposition fluxes are summarised in Table A.2. For lead and cadmium relative bias is within ±30% for air concentrations and for wet deposition fluxes. For most of stations the difference between modelled and observed values matches a factor of two. Spatial correlation coefficients for concentrations in air are higher than those for wet deposition. It is explained by the fact that wet deposition fluxes depend on precipitation amounts, which uncertainty also influences the model performance.

The modelled concentrations of mercury match the observed ones within ±6% on average. However, the correlation coefficient is lower compared to that of lead and cadmium. Mercury has long residence time in the atmosphere. Therefore, mercury is dispersed globally, reaching almost uniform concentrations in air. The difference between modelled and observed concentrations in air has the same order of magnitude as the model uncertainty of calculated concentrations. Therefore, low spatial correlation is caused by small spatial gradients of modelled and observed concentrations. Spatial correlation coefficient between modelled and observed wet deposition fluxes is much higher (almost 0.6) than that for air concentrations. Some positive bias (35%) can be explained by uncertainties of mercury atmospheric chemistry and of speciation of mercury anthropogenic emissions. Information on emission speciation is not reported by countries and not prepared by CEIP in the emission data for modelling. Therefore, expert estimates [*AMAP/UNEP*, 2013] are used to establish the speciation for each EMEP country.

***Table A2.*** *Main statistical indicators of agreement between annual modelled and measured levels of air concentrations and wet deposition fluxes in 2014*

| | Lead | | Cadmium | | Mercury | |
|---|---|---|---|---|---|---|
| | $C_{air}$ | Wet Dep | $C_{air}$ | Wet Dep | $C_{air}$ | Wet Dep |
| Mean relative bias, % | 22 | -5 | -6 | -29 | -6 | 32 |
| Correlation coefficient | 0.83 | 0.45 | 0.70 | 0.60 | 0.39 | 0.56 |
| NRMSE | 0.54 | 0.59 | 0.56 | 0.41 | 0.09 | 0.49 |
| F2, % | 81 | 71 | 83 | 82 | 100 | 81 |
| F3, % | 93 | 88 | 93 | 91 | 100 | 95 |
| N | 42 | 49 | 40 | 44 | 12 | 21 |

$C_{air}$ – concentration in air
Wet Dep – wet deposition flux
NRMSE – Normalized Root Mean Square Error
F2 – fraction of values fitting to factor of 2 difference
F3 – fraction of values fitting to factor of 3 difference
N – number of model-observation pairs

Statistical indices summarized in Table A2 describe the agreement between modelled and measured concentrations and deposition fluxes in general. However, in various parts of the EMEP region the

situation can differ considerably. Combination of gridded maps of modelled pollution levels and observations in particular points allows to identify regions where the discrepancies between modelled and observed values are higher or lower than that on average.

Relatively good agreement between modelled and measured concentrations in air is noted for stations located in Poland, Belgium, the United Kingdom, Hungary, where bias between annual mean values is within ±50% range (Fig. A.1a). Similar range of deviation also takes place for most of stations in Germany and Spain. Underestimation of the observed levels is noted for stations located in Scandinavia (Finland, Norway). At stations in the Czech Republic, Latvia, Slovenia, Denmark, most of stations in France and some stations in Germany the model overestimates the observed concentrations in air. Modelled wet deposition fluxes match the observed fluxes within ±50% at stations located in Belgium, the Czech Republic, the Netherlands, Belgium, Slovakia, most or stations in Finland, the United Kingdom, Sweden and France (Fig. A.1b). At stations in Poland as well as some stations in the United Kingdom, Germany and France the modelled wet deposition fluxes exceed the observed ones by more than 50%.

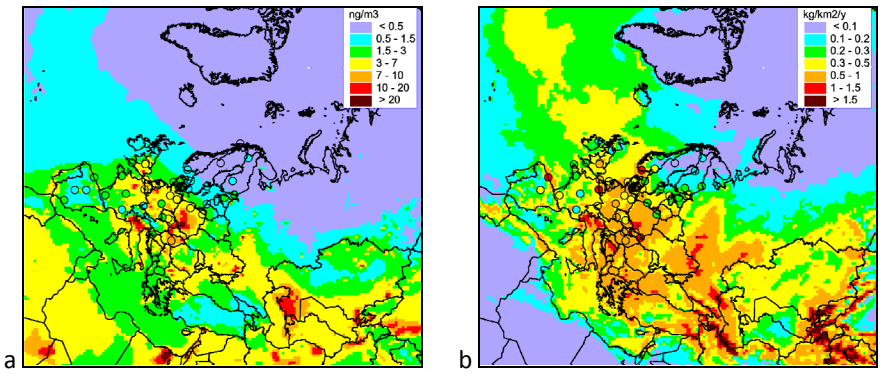


***Fig. A.1.*** *Spatial distribution of modelled and observed lead concentrations in air (a) and wet deposition fluxes (b) in 2015*

At most of stations modelled concentrations of cadmium in air agree with the observed concentrations within ±50% range (Fig. A.2a). Underestimation of the observed concentrations takes place at station in Latvia and at most of stations in Finland and Norway. Some overestimation of observed levels takes place at single stations in Germany, the Netherlands, Cyprus, the United Kingdom and Sweden. In spite of general tendency to underestimate cadmium wet deposition fluxes, at most of stations the bias of modelled from observed values varies within ±50% limits (Fig. A.2b). Underestimation of the observed values exceeding 50% is obtained for stations located in Belgium, Estonia, some stations in Finland and Slovakia. At stations GB48, HU2, NL91 and SK7 the model tends to overestimate cadmium wet deposition flux by more than 50%.

Mercury modelled and observed concentrations in air agree within ±15% (Fig. A.3a). Both modelled and observed concentrations demonstrate quite smooth spatial distribution in the EMEP region. The bias for wet deposition fluxes varies from -20% to 50% at most of stations (Fig. A.3b). Higher bias is noted for stations located in the United Kingdom and for particular station in other countries (DE1, SI8, FI36).

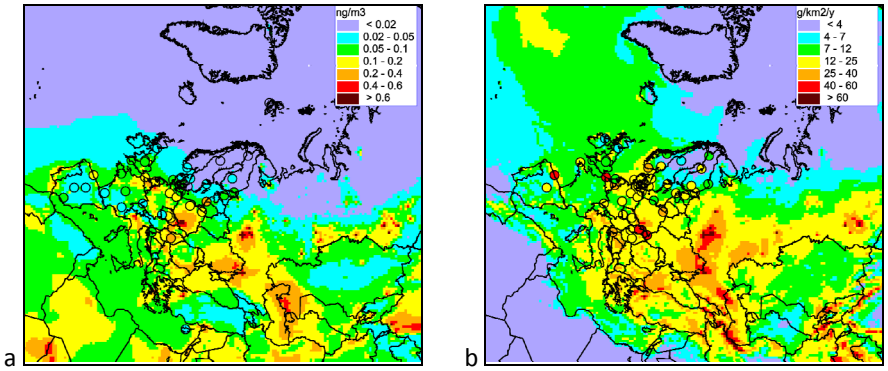


***Fig. A.2.*** *Spatial distribution of modelled and observed cadmium concentrations in air (a) and wet deposition fluxes (b) in 2015*

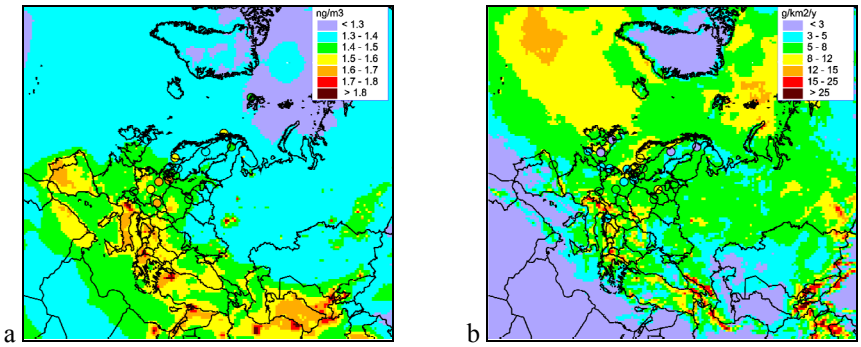


***Fig. A.3.*** *Spatial distribution of modelled and observed mercury concentrations in air (a) and wet deposition fluxes (b) in 2015*

Reasons leading to discrepancies between modelled and measured values may differ for particulate stations. Overestimation of the observed concentrations of lead and cadmium in air or their wet deposition fluxes can often be explained by too high contribution of wind re-suspension to total modelled value. One of planned tasks in the framework of transition from old to new EMEP grid is adaptation of re-suspension scheme to new grid and new land-cover data. Overestimation of mercury wet deposition fluxes may be explained by uncertainties of mercury atmospheric chemistry. It is planned to modify the model scheme of mercury transformations in the atmosphere. Another reason is uncertainties of mercury speciation of anthropogenic emissions. Underestimation of the observed values by the model can be explained by insufficient emissions of the metals from specific emission source categories or by unaccounted local emission sources.

Another aspect is representativeness of measurement stations. It is assumed that modelled concentrations or deposition characterize pollution level average over the model gridcell. Measurements are carried out at “points”. Theoretically, the “point” of station location should be representative to the surrounding area comparable with modelled gridcell. In other words, the station should not be affected by significant emission sources and local geographical peculiarities (relief, local wind circulation etc.). However, there is a need to examine what area is characterized by each station of the EMEP network.

## METEOROLOGICAL CONDITIONS OF 2015

Pollution levels in the EMEP region are strongly influenced by meteorological conditions. The main characteristics of meteorological conditions of a particular year affecting atmospheric transport and deposition of heavy metals and persistent organic pollutants (POPs) are precipitation amounts, air temperature and peculiarities of atmospheric transport patterns. Precipitation scavenging is major removal mechanism for most of considered pollutants. Air temperature affects rates of chemical reactions and partitioning between gaseous and particulate phases for a number of POPs. Atmospheric circulation determines predominant transport patterns of atmospheric pollutants from source regions to receptors and it markedly affects source-receptor relationships. Besides, combination of precipitation regime and wind strength influences origin of wind suspension dust containing heavy metals.

The year 2015 is exceptionally warm compared to other years of meteorological observations. In particular, its global temperature is 1°C warmer than that in pre-industrial time and concentration of carbon dioxide measured at Mauna Loa observatory exceeded 400 ppm [*Blunden and Arndt*, 2016]. This year is also the warmest in a number of the EMEP countries [*WMO*, 2015]. For Europe as a whole the annual mean temperature anomaly in 2015 relative to climatic value (mean for 1961-1990 period) is 1.46° C. The strongest anomalies (2-4°C) are noted for the Arctic area of Europe (Fig. B.1). Somewhat lower anomalies take place over European Russia, Scandinavia, eastern and central Europe. The northern part of Atlantic is characterised by small (0-1°C) increase of annual mean temperature compared to the climatic mean value.

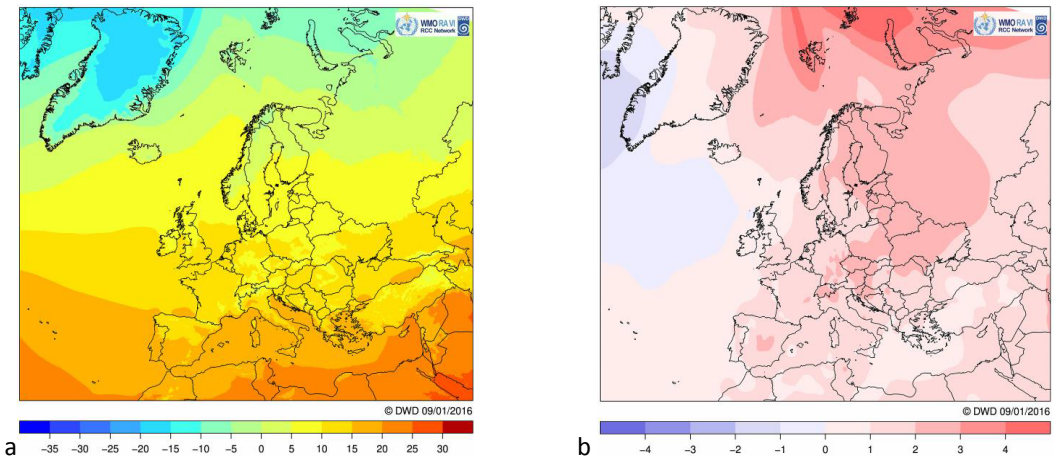


***Fig. B.1.*** *Annual mean air temperature (a) and its anomaly (b) for 2015, °C, relative to period of 1961-1990. Source: [http://www.dwd.de/rcc-cm](http://www.dwd.de/rcc-cm)*

Over most part of Europe precipitation amounts in 2015 were higher than the climatic norm, derived from averaging over period from 1951 to 2000. Precipitation anomalies are noted for most part of Scandinavia, European part of Russia, southern part of the Balkan Peninsula, Greenland (Fig. B.2). Drier than normal conditions are observed over Iberian Peninsula, France, southern Germany, northern Italy, Estonia and Poland.

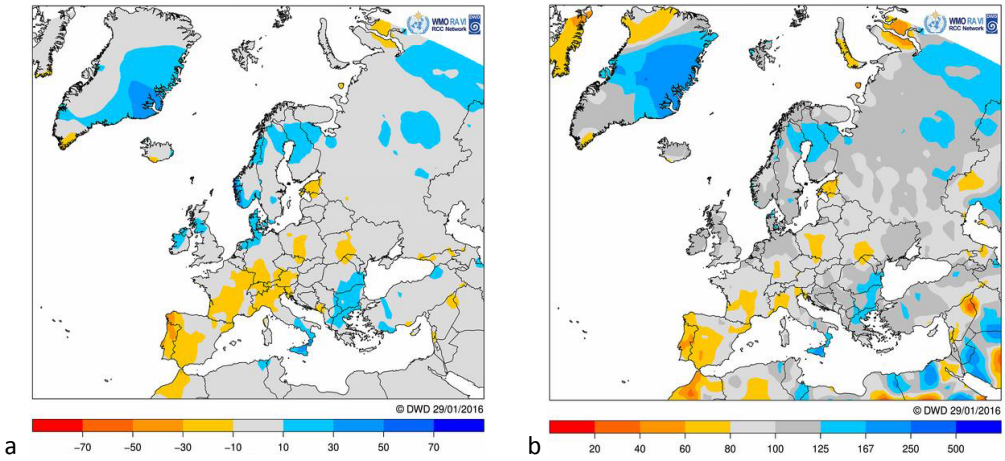


***Fig. B.2.*** *Absolute (a, mm/month) and relative (b, %) anomaly of annual precipitation sums in 2015 relative to climatic mean value for the period from 1951 to 2000. Source: http://www.dwd.de/rcc-cm*

Strength and direction of wind depends on gradient of atmospheric pressure. In 2015 surface pressure over the Icelandic Low is lower, and over the Azores High – higher than normal (relative to 1961-1990). It conditioned stronger westerly atmospheric transport, especially in winter period. Compared to climatic mean characteristics, in the EMEP region zonal component of atmospheric circulation was more (25-60%) intensive in winter time, while in the other part of the year it was close to the norm [*HMCR*, 2017]. Intensity of meridional component was close to normal value almost throughout the whole year 2015.

ANNEX C

# PROPOSALS FOR THE WORKPLAN FOR 2018-2019 AND UPDATED MANDATE OF MSC-E

This annex presents proposals of MSC-E for the future mandatory work and research activity on assessment of heavy metal and POP pollution level assessment. There are some items e.g., country-scale assessment of heavy metals and POPs in Russia, which inclusion in the proposal is under discussion. Besides, new proposal on assessment of mercury pollution levels in Germany has been recently presented by national experts from this country.

## *Proposal of MSC-E Mandate*

(a) Prepare data on anthropogenic emissions of heavy metals and POPs on regional (EMEP domain) and global scales including auxiliary parameters (e.g. emission height, temporal variation, chemical composition etc.) as input for operational modelling based on gridded emission dataset provided by Centre for Emission Inventories and Projections (CEIP) and expert estimates;

(b) Generate meteorological data for operational and research modelling on different scales (global, regional) based on datasets of the European Centre for Medium-Range Weather Forecasts (ECMWF);

(c) Prepare input data required for modelling of heavy metals and POPs on regional and global scales, including wind suspension of mineral dust as well as atmospheric concentrations of chemical reactants and particulate matter;

(d) Collect and process measurement data for evaluation of model performance from various monitoring networks and databases (e.g. EBAS, AirBase, GMOS, UNEP SC GMP Data Warehouse, etc.);

(e) Update the modelling tools with new findings and improved parameterizations developed by the Centre in its research activities in accordance with the bi-annual work-plan and cooperation with scientific community;

(f) Perform simulations of heavy metals and POPs dispersion on a global scale for evaluation of intercontinental transport and initial and boundary conditions for regional-scale assessment of pollution levels;

(g) Perform further testing and evaluation of model performance in simulations of air concentration and deposition levels as well as source-receptor relationships of heavy metals and POPs on the new EMEP grid;

(h) Perform operational model assessment of heavy metal (Pb, Cd, and Hg) and POP (PAHs, PCBs, PCDD/Fs, and HCB) pollution levels over the EMEP domain;

(i) Perform quality assurance and quality control of modelling results through evaluation against

measurements from the EMEP and other monitoring networks;

(j) Provide support of Parties to the Convention with use of the model assessment results and access to the modeling tools.

(k) Contribute to the work of the subsidiary bodies and task forces:

- Task Force on Measurements and Modelling (TFMM): Continue cooperation on the evaluation of model performance and improvement of modeling approaches in the field of heavy metal and POP pollution assessment; present and discuss results of the national scale case studies and other research activities on heavy metal and POP pollution with fine resolution;
- Task Force on Hemispheric Transport of Air Pollution (TFHTAP): Cooperate on assessment of intercontinental transport of Hg and POPs and its impact on pollution levels in the EMEP countries;
- Working Group on Effects: Continue collaboration with ICP-Vegetation on evaluation of heavy metal pollution levels in Europe using modeling results and measurements in mosses and develop cooperation with other International Cooperative Programmes; provide support of the Coordination Centre for Effects (CCE) with information on ecosystem-specific deposition heavy metals and POPs for assessment of critical load exceedances; contribute to the Task Force on Health with information on toxic substances (PAHs, PCDD/Fs and others);

(l) Cooperate on dissemination of information and data exchange with international bodies including UNEP, AMAP, Stockholm Convention, Minamata Convention, HELCOM, etc.;

(m) Prepare annual Status Reports and individual country reports for the EMEP countries and make results of model calculations available online at the MSC-E website; develop and maintain a website in Russian to facilitate access to information by countries in Eastern Europe, the Caucasus and Central Asia;

(n) Report on its activities and deliverables to the Steering Body to EMEP and Working Group on Effects and participate in annual meetings of the relevant Task Forces (TFMM, TFHTAP).

***Proposal for the workplan of MSC-E future research activities for 2018-2019***

| Title | Description/Objectives | Deliverables | Collaboration |
|---|---|---|---|
| *Country-scale assessment of HM and POP pollution (Case Studies)* | 1) Assessment of country-specific HM and POP pollution using detailed national emission and monitoring data for Poland (Cd, BaP), Spain (BaP), France (BaP), UK (Pb, Cd - ?), Russia (Pb, Cd - ?).<br>2) Evaluation of pollution levels in high-emission and high-impact (e.g. urban) areas using data fusion approaches.<br>3) Analysis of factors affecting quality of HM and POP pollution modeling with fine spatial resolution. | 1) Model estimates of pollution levels with high spatial resolution;<br>2) Analysis of discrepancies between modeled and observed pollution levels;<br>3) Estimates of contributions of LPS, national, regional, and non-EMEP emissions as well as key source categories to pollution;<br>4) Estimates of air pollution levels in urban areas based on combined use of modeling results and measurements<br>5) Recommendations for improvement of model assessment quality in the EMEP region.<br>6) Overview of main results of Case Studies (since 2011) | TFMM, Poland (IEP-NRI), Czech Republic (CHMI), Spain (CIEMAT), France (INERIS), UK (CEH), Russia (IGCE) |
| Evaluation of multi-compartment intercontinental transport of Hg and POPs | 1) Assessment of Hg, PCDD/Fs and PCB pollution of the EMEP countries and other regions (e.g. the Arctic) from regional and global sources<br>2) Analysis of the key factors affecting POP and Hg accumulation in and exchange between the environmental media<br>3) Evaluation of secondary emissions of selected POPs (PCDD/Fs, PCB) and Hg and their contribution to pollution of the EMEP countries. | 1) Source apportionment of Hg, PCDD/Fs, and PCB pollution levels in the EMEP countries including regional and global sources<br>2) Evaluation of Hg deposition to sensitive ecosystems (e.g. wetlands, in-land waters and catchment areas, marginal seas, the Arctic)<br>3) Contribution to EMEP Global Mercury Assessment 2018<br>4) Development of model parameterizations for Hg aquatic chemistry and air-surface exchange processes<br>5) Evaluation and refinement of model parameterizations of PCDD/Fs and PCB processes in terrestrial and aquatic compartments | TFHTAP, TFMM, WGE/ICP-Waters, UNEP, AMAP, Stockholm Convention, Minamata Convention |
| Analysis of effectiveness of implementation of Protocol on POPs | Contribution to evaluation of stricter measures for mitigation of BaP pollution levels | 1) Analysis of long-term trends of BaP pollution levels in the EMEP countries<br>2) Assessment of BaP pollution levels with focus on densely populated areas and comparison with air quality guidelines (health effects)<br>3) Evaluation of the key source categories contribution to BaP pollution levels<br>4) Projections of future BaP pollution levels on the basis of emission scenarios (if available) | TFTEI |